

Polimery w Medycynie

Polymers in Medicine

BIANNUAL ISSN: 0370-0747 e-ISSN: 2451-2699

www.polimery.umw.edu.pl

2022, Vol. 52, No. 1 (January–June)

Ministry of Science and Higher Education – 70 pts.
Index Copernicus (ICV) – 120.63 pts.



WROCLAW
MEDICAL UNIVERSITY

Polimery w Medycynie
Polymers in Medicine



Polimery w Medycynie

Polymers in Medicine

ISSN 0370-0747 (PRINT)

ISSN 2451-2699 (ONLINE)

www.polimery.umw.edu.pl

BIANNUAL
2022, Vol. 52, No. 1
(January–June)

“Polymers in Medicine” is an independent, multidisciplinary forum to exchange scientific and clinical information, which publishes original papers (technical, analytical, experimental, clinical), preliminary reports and reviews regarding the use of polymers (natural and synthetic) and biomaterials in different specialties of medicine (biochemistry, clinical medicine, pharmacology, dentistry, implantology), biotechnology and veterinary science.

Address of Editorial Office

Marcinkowskiego 2–6
50-368 Wrocław, Poland
Tel.: +48 71 784 11 33
E-mail: redakcja@umw.edu.pl

Publisher

Wrocław Medical University
Wybrzeże L. Pasteura 1
50-367 Wrocław, Poland

Online edition is the original version of the journal

Editor-in-Chief

Prof. Witold Musiał

Deputy Editor

Dr. Konrad Szustakiewicz, DSc., Eng.

Statistical Editors

Wojciech Bombała, MSc
Katarzyna Giniewicz, MSc Eng.
Anna Kopszak, MSc
Dr. Krzysztof Kujawa

Scientific Committee

Prof. Mirosława El-Fray
Prof. Franciszek Główka
Prof. Jörg Kreßler
Dr. Anna Krupa
Prof. Maciej Małecki
Prof. Bożena B. Michniak-Kohn

Prof. Wojciech Milyk
Prof. Masami Okamoto
Prof. Elżbieta Pamała
Prof. Wiesław Sawicki
Prof. Szczepan Zapotoczny

Section Editors

Dr. Tomasz Urbaniak
(synthesis, evaluation, medical use
of polymers, sensitive to environmental
factors, applied in controlled and targeted
drug delivery)

Dr. Monika Gasztych
(preparation, assessment and application
of polymers in pharmaceutical technology
and medical devices)

Dr. BEng., Agnieszka Gadomska-Gajadur
(synthesis and characterization of polymers
having biomedical potential, composites for
regenerative medicine)

Manuscript editing

Marek Misiak, Jolanta Krzyżak

Editorial Policy

During the review process, the Editorial Board conforms to the "Uniform Requirements for Manuscripts Submitted to Biomedical Journals: Writing and Editing for Biomedical Publication" approved by the International Committee of Medical Journal Editors (<http://www.icmje.org/>). Experimental studies must include a statement that the experimental protocol and informed consent procedure were in compliance with the Helsinki Convention and were approved by the ethics committee.

For more information visit the following page: <http://www.polimery.umw.edu.pl>

Indexed in: OCLC, WorldCat, PBL, EBSCO, MEDLINE, Index Copernicus

Typographic design: Monika Kołęda, Piotr Gil

Cover: Monika Kołęda

DTP: Wrocław Medical University Press

Printing and binding: ARG1

Circulation: 11 copies

Contents

Original papers

- 5 Jenan A. Ghafil, Bashar Mohammed Salih Ibrahim, Ayaid Khadem Zgair
Coating indwelling urinary catheters with moxifloxacin prevents biofilm formation by *Burkholderia cepacia*
- 11 Parham Pedram, Shiva Jafarnia, Sima Shahabi, Sogol Saberi, Hamidreza Hajizamani
Comparative evaluation of fiber-reinforced, bulk-fill and conventional dental composites: Physical characteristics and polymerization properties

Reviews

- 17 Dominik Strojewski, Anna Krupa
Kollidon® VA 64 and Soluplus® as modern polymeric carriers for amorphous solid dispersions
- 29 Mohd Imran, Monalisha Samal, Abdul Qadir, Asad Ali, Showkat R. Mir
A critical review on the extraction and pharmacotherapeutic activity of piperine
- 35 Tomasz Kubiak
Polymeric capsules and micelles as promising carriers of anticancer drugs

Coating indwelling urinary catheters with moxifloxacin prevents biofilm formation by *Burkholderia cepacia*

Jenan A. Ghafil^{1,A,B}, Bashar Mohammed Salih Ibrahim^{2,C,F}, Ayaid Khadem Zgair^{2,B-D}

¹ Department of Biology, College of Science, University of Baghdad, Iraq

² Department of Pharmaceutical Microbiology, College of Pharmacy, Süleyman Demirel University, Isparta, Turkey

A – research concept and design; B – collection and/or assembly of data; C – data analysis and interpretation; D – writing the article; E – critical revision of the article; F – final approval of the article

Polymers in Medicine, ISSN 0370-0747 (print), ISSN 2451-2699 (online)

Polim Med. 2022;52(1):5–9

Address for correspondence

Bashar Mohammed Salih Ibrahim
E-mail: basharibrahim@sdu.edu.tr

Funding sources

None declared

Conflict of interest

None declared

Received on March 10, 2022

Reviewed on May 9, 2022

Accepted on May 11, 2022

Published online on June 27, 2022

Abstract

Background. *Burkholderia cepacia* adhesion and biofilm formation onto abiotic surfaces is an important feature of clinically relevant isolates. The in vitro biofilm formation of *B. cepacia* onto coated indwelling urinary catheters (IDCs) with moxifloxacin has not been previously investigated.

Objectives. To examine the ability of *B. cepacia* to form biofilms on IDCs and the effect of coating IDCs with moxifloxacin on biofilm formation by *B. cepacia* in vitro.

Materials and methods. The adhesion of *B. cepacia* to coated and uncoated IDCs with moxifloxacin was evaluated. Pieces of IDCs were coated with moxifloxacin (adsorption method). The spectrophotometric method was used to check moxifloxacin leaching into tubes. Coated and uncoated tubes were incubated with 10^7 colony forming units (cfu)/mL of *B. cepacia*. The viable bacterial count was used to count the number of bacteria adhered to coated and uncoated IDC pieces.

Results. A significant adhesion of *B. cepacia* to uncoated IDC pieces started 15 min after the incubation in a bacterial suspension (10^7 cfu/mL). A maximum adhesion was observed at 48 h. The pretreatment of IDCs with 100 µg/mL of moxifloxacin produced the best adsorption of antibiotic onto the IDCs. Coating IDC pieces with moxifloxacin significantly reduced the adhesion and biofilm formation of *B. cepacia* ($p < 0.05$) at various time intervals (1 h, 4 h and 24 h).

Conclusions. The present study has demonstrated for the first time that coated IDCs with moxifloxacin reduce *B. cepacia* adhesion and biofilm formation. This finding has opened the door to the production of the new generation IDCs that prevent bacteria from attaching and forming biofilms.

Key words: adhesion, biofilm formation, *Burkholderia cepacia*, indwelling urinary catheter, moxifloxacin

Cite as

Ghafil JA, Ibrahim BMS, Zgair AK. Coating indwelling urinary catheters with moxifloxacin prevents biofilm formation by *Burkholderia cepacia*. Polim Med. 2022;52(1):5–9. doi:10.17219/pim/149986

DOI

10.17219/pim/149986

Copyright

Copyright by Author(s)

This is an article distributed under the terms of the Creative Commons Attribution 3.0 Unported (CC BY 3.0) (<https://creativecommons.org/licenses/by/3.0/>)

Background

Burkholderia cepacia is a non-fermenting Gram-negative (NFGN) bacteria responsible for a significant number of hospital infections.¹ It has been indicated in chronic nosocomial infections such as septicemia, respiratory tract infections, genitourinary system infections, intracranial infections, endocarditis, gastrointestinal system infections, and surgical site infections.² It is classified as an important emerging opportunistic pathogen, especially in immunocompromised hosts. Studies have shown that these bacteria maintain their vitality by attaching to any surface and forming biofilms rather than remaining in their planktonic form.³

In addition to having an important role in bacterial adherence and resistance to antibiotics and phagocytosis, biofilms allow bacteria to gain the ability to adapt to the environment by forming a community with new genetic modulations. These help mediate cell–cell and cell–surface interactions critical for biofilm formation and for stabilization of the extracellular exopolysaccharide, produced by bacterial cells.^{4,5}

Burkholderia cepacia is capable of surviving and multiplying in urine, intravenous fluids and respiratory secretions. Previous studies have shown that *B. cepacia* causes many clinical problems by attaching to biotic and abiotic surfaces.^{6,7} It can be found in humid areas in the hospital such as food, sinks, toilets, floor cleaning cloths, respiratory equipment, dialysis equipment, plastic tubing of catheters, and even disinfectant solutions.⁸ The experimental work on the adhesion of *B. cepacia* to the plastic tubing of indwelling urinary catheters (IDCs) is not clearly described in the literature. Subinhibitory concentrations (sub-minimum inhibitory concentrations (sub-MICs)) are defined as concentrations of an antibiotic below the MICs. The sub-MICs of antibiotics can alter the physical and chemical cell–surface features of bacteria, and may hinder the expression of some virulence properties and functionality of bacteria, such as bacterial adherence.⁹ In recent years, researchers have been interested in identifying alternative treatments that inhibit biofilms and increase the effectiveness of antibacterial drugs, i.e., using heavy metal nanoparticles, enzymes and plant extracts.¹⁰

It has been reported that these alternative treatments affect the structure of the biofilm by various mechanisms.¹⁰ However, more studies are needed on this subject. Currently, many research projects have been conducted to find new antibacterial targets. Studies focused on preventing the communication between bacteria instead of directly killing them have proposed promising new strategies for the future, but these solutions have yet to be put into practice.¹¹ In this study, we aimed to evaluate the adhesion of *B. cepacia* to abiotic surfaces, biofilm formation, and the role of subinhibiting doses of moxifloxacin in reducing the ability of this bacterium to form biofilms on IDCs.

Materials and methods

Clinical isolates

In our study, clinical isolates of *B. cepacia* obtained from the Medical School's Department of Medical Microbiology in Chandigarh, India, were preserved by lyophilization. To determine biofilm formation, subcultures were prepared every week by inoculating Luria-Bertani Agar (LB; HiMedia, Mumbai, India) medium at 37°C.

IDC tubes

Female 2-way latex foley catheters (Well Lead Medical Co., Ltd., Guangzhou, China) were used in the current study. The catheters are made from natural latex. They have a silicone-coated surface (to reduce allergic reaction), a length of 270 mm, CE and ISO 13485 certificates, and are single-use only. The catheters were opened and the tubes were cut under sterile conditions.

Bacterial adhesion to pieces of IDC tubes

The isolates were grown overnight at 37°C in individual sterile bottles containing trypticase soy water (tryptica soy broth (TSB); HiMedia). A cell pellet was obtained by centrifugation (10,000 g for 5 min at 4°C). The pellet was washed twice with phosphate-buffered saline (PBS, 0.01 M, pH 7.2) and resuspended in sterile PBS (0.01 M, pH 7.2) to adjust the bacterial count to 1×10^7 colony forming units (cfu)/mL. Several pieces of IDC tubing measuring 1 cm² were placed in test tubes containing *B. cepacia* (1×10^7 cfu/mL) and then incubated at 37°C for different time intervals: 0 min, 15 min, 30 min, 1 h, 2 h, 4 h, 24 h, and 48 h. After the incubation, each piece of tubing was gently washed 3 times with PBS (0.01 M, pH 7.2) solution to remove any unbound bacteria. Each piece was individually scratched in 1 mL of PBS solution. Then, 100 µL were serially diluted and plated on double plates of LB agar (HiMedia). A bacterial count was performed after 18 h of incubation at 37°C.¹² The experiment was repeated 3 times.

Adsorption of moxifloxacin to IDC tubes

According to the method of Reid et al., 1-cm sections of IDC tubing were placed in 3 test tubes containing moxifloxacin at concentrations of 100 µg/mL, 50 µg/mL and 25 µg/mL, and were incubated for 24 h at room temperature.¹³ After the incubation, the pieces were carefully washed with 2 mL of PBS (pH 7.1 ± 0.1). The IDC pieces were then incubated in 2 mL of PBS (pH 7.0 ± 0.1) for additional 60 min. Leakage of moxifloxacin into the solution from the IDC tubing was determined using the spectrophotometer analysis. The remaining moxifloxacin in the tube containing the IDC fragments (test) was estimated after 24 h of incubation at room temperature

(spectrophotometric method). The decrease in concentrations of moxifloxacin indicates the amount of moxifloxacin bound to the IDC pieces. These amounts were compared with the level of moxifloxacin in control tubes (3 test tubes containing 100 µg/mL, 50 µg/mL and 25 µg/mL of moxifloxacin without IDC pieces). The larger the decrease in the concentration of the antibiotic, the better the adsorption of the antibiotic onto IDC pieces. The solutions were filtered through 0.2-µm pore-size Acrodisc filter units in Wheaton liquid chromatography vials. The quantity of moxifloxacin was calculated using maximum A290 values that were checked with UV Visible Scanning Spectrophotometer (Thermo Fisher Scientific, Waltham, USA). All experiments were repeated in triplicate.¹³

Adhesion of *B. cepacia* to tubes coated with moxifloxacin

A similar procedure aimed at measuring the adhesion of *B. cepacia* to uncoated IDC tubes as mentioned above was followed. It allowed us to study the ability of *B. cepacia* to adhere to coated tubes in terms of the number (cfu/cm²) of *B. cepacia* that adhered to coated IDC tubes at different time intervals (1 h, 4 h and 24 h).

Statistical analyses

Calculations were performed to obtain a mean value and standard deviation (SD). The differences were analyzed by means of the Student's t-test using Origin v. 8.0 software (OriginLab, Northampton, USA). A value of $p < 0.05$ was considered statistically significant.

Results

Adhesion of *B. cepacia* to IDC tubes

In this study, the kinetics of *B. cepacia* adhesion to pieces of uncoated IDC tubes at various time intervals (15 min, 1 h, 2 h, 4 h, 24 h, and 48 h) was investigated. The kinetics of *B. cepacia* adhesion to pieces of IDC tubes was confirmed by counting the viable bacterial count in cfu/cm² (biofilm formation). The study showed the ability of the isolates to adhere to IDC tubes with high efficiency. A significant bacterial adhesion started 15 min after the incubation, with maximum adhesion observed at 48 h (Fig. 1). The result of the present study showed a high and rapid ability of *B. cepacia* to adhere and form biofilm on IDCs.

Attachment of moxifloxacin to pieces of IDC tubes

The optimum wavelength used in this experiment was estimated after studying different wavelengths to determine which one of them achieved the highest absorbance

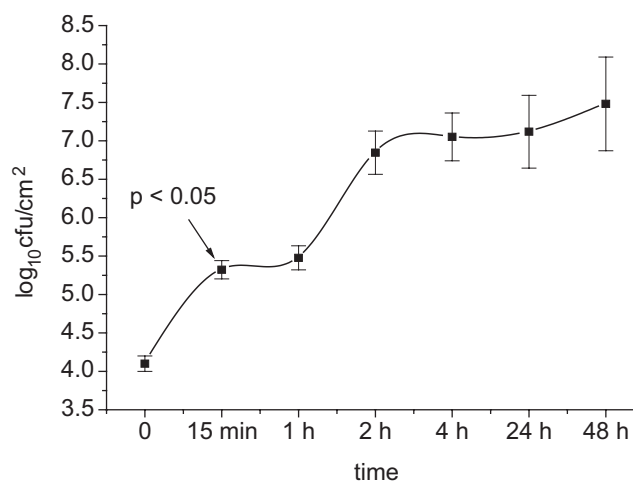


Fig. 1. Kinetics of *Burkholderia cepacia* adhesion to pieces of indwelling urinary catheter (IDC) tubes. Significant adhesion started as early as 15 min after the bacterial incubation

of moxifloxacin (100 µg/mL). Figure 2A shows that the maximum absorbance of moxifloxacin (100 µg/mL) was at 290 nm. This wavelength was used in further experiments to check the efficiency of adsorption of moxifloxacin to IDC tubes. The absorbance (at 290 nm) was measured in test tube solutions containing 100 µg/mL, 50 µg/mL or 25 µg/mL of moxifloxacin with IDC pieces. The test tube solutions were incubated for 24 h. The results were compared with control tubes (100 µg/mL, 50 µg/mL or 25 µg/mL of moxifloxacin without IDC pieces). Figure 2B showed that the absorbance of test tubes (50 µg/mL or 100 µg/mL of moxifloxacin and IDC pieces) at 290 nm was significantly lower than the absorbance of control tubes (50 µg/mL or 100 µg/mL of moxifloxacin without IDC pieces). No significant difference was observed between test tubes containing 25 µg/mL ($p > 0.05$) of moxifloxacin with IDC pieces and control tubes (25 µg/mL of moxifloxacin only). The present study showed that the best adsorption of moxifloxacin was observed after a 24-h exposure of the pieces of IDC to 100 µg/mL of moxifloxacin at room temperature. Thus, the deposition of moxifloxacin on catheters was dependent on moxifloxacin concentration. Therefore, the pieces of IDC exposed to 100 µg/mL of moxifloxacin were used to evaluate the effect of moxifloxacin-coated IDCs on *B. cepacia* adhesion and biofilm formation.

Role of moxifloxacin in reducing bacterial biofilm formation

In the current study, the ability of *B. cepacia* to attach to coated IDC tubes with 100 µg/mL of moxifloxacin was evaluated. The effects of moxifloxacin-coated IDC tubes on the ability of *B. cepacia* to attach to these tubes were examined. This ability was evaluated at various time intervals (1 h, 4 h and 24 h). The results were compared with controls (uncoated pieces of IDC). Figure 3 shows

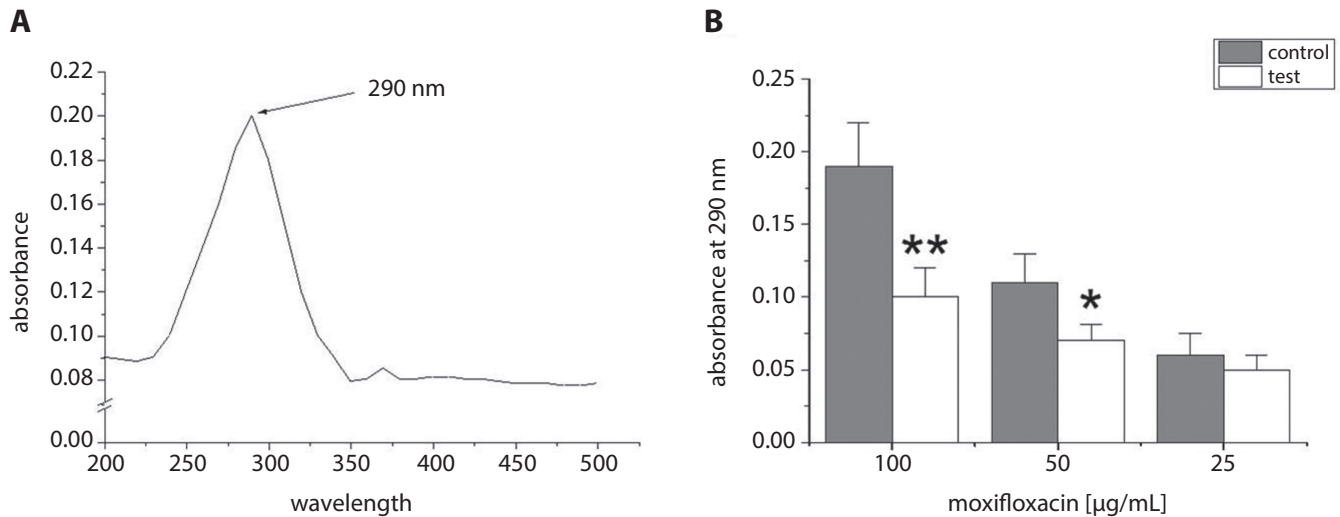


Fig. 2. Absorbance of moxifloxacin (100 µg/mL) at different wavelengths. A. Maximum absorbance was found at a wavelength of 290 nm; B. Absorbance of moxifloxacin at 290 nm for control tubes (25 µg/mL, 50 µg/mL and 100 µg/mL of moxifloxacin) and test tubes (25 µg/mL, 50 µg/mL and 100 µg/mL of moxifloxacin and indwelling urinary catheter (IDC) pieces of 1 cm²) incubated overnight at room temperature. Asterisks indicate significant differences from controls (* p < 0.05; ** p < 0.01)

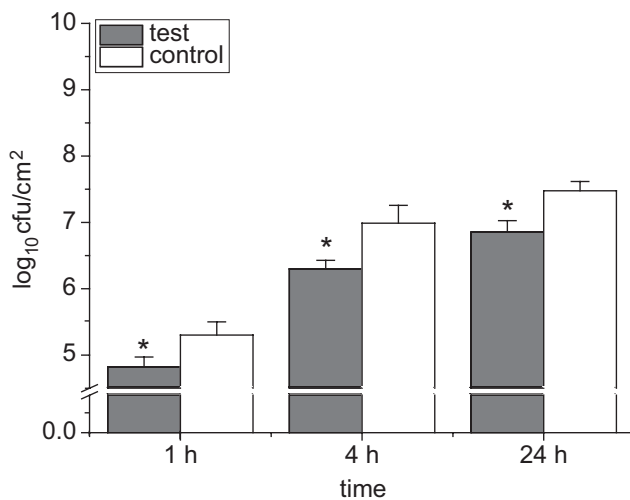


Fig. 3. Bacterial adhesion to coated pieces of indwelling urinary catheters (IDCs) with 100 µg/mL of moxifloxacin (test) and uncoated IDCs without moxifloxacin (control). Asterisks indicate a significant difference from controls (p < 0.05)

a significant difference between the number of adhered bacteria (cfu/cm²) on coated and uncoated IDC tubes at all time points (1 h, 4 h and 24 h) after the incubation with bacterial suspensions (10⁷ cfu/mL). The current study suggests that coating IDCs with moxifloxacin significantly reduces *B. cepacia* attachment to IDCs.

Discussion

Burkholderia cepacia can colonize moist surfaces and cause opportunistic infections, especially in intensive care patients. Multiple studies have shown that these bacteria maintain their vitality by forming biofilms and attaching

to any surface rather than remaining in the planktonic form.³ Biofilms that form on biomaterials, medical devices, host epithelial cells, and mucosal surfaces cause serious medical and industrial problems as they become sources of contamination.^{13,14} Studies have demonstrated that *B. cepacia* has the ability to adhere to a variety of plastic catheter surfaces by forming biofilms. This represents a big challenge in treating infections with these bacteria, especially in hospitalized patients who require IDC tubes as part of their medical care.^{8,15} This study was aimed at finding a solution to this problem.

The current study showed a high and rapid ability of these bacteria to adhere to catheters. Its adherence was significant within only 15 min after the catheter was treated with a standard inoculum of *B. cepacia*. Our findings are consistent with the results of previous studies, showing that these bacteria have the ability to adhere and form biofilms on biotic and abiotic surfaces.^{12,16} The ability of *B. cepacia* to adhere and form a biofilm is due to several factors including quorum sensing, as well as the effect of structural appendages such as flagella.^{12,17}

In the current study, a good method of adhesion elimination and biofilm formation of *B. cepacia* in IDC tubes was found. The method was dependent on coating IDC tubes with moxifloxacin. It was found that the adhesion of bacteria (*B. cepacia*) and biofilm formation were significantly reduced in the coated IDC tubes compared to uncoated IDC tubes. Our study is a pioneer research that successfully used coated IDC tubes with moxifloxacin to eradicate *B. cepacia* adhesion and biofilm formation. This project opens the door to new research aimed at manufacturing IDC tubes that do not allow bacteria to adhere and form a biofilm. Such feature of medical equipment could prevent the causes of dangerous infections in hospitalized patients.

Conclusions


Our study demonstrated the adhesion ability of *B. cepacia* to IDC tubes. Moreover, by coating IDCs with moxifloxacin, the ability of *B. cepacia* to adhere to IDC tubes and form biofilms was significantly reduced. We hope that these findings may help in reducing the chance of serious infections with *B. cepacia*, especially in patients suffering from kidney or urinary tract conditions.

ORCID iDs

Jenan A. Ghafil  <https://orcid.org/0000-0003-1461-302X>

Bashar Mohammed Salih Ibrahim

 <https://orcid.org/0000-0003-3086-0995>

Ayad Khadem Zgair  <https://orcid.org/0000-0002-2356-3338>

References

- Srinivasan S, Arora NC, Sahai K. Report on the newly emerging nosocomial *Burkholderia cepacia* in a tertiary hospital. *Med J Armed Forces India*. 2016;72(Suppl 1):S50–S53. doi:10.1016/j.mjafi.2016.03.003
- Bilgin H, Gelmez GA, Bayrakdar F, et al. An outbreak investigation of *Burkholderia cepacia* infections related with contaminated chlorhexidine mouthwash solution in a tertiary care center in Turkey. *Antimicrob Resist Infect Control*. 2021;10(1):143. doi:10.1186/s13756-021-01004-8
- Kovalchuk VP, Nazarchuk OA, Burkot VM, Fomina NS, Prokopchuk ZM, Dobrovanov O. Biofilm forming activity of non-fermenting Gram-negative bacteria. *Wiad Lek*. 2021;74(2):252–256. doi:10.36740/WLek 202102114
- Zgair AK, Chhibber S. Immunological and biological relationship among flagellin of *Pseudomonas aeruginosa*, *Burkholderia cepacia* and *Stenotrophomonas maltophilia*. *Microbiologia*. 2012;81(3):371–376. PMID:22880399.
- Murphy MP, Caraher E. Residence in biofilms allows *Burkholderia cepacia* complex (Bcc) bacteria to evade the antimicrobial activities of neutrophil-like dHL60 cells. *Pathog Dis*. 2015;73(8):ftv069. doi:10.1093/femspd/ftv069
- Zgair AK. Flagellin administration protects respiratory tract from *Burkholderia cepacia* infection. *J Microbiol Biotechnol*. 2012;22(7):907–916. doi:10.4014/jmb.1112.11079
- Pimenta AI, Mil-Homens D, Fialho AM. *Burkholderia cenocepacia*-host cell contact controls the transcription activity of the trimeric autotransporter adhesin BCAM2418 gene. *Microbiologyopen*. 2020;9(4):e998. doi:10.1002/mbo3.998
- Decho AW, Gutierrez T. Microbial extracellular polymeric substances (EPSs) in ocean systems. *Front Microbiol*. 2017;8:922. doi:10.3389/fmicb.2017.00922
- Pompilio A, Catavittello C, Picciani C, et al. Subinhibitory concentrations of moxifloxacin decrease adhesion and biofilm formation of *Stenotrophomonas maltophilia* from cystic fibrosis. *J Med Microbiol*. 2010;59(Pt 1):76–81. doi:10.1099/jmm.0.011981-0
- Mubeen B, Ansar AN, Rasool R, et al. Nanotechnology as a novel approach in combating microbes providing an alternative to antibiotics. *Antibiotics (Basel)*. 2021;10(12):1473. doi:10.3390/antibiotics 10121473
- Preda VG, Săndulescu O. Communication is the key: Biofilms, quorum sensing, formation and prevention. *Discoveries (Craiova)*. 2019;7(3):e100. doi:10.15190/d.2019.13
- Zgair AK, Chhibber S. Immunoassay method to check the flagellin mediated binding of *Stenotrophomonas maltophilia* to polystyrene. *Microbiology*. 2011;80:136–138. doi:10.1134/S0026261711010206
- Reid G, Sharma S, Advikolanu K, Tieszer C, Martin RA, Bruce AW. Effects of ciprofloxacin, norfloxacin, and ofloxacin on in vitro adhesion and survival of *Pseudomonas aeruginosa* AK1 on urinary catheters. *Antimicrob Agents Chemother*. 1994;38(7):1490–1495. doi:10.1128/AAC.38.7.1490
- Sousa SA, Ramos CG, Leitão JH. *Burkholderia cepacia* complex: Emerging multihost pathogens equipped with a wide range of virulence factors and determinants. *Int J Microbiol*. 2011;2011:607575. doi:10.1155/2011/607575
- Khatoun Z, McTiernan CD, Suuronen EJ, Mah TF, Alarcon EI. Bacterial biofilm formation on implantable devices and approaches to its treatment and prevention. *Heliyon*. 2018;4(12):e01067. doi:10.1016/j.heliyon.2018.e01067
- Coenye T. Social interactions in the *Burkholderia cepacia* complex: Biofilms and quorum sensing. *Future Microbiol*. 2010;5(7):1087–1099. doi:10.2217/fmb.10.68
- Ganesh PS, Vishnupriya S, Vadivelu J, Mariappan V, Vellasamy KM, Shankar EM. Intracellular survival and innate immune evasion of *Burkholderia cepacia*: Improved understanding of quorum sensing-controlled virulence factors, biofilm, and inhibitors. *Microbiol Immunol*. 2020;64(2):87–98. doi:10.1111/1348-0421.12762

Comparative evaluation of fiber-reinforced, bulk-fill and conventional dental composites: Physical characteristics and polymerization properties

Parham Pedram^{1,A–C,E}, Shiva Jafarnia^{2,B–D}, Sima Shahabi^{1,3,A,B,E,F}, Sogol Saberi^{3,A–D}, Hamidreza Hajizamani^{1,B,D}

¹ Department of Dental Biomaterials, School of Dentistry, Tehran University of Medical Sciences, Iran

² Department of Dental and Biomedical Materials Science, Graduate School of Biomedical Sciences, Nagasaki University, Japan

³ Laser Research Center, Dentistry Research Institute, Tehran University of Medical Sciences, Iran

A – research concept and design; B – collection and/or assembly of data; C – data analysis and interpretation; D – writing the article; E – critical revision of the article; F – final approval of the article

Polymers in Medicine, ISSN 0370-0747 (print), ISSN 2451-2699 (online)

Polim Med. 2022;52(1):11–16

Address for correspondence

Sogol Saberi

E-mail: Saberisogol@gmail.com

Funding sources

None declared

Conflict of interest

None declared

Received on January 8, 2022

Reviewed on May 24, 2022

Accepted on July 4, 2022

Published online on July 8, 2022

Cite as

Pedram P, Jafarnia S, Shahabi S, Saberi S, Hajizamani H. Comparative evaluation of fiber-reinforced, bulk-fill and conventional dental composites: Physical characteristics and polymerization properties. *Polim Med.* 2022;52(1):11–16. doi:10.17219/pim/151857

DOI

10.17219/pim/151857

Copyright

Copyright by Author(s)

This is an article distributed under the terms of the Creative Commons Attribution 3.0 Unported (CC BY 3.0) (<https://creativecommons.org/licenses/by/3.0/>)

Abstract

Background. Resin composites have various applications. At the same time, they have some drawbacks, such as polymerization shrinkage. Conventional composites are polymerized in 2-mm thick layers. However, in posterior restoration, the 2-mm depth of cure is not satisfactory. To find a solution, resin composites have been vastly improved in terms of fillers, matrix and initiators.

Objectives. To evaluate polymerization properties and physical characteristics of fiber-reinforced composites and compare them with bulk-fill composites that are designed for large posterior restorations.

Materials and methods. Samples were prepared from each resin composite. The 3-point bending test was performed to evaluate the flexural strength of all composites. The depth of cure of the composite from 1 mm to 4 mm of depth was analyzed using Vickers hardness test (VHN). To analyze the degree of conversion, Fourier-transform infrared spectroscopy (FTIR) of the top and bottom surfaces of the samples with 4-mm thickness was calculated. The data were analyzed using one-way analysis of variance (ANOVA) test followed by post hoc test (95% confidence interval (95% CI)).

Results. The Filtek showed the highest flexural strength followed by everX and X-tra fil. At 1-mm depth, X-tra fil had the highest and Gradia had the lowest microhardness. At the 4-mm depth, the microhardness trend was as follows: everX > Filtek > X-tra fil > Gradia > Beautifil. The everX composite had the lowest reduction of the degree of conversion at 4-mm thickness, which showed a significant difference in comparison with Filtek, Gradia and X-tra fil composites.

Conclusions. Based on the results of our study, it can be concluded that the fiber-reinforced composite everX showed more favorable results regarding polymerization properties, such as the degree of conversion and the depth of cure. However, the flexural strength results in Filtek were better than those in everX.

Key words: FTIR, resin composite, depth of cure, degree of conversion, physical properties

Background

Considering an increasing aesthetic demand among patients, tooth-colored restorative materials have received a lot of attention.¹ Resin composites have various applications in restorative dentistry because of their aesthetic and safety values.² At the same time, they have some drawbacks such as polymerization shrinkage, wear and technique sensitivity in posterior restorations, as well as discoloration, which lead to a debate among scientists regarding the effectiveness of composite restorations.³ Brunthaler et al. reported that the main reasons for restoration failure and replacement are fracture and secondary caries.⁴ Conventional composites are polymerized in layers with 2-mm thickness. However, in posterior restoration, the 2-mm depth of cure is not satisfactory.⁵ To find a solution for this concern, resin composites have improved vastly in terms of fillers, matrix and initiators.^{6,7} Fillers with higher translucency and loading in bulk-fill composites enable better light penetration and reduce polymerization shrinkage in a more efficient polymerization.⁸ In conventional composites, the objective was to increase the amount of filler in order to improve their mechanical properties, and at the same time reduce the size of the fillers to improve their optical properties.⁹ However, since the goal for posterior restoration is higher depth of cure, fillers in bulk-fill composites are fewer in number, greater in size and more translucent.¹⁰ Factors such as color and thickness of composite layers alongside the chemical composition of the resin composite affect the polymerization of these materials.¹¹ The reduction of the light energy leads to a lower degree of conversion and reduced polymerization, which in turn cause poor mechanical properties of the composite. The difficulties in curing conventional composites increase the treatment time and chance of clinical errors.¹² Also, a complete polymerization of the composite is crucial for the restoration to achieve adequate physical and mechanical properties. An inadequate polymerization of the resin composite can lead to marginal microleakage,¹³ discoloration,¹⁴ reduced bond strength,¹⁵ and recurrent caries. An incomplete polymerization also results in increased monomer release from composites, which compromises the biocompatibility.^{16,17} Therefore, because of characteristics such as high polymerization depth which results in less chairside time and higher physicommechanical performance,

bulk-fill composites have become more popular.¹⁸ A newly introduced fiber-reinforced composite for large posterior restoration has several advantages such as the high depth of cure and mechanical properties similar to the dentin.¹⁹ Although there are some studies on the physical and mechanical properties of bulk-fill composites, the scope of research regarding the comparison of polymerization kinetics and mechanical properties of fiber-reinforced composite with bulk-fill and conventional resin composites is limited. Different techniques have been used to evaluate the degree of conversion and depth of cure of resin composites, such as microhardness evaluation and Fourier-transform infrared spectroscopy (FTIR) spectra by the comparison of the unpolymerized residual monomer bands.^{20,21} To guarantee the exact polymerization behavior of resin composites, both the depth of cure and the degree of conversion are essential.

Accordingly, the purpose of this study was to evaluate and compare fiber-reinforced and bulk-fill composites, designed for large posterior restoration, with each other and with a conventional resin composite, in terms of degree of conversion, depth of cure and flexural strength, at different thicknesses. The null hypothesis states that there are no significant differences between all resin composites regarding the abovementioned properties.

Materials and methods

Materials

The bulk-fill composites investigated in the current study included Beautifil-Bulk (SHOFU, Kyoto, Japan), Filtek Bulk Fill (3M Oral Care, St. Paul, USA) and X-tra fil (VOCO, Cuxhaven, Germany). The fiber-reinforced composite investigated in the study was everX Posterior (GC Dental, Tokyo, Japan), and the conventional composite was Gradia Direct (GC Dental). The detailed information on the materials is shown in Table 1.

Mini-flexural strength test

Cylindrical composite samples were made using rectangular shape molds with the size of 1.2×1.2×12.5 mm. The molds were cleaned using sterile gas and alcohol, and

Table 1. Detailed information on resin composites used in this evaluation

Manufacturer	Name	LOT No.	Composition	Filler (w%/v%)
GC Dental	Gradia Direct	1704241	UDMA, ethylen dymethacrylate	73/65
GC Dental	everX Posterior	1610061	Bis-GMA, TEGDMA	74.2/53.6
SHOFU	Beautifil-Bulk	101725	Bis-GMA, UDMA, Bis-MPEPP, TEGDMA	87/74.5
3M Oral Care	Filtek Bulk Fill	N782245	AUDMA, UDMA and 1,12-dodecane-DMA	76.5/58.4
VOCO	X-tra fil	1715341	Bis-GMA, UDMA and EBPDMA	86/70.1

UDMA – urethane dimethacrylate; Bis-GMA – 2,2-bis(4-(2-hydroxy-3-methacryloyloxypropoxy)phenyl) propane; TEGDMA – triethylene glycol dimethacrylate; EBPDMA – ethoxylated bisphenol A dimethacrylate; Bis-MPEPP – 2,2-bis(4-(2-methacryloxyethoxyphenyl) propane; AUDMA – aromatic urethane dimethacrylate.

the releasing agent was applied for stress-free separation of samples (Al-Cote; Dentsply, Woodbridge, Canada). The resin composite paste was placed inside the molds and the excessive material was removed. The samples were covered with Mylar matrix, fixed to a 1-mm thick glass slab and photopolymerized using a light-curing unit (BlueLEX LD-105; Monitex Industrial Co., Taipei, Taiwan) 2 times for 20 s in overlapping fragments. The intensity of light emitted from the light-curing unit was controlled using a radiometer. After light polymerization, the glass was separated and the samples were removed from the molds. The specimens were washed with water and kept in an incubator in a dark place for 24 h in order to complete the process of polymerization. To evaluate the flexural strength, the samples were placed in an Universal Testing Machine (Santam, Tehran, Iran) with 0.5 mm/min crosshead speed. The maximum fracture load was recorded, and the flexural strength (MPa) was calculated using the following equation (Equation 1):

$$FS = 3Fl/2bh^2 \quad (1)$$

Microhardness evaluation

In order to evaluate the depth of cure for each resin composite, the measurement of the composite microhardness in different thicknesses was performed. A mold with the height of 4 mm was prepared and the resin composite was inserted into the mold. Each sample was photopolymerized using light-emitting diode (LED) curing unit from the top of the mold. In every millimeter, 3 indentations were made, and the average hardness was measured and reported. For this purpose, the Vickers microhardness device (Bareiss, Oberdischingen, Germany) was used. The force applied by the device was set at 0.49 N (50 g for 15 s). The microhardness results for each depth were recorded. The adequate depth of cure for each specimen was considered at the minimum threshold of the 80% of the microhardness value of the sample surface.

ATR-FTIR analysis

The degree of conversion on the surface and at the 4-mm depth of cure of each resin composite was measured using the FTIR analysis. Samples were made from each resin composite in a disc with 4-mm thickness. Each specimen was analyzed using FTIR with an attenuated total reflectance sensor (ATR-FTIR; NICOLET™ iS™ 10; Thermo Fisher Scientific, Waltham, USA). The spectra were acquired at the range of 500–4000 cm^{-1} . The area under the absorption peaks graph with wavelengths of 1720 cm^{-1} as the internal standard and 1637 cm^{-1} as the aliphatic absorbance peak area was measured, and the degree of conversion (DC) was calculated based on the formula below (Equation 2):

$$DC = \left(1 - \frac{\frac{\text{aliphatic}}{\text{aromatic}} \text{ area cured material}}{\frac{\text{aliphatic}}{\text{aromatic}} \text{ area uncured material}} \right) \times 100 \quad (2)$$

It should be noted that aliphatic carbon varied during polymerization and aromatic carbon stayed constant, and the ratio of these 2 determines the variations in polymerization. In each group, the samples were compared to the uncured state of the same composite so that the polymerization rate could be calculated. These calculations were made for the surface of the composite and at 4-mm depth of cure.

Statistical analyses

All the data were analyzed using SPSS software.²² The obtained data were examined using analysis of variance (ANOVA) performed for the significant differences between different composites, followed by post hoc test (95% confidence interval (95% CI)) for each variable on datasets ($p < 0.05$).

Results

Flexural strength

The results of the flexural strength measured from samples of each group showed that the highest flexural strength value belonged to the Filtek (289.86 \pm 31.92 MPa), followed by everX (274.30 \pm 37.95 MPa) and X-tra fil (258.95 \pm 40.88 MPa) (Fig. 1). The Beautifil and Gradia flexural strength results were 170.59 \pm 28.62 MPa and 160.40 \pm 14.95 MPa, respectively. The statistical analysis confirmed that these 2 groups had significantly lower flexural strength compared to other composites ($p < 0.05$).

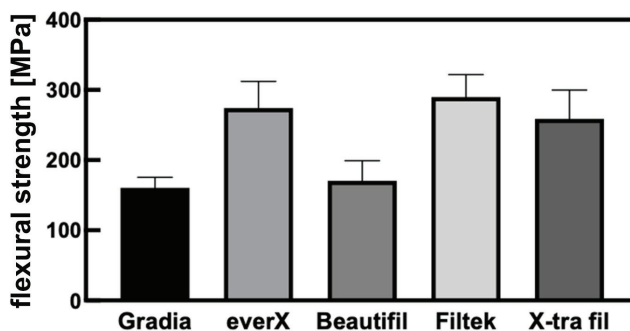


Fig. 1. Bar graph illustrating flexural strength results of all resin composite groups

Microhardness

The microhardness evaluation was carried out in 1-mm to 4-mm thick composites, and the results were reported as an average of the 10 samples (Fig. 2). At the 1st millimeter, the order of the microhardness values for all the groups was as follows: X-tra fil > Filtek > Beautifil > everX > Gradia. The highest microhardness value at the 1st millimeter was attributed to the X-tra fil which was 64.85. The Gradia microhardness results at the first 3 mm were 32.83, 30.83

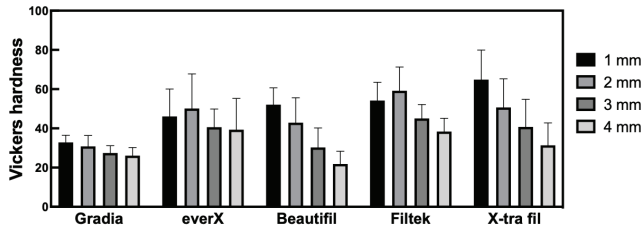


Fig. 2. Vickers microhardness results of each resin composite at 4 different depths of cure

Table 2. Ratio of microhardness in 2-mm to 4-mm thickness to the surface microhardness of each composite

Composite	Group	Ratio
Gradia	2 mm/1 mm	94.4450
	3 mm/1 mm	84.0332
	4 mm/1 mm	79.5819*
everX	2 mm/1 mm	112.0892
	3 mm/1 mm	92.5081
	4 mm/1 mm	88.5457
Beautifil	2 mm/1 mm	82.3630
	3 mm/1 mm	57.9888*
	4 mm/1 mm	42.4291*
Filtek	2 mm/1 mm	112.1046
	3 mm/1 mm	84.5168
	4 mm/1 mm	72.3740*
X-tra fil	2 mm/1 mm	80.3615
	3 mm/1 mm	65.1734*
	4 mm/1 mm	48.1461*

* star-selected values indicate more than 20% decrease in microhardness among deep layers.

and 27.64, respectively, which was the lowest hardness among all examined composites. The microhardness trend at the 4-mm depth was as follows: everX > Filtek > X-tra fil > Gradia > Beautifil. At 4-mm thickness, the hardness values of Gradia and Beautifil were 26.10 and 21.84, respectively, that being the lowest values compared to other composites.

The hardness ratio for each millimeter in each composite was reported as a percentage of the 1st millimeter (Table 2). In a separate analysis of each group, the microhardness result showed an acceptable depth of cure; however, it significantly decreased at 3-mm and 4-mm thickness. In Filtek, Gradia, X-tra fil, and Beautifil composites, the decrease in hardness value at 4 mm constituted more than 20% of the surface hardness ($p < 0.05$).

FTIR

The average degree of conversion of the top and bottom surface of composite samples was measured using FTIR (Fig. 3). The results obtained during the FTIR analysis at the 1-mm and 4-mm depth and their comparison between composites showed a statistically significant difference between the groups.

The order of the degree of conversion values at the top surface of the specimens were as follows: everX > Filtek >

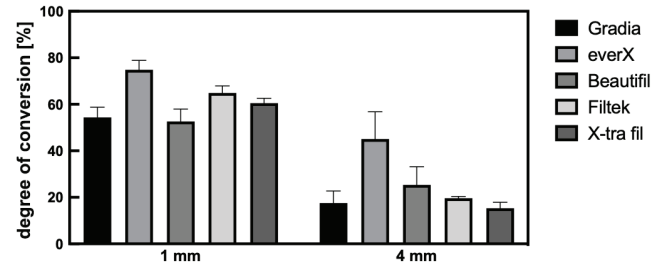


Fig. 3. Average degree of conversion for each resin composite at 1- and 4-mm depth

X-tra fil > Gradia > Beautifil. The everX degree of conversion at the 1 mm was 74.85, which was significantly higher compared to the other groups. At the 4 mm, the order of the degree of conversion was changed and was as follows: everX > Beautifil > Filtek > Gradia > X-tra fil. The everX composite showed the reduction of degree of conversion at 4-mm thickness. Also, the value of this composite was significantly higher than Filtek, Gradia and X-tra fil composites ($p < 0.05$).

Discussion

The application of resin composites is getting more attention and is becoming more popular among both clinicians and patients. However, there is still an ongoing debate among scientists regarding a complete polymerization of resin composites and their mechanical properties in posterior restoration. The newly introduced fiber-reinforced composites and bulk-fill composites have been produced specifically for large posterior restorations. The manufacturers of these composites claim that their products can provide complete polymerization and adequate physical and mechanical properties in the thickness greater than 2 mm. The aim of this study was to evaluate and compare the depth of cure, the degree of conversion and the flexural strength of fiber-reinforced, bulk-fill and conventional resin composites.

In the mini-flexural test, which was performed in our study, the sample size dimensions were smaller than those in the ISO method. Smaller dimensions, compared to conventional tests, reduce the number of possible flaws such as porosities. Additionally, the stress distribution occurs with more precision. Also, the dimensions of the specimen are more similar to the real dimensions of the samples in dental practice.²³ The results of flexural strength tests showed that Filtek had the best flexural properties compared with all other groups, followed by everX and X-tra fil. A greater flexural strength of Filtek compared to the fiber-reinforced composite can be related to the fibers of the everX that make this composite more susceptible to fracture. A conventional Gradia composite had the worst results; however, the difference between Gradia and Beautifil was not significant. Studies showed that such difference

in flexural performance of different composites can be attributed to the resin matrix mixture, filler properties and its percentage on each composite.^{8,24}

The microhardness evaluation is an index which determines the adequacy of polymerization depth. In this test, the minimum threshold is 80% of the microhardness value of the top surface, according to the standards.^{25,26} In the current study, the microhardness value of the bulk-fill composites at the 1st millimeter were higher than fiber-reinforced and conventional composites. However, at higher depths, the microhardness of Beautifil composite decreased significantly, and at the 4-mm thickness, the hardness of this composite became lower than in the conventional group. As it can be seen in Fig. 2, at the 4-mm depth, the fiber-reinforced composite everX showed the highest hardness value, which is also related to its higher depth of cure. The other composites did not show 80% of their top surface hardness at the 4-mm depth. Moreover, it is clear that the X-tra fil and Beautifil composites did not show acceptable depth of cure in terms of 80% hardness value of the top surface at the 3rd millimeter (Table 2). According to the results of our research, everX and Filtek had more stable hardness results at all depths and could be placed in bulk in posterior restorations. However, the results indicated that the Beautifil and X-tra fil composites are not suitable for single-step placement in bulk. The microhardness results of Filtek and everX showed higher hardness value at the 2nd millimeter compared to the 1st millimeter. This seems to be related to the initiation of the polymerization reaction and formation of free radicals in the composite.²⁷ At 2-mm thickness, a sufficient light penetration, the presence of free radicals from chain reactions in the 1st millimeter and heat from polymerization further stimulate free radicals and monomers, which enable this level of hardness to occur.

The FTIR analysis, which have been used in the current study, is one the most common tests for the degree of conversion analysis.^{21,28,29} There is a carbon double bond (C=C) in the resin monomers of the composites, which breaks and turns into a C–C bond. This conversion links the monomers and creates the polymer. The aliphatic C=C differs before and after the polymerization, and the absorbed wavelength of this bond is 1637 cm⁻¹. As the values reported by the FTIR device have no quantitative value, they are compared to a constant absorptive peak in order to analyze the difference before and after the polymerization and estimate the polymerization rate. The C=C bond of the aromatic ring in monomers is constant and one of the indexes used

in calculating the ratio of absorptive peaks is the wavelength absorbed by this bond (1608 cm⁻¹). Since some composites in this study did not have aromatic rings in their monomers, another constant bond in the monomer at the terminal end of the molecule (-OH) with the absorbed wavelength at the 1720 cm⁻¹ was used. The everX showed the highest degree of conversion, followed by Filter and X-tra fil. The lowest degree of conversion was attributed to Gradia and Beautifil. The e-glass fibers in the everX composite had a positive effect on its polymerization, facilitating the light penetration and scattering that result in better polymerization and higher depth of cure.³⁰ One of the modifications applied to monomers is using more urethane dimethacrylate (UDMA) in bulk-fill resin-based composites. This monomer has a low molecular weight, higher concentration of double bonds and low viscosity. Studies showed that the combinations of 2,2-bis(4-(2-hydroxy-3-methacryloyloxypropoxy) phenyl) propane (Bis-GMA) and UDMA or triethylene glycol dimethacrylate (TEGDMA) display a more rigid network and higher polymerization.^{7,31,32} The high degree of conversion in Filtek and X-tra fil may be related to UDMA in their resin matrix. Even though X-tra fil composite showed the highest decrease in polymerization, it only had a statistically significant difference in this regard when compared with everX and Beautifil composites. Nevertheless, considering the decrease in hardness at 4-mm thickness, it showed poor results.

Based on the FTIR and microhardness results obtained in the current study, it should be mentioned that although Beautifil, Filtek and X-tra fil are introduced as bulk-fill resin composites, the polymerization at the depth of 4 mm is not complete. Since incomplete polymerization results in failure of the restoration over time, it is recommended to use layering technique in the clinics to attain more durable and satisfactory results. Regarding the application of everX in the deep cavities, based on the flexural strength results of our study and manufacturer's recommendation, it is advised to cover it with a conventional composite. A layer of conventional composite causes a synergic effect, stopping crack propagation on the restoration and leading to a strong biomimetic restoration (Table 3).

Conclusions

Based on the results of our study, it can be concluded that the fiber-reinforced composite everX showed more favorable results in terms of polymerization properties

Table 3. Comparison of all measured properties

Property	Gradia	everX	Beautifil	Filtek	X-tra fil
Flexural strength [MPa]	160.4	274.3	170.59	289.86	258.95
Microhardness (VHN) 4 mm/1 mm	79.58	88.54	42.42	72.37	48.14
Degree of conversion (%) 4 mm/1 mm	32.05	60.16	48.07	30.23	25.31

VHN – Vickers hardness test.

such as degree of conversion and depth of cure. However, the results of the flexural strength in Filtek were higher than those in everX. Among the experimental bulk-fill composites, Beautiful did not show reliable results to be used in bulk concerning its polymerization properties.

ORCID iDs

Parham Pedram  <https://orcid.org/0000-0003-2322-2418>
 Shiva Jafarnia  <https://orcid.org/0000-0003-4884-6948>
 Sima Shahabi  <https://orcid.org/0000-0001-7666-3204>
 Sogol Saberi  <https://orcid.org/0000-0003-1816-8576>
 Hamidreza Hajizamani  <https://orcid.org/0000-0002-8468-132X>

References

- Lyons K. Direct placement restorative materials for use in posterior teeth: The current options. *NZ Dent J.* 2003;99(1):10–15. PMID:15330384.
- Sunbul HA, Silikas N, Watts DC. Resin-based composites show similar kinetic profiles for dimensional change and recovery with solvent storage. *Dent Mater.* 2015;31(10):e201–e217. doi:10.1016/j.dental.2015.06.003
- Leprince JG, Palin WM, Hadis MA, Devaux J, Leloup G. Progress in dimethacrylate-based dental composite technology and curing efficiency. *Dent Mater.* 2013;29(2):139–156. doi:10.1016/j.dental.2012.11.005
- Brunthaler A, König F, Lucas T, Sperr W, Schedle A. Longevity of direct resin composite restorations in posterior teeth. *Clin Oral Investig.* 2003;7(2):63–70. doi:10.1007/s00784-003-0206-7
- ALShaafi MM, Haenel T, Sullivan B, Labrie D, Alqahtani MQ, Price RB. Effect of a broad-spectrum LED curing light on the Knoop microhardness of four posterior resin based composites at 2, 4 and 6-mm depths. *J Dent.* 2016;45:14–18. doi:10.1016/j.jdent.2015.11.004
- Rodrigues SA, Scherrer SS, Ferracane JL, Bona AD. Microstructural characterization and fracture behavior of a microhybrid and a nano-fill composite. *Dent Mater.* 2008;24(9):1281–1288. doi:10.1016/j.dental.2008.02.006
- Zorzin J, Maier E, Harre S, et al. Bulk-fill resin composites: Polymerization properties and extended light curing. *Dent Mater.* 2015;31(3):293–301. doi:10.1016/j.dental.2014.12.010
- Leprince JG, Palin WM, Vanacker J, Sabbagh J, Devaux J, Leloup G. Physico-mechanical characteristics of commercially available bulk-fill composites. *J Dent.* 2014;42(8):993–1000. doi:10.1016/j.jdent.2014.05.009
- Ferracane JL. Current trends in dental composites. *Crit Rev Oral Biol Med.* 1995;6(4):302–318. doi:10.1177/10454411950060040301
- Czasch P, Ilie N. In vitro comparison of mechanical properties and degree of cure of bulk fill composites. *Clin Oral Invest.* 2013;17(1):227–235. doi:10.1007/s00784-012-0702-8
- Thomé T, Steagall Jr. W, Tachibana A, Braga SRM, Turbino ML. Influence of the distance of the curing light source and composite shade on hardness of two composites. *J Appl Oral Sci.* 2007;15(6):486–491. doi:10.1590/S1678-77572007000600006
- Fleming GJP, Awan M, Cooper PR, Sloan AJ. The potential of a resin-composite to be cured to a 4 mm depth. *Dent Mater.* 2008;24(4):522–529. doi:10.1016/j.dental.2007.05.016
- Kusgoz A, Ülker M, Yesilyurt C, Yoldas OH, Ozil M, Tanriver M. Silorane-based composite: Depth of cure, surface hardness, degree of conversion, and cervical microleakage in class II cavities. *J Esthet Restor Dent.* 2011;23(5):324–335. doi:10.1111/j.1708-8240.2011.00411.x
- Aguiar FHB, Georgetto MH, Soares GP, et al. Effect of different light-curing modes on degree of conversion, staining susceptibility and stain's retention using different beverages in a nanofilled composite resin. *J Esthet Restor Dent.* 2011;23(2):106–114. doi:10.1111/j.1708-8240.2011.00406.x
- Dalli'Magro E, Sinhoreti MAC, Correr AB, et al. Effect of different modes of light modulation on the bond strength and knoop hardness of a dental composite. *Braz Dent J.* 2008;19(4):334–340. doi:10.1590/S0103-64402008000400009
- Yap AUJ, Soh MS, Han TTS, Siow KS. Influence of curing lights and modes on cross-link density of dental composites. *Oper Dent.* 2004;29(4):410–415. PMID:15279480.
- Yap AUJ, Wong NY, Siow KS. Composite cure and shrinkage associated with high intensity curing light. *Oper Dent.* 2003;28(4):357–364. PMID:12877420.
- Tsujimoto A, Barkmeier WW, Takamizawa T, Latta MA, Miyazaki M. Depth of cure, flexural properties and volumetric shrinkage of low and high viscosity bulk-fill composites and resin composites. *Dent Mater J.* 2017;36(2):205–213. doi:10.4012/dmj.2016-131
- Garoushi S, Säilynoja E, Vallittu PK, Lassila L. Physical properties and depth of cure of a new short fiber reinforced composite. *Dent Mater.* 2013;29(8):835–841. doi:10.1016/j.dental.2013.04.016
- Cekic-Nagas I, Egilmez F, Ergun G. The effect of irradiation distance on microhardness of resin composites cured with different light curing units. *Eur J Dent.* 2010;4(4):440. PMID:20922164.
- Galvão MR, Caldas SGFR, Bagnato VS, de Souza Rastelli AN, de Andrade MF. Evaluation of degree of conversion and hardness of dental composites photo-activated with different light guide tips. *Eur J Dent.* 2013;7(1):86–93. PMID:23407620.
- Nie NH, Bent D, Hull C. *SPSS: Statistical Package for the Social Sciences.* 2nd ed. New York, USA: McGraw-Hill; 1975.
- Yap AUJ, Teoh SH. Comparison of flexural properties of composite restoratives using the ISO and mini-flexural tests. *J Oral Rehabil.* 2003;30(2):171–177. doi:10.1046/j.1365-2842.2003.01004.x
- Jafarnia S, Valanezhad A, Shahabi S, Abe S, Watanabe I. Physical and mechanical characteristics of short fiber-reinforced resin composite in comparison with bulk-fill composites. *J Oral Sci.* 2021;63(2):148–151. doi:10.2334/josnurd.20-0436
- Bouschlicher MR, Rueggeberg FA, Wilson BM. Correlation of bottom-to-top surface microhardness and conversion ratios for a variety of resin composite compositions. *Oper Dent.* 2004;29(6):698–704. PMID:15646227.
- Johnston WM, Leung RL, Fan PL. A mathematical model for post-irradiation hardening of photoactivated composite resins. *Dent Mater.* 1985;1(5):191–194. doi:10.1016/S0109-5641(85)80017-8
- Tarle Z, Attin T, Marovic D, Andermatt L, Ristic M, Tauböck TT. Influence of irradiation time on subsurface degree of conversion and microhardness of high-viscosity bulk-fill resin composites. *Clin Oral Invest.* 2015;19(4):831–840. doi:10.1007/s00784-014-1302-6
- Acquaviva PA, Cerutti F, Adami G, et al. Degree of conversion of three composite materials employed in the adhesive cementation of indirect restorations: A micro-Raman analysis. *J Dent.* 2009;37(8):610–615. doi:10.1016/j.jdent.2009.04.001
- Sgarbi SC, Pereira SK, Martins JMH, Oliveira MAC, Mazur RF. Degree of conversion of resin composites light activated by halogen light and led analyzed by ultraviolet spectrometry. *Arch Oral Res.* 2010;6(3):223–230. <https://puopr.emnuvens.com.br/oralresearch/article/view/23159/22251>. Accessed July 5, 2022.
- Le Bell AM, Tanner J, Lassila LVJ, Kangasniemi I, Vallittu PK. Depth of light-initiated polymerization of glass fiber-reinforced composite in a simulated root canal. *Int J Prosthodont.* 2003;16(4):403–408. PMID:12956496.
- Gonçalves F, Kawano Y, Braga RR. Contraction stress related to composite inorganic content. *Dent Mater.* 2010;26(7):704–709. doi:10.1016/j.dental.2010.03.015
- Sideridou I, Tserki V, Papanastasiou G. Effect of chemical structure on degree of conversion in light-cured dimethacrylate-based dental resins. *Biomaterials.* 2002;23(8):1819–1829. doi:10.1016/S0142-9612(01)00308-8

Kollidon® VA 64 and Soluplus® as modern polymeric carriers for amorphous solid dispersions

Kollidon® VA 64 i Soluplus® jako nowoczesne nośniki polimerowe dla amorficznych stałych rozproszeń

Dominik Strojewski^{A–D}, Anna Krupa^{A,E,F}

Department of Pharmaceutical Technology and Biopharmaceutics, Jagiellonian University Medical College, Kraków, Poland

A – research concept and design; B – collection and/or assembly of data; C – data analysis and interpretation;

D – writing the article; E – critical revision of the article; F – final approval of the article

Polymers in Medicine, ISSN 0370-0747 (print), ISSN 2451-2699 (online)

Polim Med. 2022;52(1):17–27

Address for correspondence

Anna Krupa
E-mail: a.krupa@uj.edu.pl

Funding sources

The study was funded by Sonata Bis grant No. DEC-2019/34/E/NZ7/00245 from the National Science Centre in Kraków, Poland.

Conflict of interest

None declared

Received on March 21, 2022

Reviewed on May 19, 2022

Accepted on May 20, 2022

Published online on June 29, 2022

Cite as

Strojewski D, Krupa A. Kollidon® VA 64 and Soluplus® as modern polymeric carriers for amorphous solid dispersions. *Polim Med.* 2022;52(1):17–27. doi:10.17219/pim/150267

DOI

10.17219/pim/150267

Copyright

Copyright by Author(s)

This is an article distributed under the terms of the Creative Commons Attribution 3.0 Unported (CC BY 3.0) (<https://creativecommons.org/licenses/by/3.0/>)

Abstract

As the number of new drug candidates that are poorly soluble in water grows, new technologies that enable the enhancement of their solubility are needed. This is the case with amorphous solid dispersions (ASDs) that, nowadays, not only ensure the solubility, but can also be used to control the release rate of poorly soluble drugs. However, this dosage form must overcome the major disadvantage of ASDs, which is limited stability upon storage. Thus, a thorough knowledge on polymeric carriers that can enhance drug solubility while ensuring stability in the amorphous form is necessary. In this review, the state of the art in the application of Kollidon® VA 64 (copovidone) and Soluplus® (graft copolymer of polyvinyl caprolactam-polyvinyl acetate and poly(ethylene glycol) (PEG)) in the manufacturing of ASDs over the last 20 years is presented. Apart from the classical methods, namely solvent evaporation or melting, more advanced technologies such as pulse combustion drying, high-speed electrospinning and single-step 3D printing are described. It has been shown that both the dissolution rate (in vitro) and enhancement in bioavailability (in vivo) regarding poorly soluble active ingredients of natural or synthetic origin are possible using these matrix-forming polymers.

Key words (in English): solid dispersions, spray drying, hot-melt extrusion, copovidone, Soluplus

Streszczenie

Wraz ze zwiększaniem się liczby nowych substancji leczniczych, które charakteryzują się ograniczoną rozpuszczalnością w wodzie, optymalizowane są nowe technologie, które umożliwiają poprawę ich rozpuszczalności. Jedną z metod jest opracowanie amorficznych stałych rozproszeń (amorphous solid dispersions (ASDs)), dzięki którym można obecnie uzyskać nie tylko poprawę rozpuszczalności, ale również kontrolę szybkości uwalniania trudno rozpuszczalnych substancji leczniczych z finalnych postaci leków. Taka strategia musi jednak równocześnie gwarantować stabilność ASDs podczas przechowywania. Konieczna jest zatem dogłębna znajomość właściwości nośników polimerowych stosowanych w procesie ich wytwarzania. W niniejszym artykule przedstawiono aktualny stan wiedzy w zakresie zastosowania dwóch nośników do sporządzania ASDs – analizowane były Kollidon® VA 64 (kopowidon) i Soluplus® (kopolimer glikolu polietylenowego, winylokaprolaktamu i octanu winylu). Oprócz klasycznych metod otrzymywania ASDs, takich jak odparowanie rozpuszczalnika lub stapianie, opisano bardziej zaawansowane technologie, np. suszenie z zastosowaniem spalania pulsacyjnego, elektroprzędzenie oraz jednoetapowy druk 3D. Wykazano, że dla trudno rozpuszczalnych substancji czynnych pochodzenia naturalnego lub syntetycznego zwiększenie szybkości rozpuszczania w warunkach in vitro i biodostępności w warunkach in vivo jest możliwe przy użyciu tych polimerów.

Słowa kluczowe: suszenie rozpyłowe, ekstruzja topliwa, stałe rozproszenia, kopowidon, Soluplus

Introduction

Nowadays, about 40% of drugs used in pharmacotherapy and 90% of new chemical entities (NCEs) being developed are poorly soluble in water.¹ If the drug does not dissolve in the gastrointestinal aqueous environment, its absorption after oral administration can be limited. Even though NCEs often show promising properties *in vitro* when organic solvents are used, they ultimately have no clinical application. To solve this problem, the production of amorphous solid dispersions (ASDs) was proposed and this approach has attracted growing attention over recent years.

Amorphous solid dispersions are defined as molecular mixtures of poorly water-soluble drugs with hydrophilic carriers.² The first report on using solid dispersions to improve bioavailability was provided in 1961 by Sekiguchi and Obi.³ Since then, they have been widely explored as a formulation strategy to improve the performance of drugs with unfavorable physicochemical properties and, consequently, limited solubility. As compared to other methods used to enhance solubility such as chemical modifications of the structure of the drug (e.g., salt or prodrug formation), performing clinical trials are not necessary. Furthermore, the modification of the chemical is not always possible, e.g., in neutral compounds that do not have easily reacting acidic or basic groups.^{4,5}

The preparation of solid dispersions enables the reduction of drug particle size, improves the wettability of hydrophobic particles, and transforms the ordered crystalline

drug structure into a disordered metastable amorphous form with better solubility. In addition to enhanced solubility and bioavailability, the advantage of solid dispersions is that they can control the release of a drug and sometimes mask the unpleasant taste of a drug.⁶ On the other hand, the drawbacks of ASDs include the risk of crystal growth, phase separation or recrystallization of amorphous drugs induced by inappropriate storage temperatures or insufficient package needed to prevent exposure to humidity.^{5,7,8} Thus, a proper selection of the matrix-forming ingredients and manufacturing technologies is necessary to develop stable ASDs with properties adjusted to patient's needs.

Taking into account the compositions that have been developed so far, they can be divided into 4 generations (Table 1).⁹ The 1st-generation ones are prepared by using low-molecular-weight crystalline carriers such as urea or sugars. As the system is fully crystalline, drug release can be slow, but these systems are usually stable. The 2nd-generation compositions are prepared using amorphous polymeric carriers, such as polyvinylpyrrolidone (PVP), poly(ethylene glycol) (PEG) and cellulose derivatives. If possible, a poorly soluble drug and a carrier should be mixed at the molecular level.⁵ The 3rd-generation solid dispersions are prepared with the use of surface active agents and self-emulsifiers. These allow for the chemical and physical stability of the final formulation and can enhance the drug dissolution profile. In addition, the presence of a surfactant may improve the miscibility of the drug and polymer, preventing phase separation. The plasticizing

Table 1. Generations of solid dispersions distinguished on the basis of their composition

Generation	Type of formulation	Type of carrier	Surfactants or self-emulsifying carriers	Advantages	Disadvantages
1 st	eutectic mixtures or molecular dispersions	low-molecular-weight crystalline, highly water-soluble: citric acid, galactose, mannitol, sorbitol, succinic acid, sucrose, trehalose, urea	N/A	stable	drug release can be slow
2 nd	molecular dispersions: amorphous solid solutions (1 phase), amorphous solid suspensions (2 phases), or mixed types	amorphous, mostly polymers: EC, HPC, HPMC, HPMCAS, HPMCP, PVP, crospovidone, PVPVA, PEG, poly(methacrylates), starch derivatives, e.g., cyclodextrines	N/A	– dissolution rate faster than from 1 st generation; – carrier dissolution governs drug release	– risk of drug precipitation and recrystallization; – high viscosity polymers may delay drug release
3 rd	surfactant-based solid dispersions	amorphous polymers: EC, HPC, HPMC, HPMCAS, HPMCP, PVP, PVPVA, PEG	Labrasol, Tweens, Gelucire 44/14, Compritol 888 ATO, poloxamers, SLS, Soluplus® alone or in mixture with polymers	– higher stability and bioavailability than 2 nd generation; – faster drug dissolution from matrices loaded with polymers with high T _g	– more than 2 excipients may be needed to form matrix; – may not be suitable for high-dose drugs
4 th	drug in molecular dispersion in matrices of controlled (sustained) release	water-soluble (swellable) polymers combined with water-insoluble polymers, e.g., EC, Eudragit RS, Eudragit RL, HPC, HPMC, Na-CMC, PEO	Soluplus®, carboxyvinyl polymer (Carbopol)	– sustained drug release; – suitable for drugs with short biological half-life; – reduced dosing frequency; – reduced risk of side effects; – better compliance	– matrix is complex; – may not be suitable for high-dose drugs

N/A – not applicable; EC – ethylcellulose; HPC – hydroxypropyl cellulose; HPMC – hypromellose; HPMCAS – hypromellose acetate succinate; HPMCP – hypromellose phthalate; Na-CMC – sodium carboxymethylcellulose; PEG – poly(ethylene glycol); PEO – poly(ethylene oxide); PVP – povidone; PVPVA – copovidone; SLS – sodium lauryl sulfate.

effect of surfactants may also give the opportunity to lower the temperature of co-processing, which might be helpful in avoiding the chemical degradation of compounds. Finally, the 4th-generation solid dispersions are known as controlled-release solid dispersions. The carriers used to form these generations can be either water-insoluble or water-soluble (Table 1).^{5,10} The combination of these 2 types of carriers ensures both controlled and extended release of the drugs, which is especially important for those with a short biological half-life.

The experience gathered over the last 6 decades of research on solid dispersions has clearly shown polymeric excipients to be the most successful carriers in the development of amorphous formulations. Most polymers used in pharmaceutical technology are amorphous by themselves. In solid dispersions, drugs can be either crystalline or amorphous. They can be dispersed or dissolved in the polymer matrix.⁹ Preferably, the amorphous drug should be dissolved in the polymer to form a solid solution. When the drug load is lower than its saturation solubility in the polymer, the system is the most stable. However, the solubility of drugs in polymers (in the solid state) is often limited. In such a case, if the drug load in the solid dispersion is higher than its solubility in the polymer, the drug may recrystallize or precipitate out of the polymer matrix. When the crystalline drug is dispersed in an amorphous polymer, Ostwald ripening can occur, resulting in the formation of big crystals with a slower dissolution rate.¹

From a technological point of view, the preparation of a molecular dispersion of a drug and polymer can be challenging since de-mixing or phase separation related to recrystallization of the amorphous drug or formation of amorphous drug clusters can occur. Therefore, polymers of either natural or synthetic origin are co-processed with drugs using various technologies.¹ To increase the stability of the amorphous form, the glass transition temperature (T_g) of the polymer should be higher than that of the drug.¹¹ There should also be an opportunity for specific interactions between the drug and polymer, e.g., hydrogen bonding.¹²

The first polymer used to prepare ASDs was PVP, which was applied to improve the solubility of sulfathiazole.¹³ This research dates back to 1969. Since then, numerous research groups have studied the suitability of PVP for the manufacturing of ASDs with many different drugs.^{14–16} However, the highly hygroscopic character and low T_g of PVP limits its practical use in many formulations. Thus, new copolymers or graft polymers with vinyl and pyrrolidone structures and more favorable properties than PVP were developed, e.g., copovidone. Apart from them, other polymers such as cellulose and polymethacrylate derivatives are also used to form ASDs (Table 1).^{17–19}

In general, ASDs can be produced by 1) melting methods, e.g., hot-melt extrusion (HME), spray congealing and melt granulation; 2) solvent evaporation methods, e.g., solvent casting, spray drying and freeze drying; and 3) others,

e.g., mechanical activation during milling or supercritical methods.^{20–22} The selection of the manufacturing method determines the solid state characteristics of ASDs, particle morphology, powder density, flow properties, moisture content, stability, and finally in vitro and in vivo performance of the drug. The technology used for processing may also govern the molecular mobility of the drug. Moreover, depending on the type of processing, different critical parameters are responsible for effective drug amorphization. In the case of spray drying, it is the rate of solvent evaporation, whereas the rate of freezing is crucial in freeze drying. The processing type may also affect the morphology of the solid particles, and hence, the dissolution rate and the stability of the ASDs. The particle shape of ASDs prepared by spray drying is usually spherical. On the other hand, the particles of freeze-dried ASDs are more irregular and typically in the shape of flakes. Therefore, the kinetics of water vapor sorption during storage and drug release from ASDs of the same composition prepared using 2 different methods may differ.²³

Among the techniques mentioned above, HME and spray drying are typically used on the industrial scale.²⁴ In contrast to spray drying, HME is a solvent-free method. However, high temperatures used for such processing may not be suitable for thermolabile drugs and drugs with high melting points, which is often the case for insoluble compounds. Moreover, a higher amount of material is necessary for HME than for spray drying, which may be problematic especially in the early phases of drug development. Grinding of homogeneous amorphous hot-melt extrudates is often necessary to obtain immediate drug release. However, such an approach may create an unstable heterogeneous formulation. Regarding, spray-dried ASDs, the presence of residual solvents may be problematic for stability and safety reasons. Additionally, low powder density, poor flowability and low yield are the most important drawbacks of spray-dried formulations.²³

The application of new techniques such as electrospraying, pulse combustion spray drying and additive manufacturing (AM) methods has been proposed for preparing ASDs.²³ Electrospraying enables the reduction of the particle size to nanometers and increases the specific surface area of ASDs, providing favorable dissolution properties to the final formulation. In turn, pulse combustion spray drying is used when improving the drying rate is necessary; however, the required equipment is not widely available and the process is noisy.^{23,25}

Limitless opportunities in designing three-dimensional (3D) objects and formulations for therapeutic applications are available regarding AM. In such process, the material is added layer upon layer to rapidly form end-use products of precisely defined geometric measurements using 3D model data.²⁶ This approach is compatible with the personalized drug manufacturing concept and allows one to adjust not only the drug dose and release rate, but also other characteristics crucial to ensure compliance (e.g.,

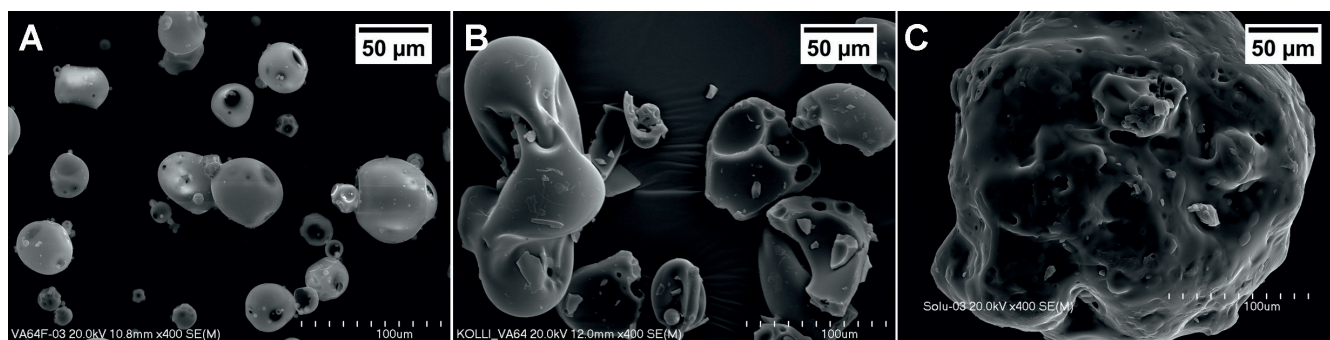


Fig. 1. Scanning electron micrographs of Kollidon® VA 64 Fine (A), Kollidon® VA 64 (B) and Soluplus® (C) taken using the Hitachi S-4700 scanning electron microscope (Hitachi Ltd., Tokyo, Japan)

short disintegration time).^{27,28} According to the ISO/ASTM 52900 standard,²⁶ 7 categories of AM technologies have been developed taking into account the processing methodology: binder jetting, directed energy deposition, material extrusion, material jetting, powder bed fusion, sheet lamination, and vat photopolymerization. Among them, fused deposition modeling (FDM), which is based on material extrusion, is the most widely used.²⁹ Before FDM, drug-loaded filaments (hot-melt extrudates) of high mechanical resistance need to be prepared. It could be a challenging step for thermolabile materials; therefore, 3D-printer modifications have been proposed in order to simplify ASD manufacturing of a final solid dosage form, e.g., 3D printed tablets (printlets).^{29,30} Ideally, it should be possible to feed raw powdered materials (i.e., drug and matrix-forming polymers) directly into a 3D printer to co-process them using the same apparatus in a single-step process without any preliminary treatment of the powder bed or additional operations on the 3D-printed dosage form.

In order to facilitate the manufacturing of ASDs, an ideal polymeric carrier should have low hygroscopic properties and low miscibility with drugs and with other polymers. It should also have a T_g at least 40°C higher than storage conditions and proper viscoelasticity for extrusion.⁴ It should be freely soluble in water and low-toxic organic solvents. Such characteristics are typical of copovidone (Kollidon® VA 64) and polyvinyl caprolactam-polyvinyl acetate-PEG graft copolymer (Soluplus®), which were selected for discussion in this review.³¹

Kollidon® VA 64 (copovidone) as a vinylpyrrolidone copolymer for ASDs

Kollidon® VA 64 is referred to by the pharmacopoeial names copovidone, copovidonum (The European Pharmacopoeia (Ph. Eur.), The United States Pharmacopoeia-National Formulary (USP-NF)), or copolyvidone (The Japanese Pharmacopoeia (JP)). It is a copolymer composed of a chain structure of 2 monomers, namely

N-vinylpyrrolidone (NVP) and vinyl acetate (VAc).³² These monomers are combined in a molar ratio of approx. 6:4 using radical polymerization. Thus, the number 64 in the trade name corresponds to the molar ratio between these monomers.

Spray-dried copovidone is a slightly yellow or white powder available in 2 commercial grades, i.e., Kollidon® VA 64 and Kollidon® VA 64 Fine (Table 2). As can be seen in Fig. 1, they differ significantly in particle size and morphology. Standard grade particle sizes range between 50 µm and 250 µm and are irregular in shape. In contrast to the standard grade, the “Fine” grade has more than 80% of particles measuring less than 50 µm, and the majority of them are spherical. As a result, their applications are different (Table 2).

Copovidone is soluble in water and alcohol but less soluble in ether and aliphatic and alicyclic hydrocarbons. Due to its high solubility in various solvents and the ability to form highly concentrated aqueous solutions with low viscosity (e.g., a solution of 20% has a viscosity of only 20 mPas at 25°C), it is a suitable carrier for manufacturing of ASDs using solvent evaporation methods. Moreover, pH values do not have an impact on the viscosity of copovidone solutions. Importantly, the T_g of copovidone is high (101°C), which helps to ensure the stability of the amorphous systems during storage. This copolymer also possesses favorable thermorheological properties and high thermal stability, with a degradation temperature of 230°C. Since polymers are usually extruded at temperatures 30–50°C above their T_g , copovidone can also be used for manufacturing ASDs using this technology. Even though copovidone, due to the lack of an amphiphilic structure, is not a typical solubilizer, multiple studies have confirmed its ability to enhance the solubility of poorly soluble drugs. All of these properties, along with the ability to form solid dispersions using methods feasible on an industrial scale, have resulted in its use in numerous drug products launched onto the market over the last 2 decades (Table 3). Moreover, multiple studies carried out on a laboratory scale have shown a high potential of this polymer for the development of stable ASDs with active pharmaceutical ingredients (APIs) of synthetic and natural origin.

Table 2. Physicochemical properties of Kollidon® VA 64 Fine, Kollidon® VA 64 and Soluplus®

Trade name/Grades	Kollidon® VA 64 Fine	Kollidon® VA 64	Soluplus®
Polymer name	copovidone		polyvinyl caprolactam-polyvinyl acetate-polyethylene glycol graft copolymer
Monomers ratio	6 parts of N-vinylpyrrolidone 4 parts of vinyl acetate		13% PEG 6000 57% vinyl caprolactam 30% vinyl acetate
Mw [g/mol]	15,000–20,000		90,000–140,000
Particle size [µm]	10–20	50–65	340
Glass transition temperature [°C]	approx. 102		approx. 70
Solubility	Less than 1%: – diethyl ether, – pentane, – cyclohexane, – liquid paraffin. More than 20%: – water, – methanol, – ethanol, – n-propanol/2-propanol, – n-butanol, – chloroform, – methylene chloride, – PEG 400, – propylene glycol, – 1,4-butanediol, – glycerol		– water – acetone up to 50% – methanol up to 45% – ethanol up to 25% – dimethylformamide up to 50%
HLB	N/A		14
Stability	prone to oxidation in the solid state and in solutions		hygroscopic
	less stable	very stable	stable
Main applications in pharmaceutical technology	dry binder	– dry binder – binder in wet granulation – film former for coating, subcoating and topical sprays	– polymeric solubilizer – matrix-forming excipient for solid solutions suitable for hot-melt extrusion and spray drying

HLB – hydrophilic-lipophilic balance; N/A – not applicable; PEG – poly(ethylene glycol); MW – molecular weight.

Table 3. Examples of drug products containing amorphous solid dispersions (ASDs) with copovidone matrix

Drug name	Drug dose [mg]	Drug product trade name	Dosage form	Indications	ASD manufacturing technology	Year of EMA approval
Ritonavir	100	Norvir®	film-coated tablets	HIV-1 therapy (>2 years old)	HME	1996
Lopinavir/Ritonavir	100/25	Kaletra®	film-coated tablets	HIV-1 therapy (>14 days old)	HME	2001
Olaparib	100; 150	Lynparza®	film-coated tablets	ovarian, breast and prostate cancer, pancreatic adenocarcinoma	HME	2014
Ledipasvir/Sofosbuvir	90/400; 45/200	Harvoni®	film-coated tablets	chronic hepatitis C (>3 years old)	SDD	2014
Sofosbuvir/Velpatasvir	400/100; 200/50	Epclusa®	film-coated tablets	chronic hepatitis C (>3 years old)	SDD	2016
Elbasvir/Grazoprevir	50/100	Zepatier®	film-coated tablets	chronic hepatitis C therapy (>12 years old)	SDD	2016
Encorafenib	50; 75	Braftovi®	hard gelatin capsules	unresectable or metastatic melanoma with the BRAF V600 mutation, metastatic colorectal cancer with BRAF V600E mutation	HME	2018

SDD – spray drying; HME – hot-melt extrusion; EMA – European Medicines Agency; HIV – human immunodeficiency virus.

Mehatha et al. prepared ASDs of ezetimibe by HME using Kollidon® VA 64 as a carrier. Ezetimibe is a practically insoluble lipid-lowering compound with a melting

point (T_m) of 163°C.³³ It was co-processed with copovidone in 3 proportions – 1:2, 1:3 and 1:4. Before the extrusion, the drug and the carrier were mixed together

in a double-cone blender. These mixtures were hot-melt-extruded in a temperature gradient distributed across 4 heating zones: 110–125–135–150°C ±10°C. The screw rotational speed was set at 100 rpm. Using diffractograms, it was confirmed that ASDs of ezetimibe in copovidone were formed regardless of the ezetimibe-to-copovidone ratio. However, the polymer load determined the concentration of ezetimibe released. The higher the polymer load, the higher amount of drug released. After 90 min, the increase in the drug release rate was roughly 4 times higher than that of the crude drug.

Sarode et al. investigated the opportunity to increase the stability of indomethacin ASDs ($T_m = 160^\circ\text{C}$) using copovidone or Eudragit EPO.²¹ In parallel, ASDs of itraconazole ($T_m = 170^\circ\text{C}$) loaded with Kollidon® VA 64 or hypromellose acetate succinate (Aquot-LF) were prepared. Both drugs were hot-melt-extruded with these polymers. First, they were mixed with the polymer in a 30:70 weight ratio. Next, HME was performed using a twin screw hot-melt extruder with 4 heating zones. Depending on the drug, the extrusion temperature and rotation speed were set at 140°C and 100 rpm for indomethacin and 150°C and 150 rpm for itraconazole. The feeding rate was set at 15 g/min. The extruded samples were placed in stability chambers for 1–12 weeks at temperatures ranging from 5°C to 50°C and relative humidity (RH) levels of 33%, 75% or 96%. In these storage conditions, copovidone was found to effectively protect amorphous indomethacin from recrystallization. After 12 weeks of storage at 50°C and 96% RH, the indomethacin release profile remained unchanged. Regarding itraconazole, the stabilizing effect of copovidone was much less pronounced. The release profile showed that phase separation, recrystallization and chemical drug degradation had occurred.

The impact of hydrophilic polymers such as poloxamer, PVP and copovidone on the solubility of sildenafil citrate in ASDs was investigated by Aldawsari et al.³⁴ The ASDs were prepared in a drug-to-polymer ratio of 1:1 using the solvent evaporation method. Sildenafil citrate and polymer were dissolved in 60 mL of a water-ethanol mixture (1:1). The solvents were evaporated at 60°C using a rotary evaporator. The produced ASDs contained sildenafil citrate in an amorphous form. Drug release tests showed a significant increase in the drug release rate from this ASDs (100%) compared to sildenafil citrate alone (29%). Furthermore, the authors demonstrated that after the administration of sildenafil ASDs loaded with copovidone, the pharmacodynamic effect was stronger than that observed for the crude drug.

Kollidon® VA 64 was also used in the spray drying process to prepare ASDs with tadalafil.³⁵ The drug was co-processed with the polymer in 9 proportions, in which the polymer load ranged from 10% to 90%. An acetone-water mixture (9:1) was used as a solvent. The results of powder X-ray diffraction (XRD), differential scanning calorimetry (DSC) and hot-stage polarized light

microscopy revealed that the ASDs successfully formed. By annealing the binary solid dispersion (1:1) above its T_g , the thermodynamic solubility of tadalafil in copovidone was established and it was equal to 20.5% at 25°C. Based on accelerated stability studies (40°C; RH = 75%), ASDs with high loads of hygroscopic copovidone were shown to be prone to recrystallization due to the plasticizing effect of adsorbed water molecules. However, after storage at 80°C and RH = 0% for 2 months, ASDs loaded with 80% or 90% copovidone were the most stable and there was no recrystallization of amorphous tadalafil.

Xu et al. proposed the manufacturing of ASDs composed of ibuprofen and copovidone in a 1:5 weight ratio using an innovative technique of solvent evaporation known as pulse combustion drying.²⁵ In this method, high-pressure shock waves of hot gas are created through cyclic explosions of a gaseous fuel (e.g., propane) mixed with combustion air in a combustion chamber located above the drying chamber. These high-speed waves of exhaust gases are used to atomize and then quickly evaporate solvents from tiny droplets of liquid samples fed into the drying chamber. Similarly to spray drying, solid particles are separated using a cyclone and collected in bag filters. The advantage of this method is a high rate of heat transfer due to the high compression and contraction forces induced by considerable fluctuations in pressure (±10 kPa) and velocity (±100 m/s) of the gases inside the combustion chamber.³⁶ By developing conditions of extreme turbulence inside the drying chamber and increasing the heat transfer, the drop drying time can be shortened below 1 s. As a result, it is possible to obtain high drying yields even at relatively low temperatures (<80°C). Interestingly, pulse combustion drying can be used to dry liquids of relatively high viscosity, that is, up to 16 Pas or up to 300 mPas for suspensions or solutions, respectively. Therefore, this process can be an interesting alternative to spray drying during ASDs development.

A Hypulcon system was used to dehydrate ibuprofen suspensions in an aqueous solution of copovidone.²⁵ The suspension was fed into the drying chamber at a rate of 8 mL/min. Drying was carried out at 65°C. The flow rate of propane and combustion air was 30–35 L/h and 900–1000 L/h, respectively. This co-processing enabled to transform crystalline ibuprofen into its amorphous form. Drug release studies showed a significant increase in ibuprofen release rates from ASDs compared to the physical mixture (PM). After 5 min, the concentration of ibuprofen released was more than 11 times higher than that recorded for the PM. For reasons of comparison, ASDs were also prepared using conventional spray drying. It was found that the spray-dried particles were much bigger, and consequently, dissolved slower than those produced by means of the Hypulcon system. From a technological point of view, the undoubted advantage of this technology is the opportunity to prepare ASDs with poorly soluble drugs without the need for organic solvents. In addition,

pulse combustion drying is an environment-friendly technology because of the low emissions of exhaust gases. However, the limited access to this kind of dryer restricts the widespread use of this technology.

Looking for a technology aimed at producing ASDs on a larger scale, Nagy et al. proposed the application of high-speed electrospinning.³⁷ Itraconazole and copovidone (6:4) were dissolved in a mixture of dichloromethane and ethanol (2:1). High-speed electrospinning was then carried out at room temperature using a voltage of 50 kV. The flow rate was 1500 mL/h and the spinneret rotational speed was set at 40,000 rpm. As a result, the obtained ASDs released more than 90% of the itraconazole within 10 min, whereas only 10% of the crude drug dissolved after 120 min. The authors showed that this technology allowed ASDs to be produced with yields as high as 450 g/h. In other solvent evaporation methods based on electrospinning, such as single-needle electrospinning, the amount of ASDs formed is much smaller, i.e., up to 6 g/h.

Recent studies by Dong et al. provided evidence that by combining hydrophilic polymers with pH modifiers, it is possible to increase the bioavailability of ionizable drugs by preparing ternary solid dispersions.³⁸ The solid dispersion of glycyrrhetic acid ($T_m = 296^\circ\text{C}$) was loaded with copovidone and alkalizing agents, namely magnesium hydroxide, sodium carbonate, meglumine, or L-arginine. The loading of glycyrrhetic acid ranged from 6.25% to 40%, whereas up to 30% of the alkalizing agent and 50–93.75% of the polymer were applied. All of these excipients were vacuum-dried, sieved and dry-blended to form physical mixtures. Next, they were hot-melt-extruded at 160°C . A significant increase in the amount of glycyrrhetic acid released was observed, which was clearly related to the amorphization of the drug in the presence of copovidone and an alkalizing agent. The most favorable results were seen when meglumine or L-arginine was used. The analysis of spectra recorded using Fourier-transform infrared (FT-IR), Raman and X-ray photoelectron (XPS) spectroscopies confirmed that ion-pair complexes were formed between glycyrrhetic acid and the alkalizing agents. Since the bonding energy is lower than that of intermolecular hydrogen bonds between the drug molecules, the solubility and release rate of glycyrrhetic acid increased. Furthermore, intermolecular H bonds formed between the alkalizers and Kollidon® VA 64, and this process was responsible for the enhanced wettability of the hydrophobic drug particles.

Kollidon® VA 64 can also be successfully combined with surfactants to improve the solubility of poorly soluble drugs.^{39,40} Vasoya et al. developed ternary solid dispersions using 5–20% carvedilol ($T_m = 116^\circ\text{C}$) loaded with 60–95% of copovidone and up to 20% of the surfactant polyoxyl glyceryl-32 stearate (Acconon C-50; Abitec, Columbus, USA).³⁹ This solid surfactant has a hydrophilic-lipophilic balance (HLB) value of 13 and a T_m of 50°C . The HME was carried out at 160°C in order to obtain homogeneous

extrudates. The DSC results showed that up to 20% of the carvedilol was miscible on a molecular level with copovidone and surfactant if the surfactant load was 20%. The surfactant tended to recrystallize out of the solid dispersion, yet this did not have a negative impact on either the miscibility of carvedilol with copovidone or its release from the solid dispersion. Finally, the most favorable properties were shown in ASDs containing the highest amount of surfactant, which improved the wettability of the particles and prevented the formation of drug-rich layers on the surface of the dissolved particles.

Ternary ASDs were also developed to enhance the solubility of active ingredients of natural origin, such as those found in plant extracts. Wang et al. investigated increasing the solubility and bioavailability of standardized Ginkgo biloba leaf extract by creating ASDs in Kollidon® VA 64 and Kolliphor RH 40 (85:15).⁴⁰ First, the polymers were spray-dried together, followed by the addition of 25% of the extract. This mixture was hot-melt-extruded using a temperature gradient ranging from 120°C to 125.7°C in 8 heating zones. After being cooled, the extrudates were milled to be analyzed in a powder form. The X-ray diffraction patterns of the hot-melt-extruded formulations showed a halo typical of that of the amorphous samples. In vitro studies confirmed that the release rate of the Ginkgo biloba leaf extract from ASDs was almost 2-fold higher compared to the PM and 2.7-fold higher than that of the crude Ginkgo biloba leaf extract. Furthermore, after oral administration of this solid dispersion to rats, a significant increase in plasma concentrations of the active ingredients in this extract was shown.

Soluplus®: A graft copolymer of amphiphilic properties for ASD manufacturing

In contrast to copovidone, Soluplus® is a graft copolymer composed of polyvinyl caprolactam, polyvinyl acetate and PEG 6000. These structures are combined in a 57:30:13 ratio (Table 2). The molecular weight of Soluplus® ranges from 90,000 g/mol to 140,000 g/mol, with an average molecular weight of 118,000 g/mol. Soluplus® is available in white to slightly yellow spherical granules (Fig. 1C). Their average particle size (340 μm) is much larger than that of standard grade Kollidon® VA 64 (50–65 μm). The T_g of Soluplus® is 70°C , which is 30°C lower than that of copovidone. However, similar to copovidone, Soluplus® has a high thermal stability and can be heated to 220°C without any sign of degradation.⁴¹

Soluplus® is freely soluble in water, acetone, methanol, ethanol, dimethylformamide, and in binary mixtures of methanol and acetone or ethanol and acetone. When placed in water, the granules swell and then slowly dissolve. Because of the presence of a hydrophilic PEG fragment

as well as a lipophilic vinylcaprolactam and VAc moiety within its structure, Soluplus® displays amphiphilic properties.⁴² According to data provided by Baden Aniline and Soda Factory (BASF), Soluplus® forms micelles of 70–100 nm in diameter when dispersed in a buffer with a pH of 7. The critical micelle concentration of this polymeric solubilizer is 7.6 mg/L. Because of the presence of colloidal micelles, Soluplus® forms a cloudy solution at high concentrations. The viscosity of a 20% aqueous solution of this polymer is 10 Pas at 20°C.⁴³

In addition to its solubilizing properties, Soluplus® can also be used to enhance the intestinal absorption of poorly soluble drugs. The research on solid solutions of danazol, fenofibrate and itraconazole showed that Soluplus® was able to effectively increase drug flux across Caco-2 cell monolayers.⁴² In addition, these findings correlated well with the values of pharmacokinetic parameters (maximum plasma concentration (C_{max}), area under the curve (AUC)).

Although there is no drug product containing the solid solutions of poorly soluble drugs in Soluplus® on the market, there has been a growing interest in the development of ASDs on a smaller scale. Initially, Soluplus® was developed as a carrier for the production of solid solutions using the HME or spray drying process.^{44,45} However, in recent years, the functionality of this excipient in forming ASDs with the use of technological processes, such as high-energy ball milling or single-step 3D printing, has been described.

Liu et al. described the preparation of ASDs containing aprepitant and Soluplus® using the solvent evaporation method.⁴⁶ The weight ratios of drug to Soluplus® were 1:3, 1:4, 1:5, and 1:6. These mixtures were dissolved in acetone, which was then removed by evaporation. The drug release rate of aprepitant increased with increasing Soluplus® load. After 180 min, approx. 93% of the aprepitant was released from the ASDs (1:5) at a pH of 6.6, which was much more than the amount of drug released from the PM (34%) or crude drug (23%). In vivo studies carried out in a rat model revealed that the pharmacokinetic profile recorded after oral administration of ASDs (1:5) was similar to the commercial drug product Emend®, in which the bioavailability of aprepitant was successfully enhanced using proprietary NanoCrystal® technology. The results of stability testing performed at 40°C and 60% RH confirmed that there was no recrystallization of the amorphous aprepitant for 3 months.

Some poorly soluble drugs, e.g., tadalafil, show limited solubility not only in water (<5 µg/mL) but also in organic solvents (<1%), listed in classes 2 and 3 by the International Conference on Harmonization (ICH).⁴⁷ Thus, the application of the solvent evaporation method to prepare ASDs is difficult and may result in low drug loadings. As a consequence, the attempts to mechanically activate the crystalline particles of the drug using high-energy ball milling were undertaken. The unquestionable advantage of the milling process is the lack of a need for organic solvents. Due

to the high hydrophobicity of tadalafil, the drug was combined with amphiphilic Soluplus® to form ASDs using high-energy ball milling.^{47,48} The diffraction patterns and thermograms confirmed the amorphization of tadalafil and the creation of molecular alloys in Soluplus® by tadalafil. In drug-release studies, the amount of tadalafil dissolved from ASDs increased with increasing Soluplus® load. Thus, the best properties were seen in the tadalafil ASDs loaded with 90% of Soluplus®. These results correlated well with the results recorded in vivo. Pharmacokinetic studies on bioavailability demonstrated the beneficial effect of tadalafil amorphization using the high-energy ball milling process. In a rat model, the relative bioavailability of tadalafil was 128% for amorphous tadalafil and 289% for ASDs in Soluplus®. The rapid absorption of tadalafil was accompanied by a slower elimination process. The concentration of tadalafil in the rat plasma was quantifiable even after 24 h in a single oral dose.

Since the dissolution rate of the matrices prepared using Soluplus® can be slowed by a viscous hydrogel layer that is formed on the surface of its particles, the drug release rate from hot-melt extrudates or tablets formed based on ASDs loaded with Soluplus® may be significantly reduced.^{43,49} Therefore, grinding, freeze drying, or the incorporation of additional surfactants or inorganic salts into the matrix of hot-melt-extruded solid solutions can help overcome this drawback and, in the end, improve the drug release rate more effectively.

Amorphous solid dispersions were designed for valsartan ($T_m = 97°C–107°C$) when 70% of Soluplus® was combined with 10% of D- α -tocopherol PEG 1000 succinate (TPGS).⁵⁰ The drug load was 30%. The PM was hot-melt-extruded at the following gradient of temperatures distributed across 6 heating zones (80–80–90–90–100–100°C) using a twin-screw extruder. After 30 min, approx. 60% of the crude valsartan was dissolved in a phosphate buffer with a pH of 6.8. When the ASDs were examined, drug release was completed in 15 min. The analysis of the plasma concentration-time profiles recorded for these ASDs showed a significant increase in AUC. It was revealed that the AUC value calculated for TPGS-loaded ASDs was almost 2 times higher than that of typical solid dispersions that do not contain this surfactant, and more than 5-fold higher than the crude drug.

Soluplus® combined with a second surfactant poloxamer (Lutrol F® 68) enabled the production of 3D-printed tablets (printlets) with high mechanical resistance and controlled release of dutasteride ($T_m = 242°C–250°C$) in a single-step 3D printing process.³⁰ The hot-melt pneumatic dispenser was used to directly eject the melted powder into the printing nozzle using compressed air. Thus, the preparation of filaments before 3D printing was not necessary. The extrusion temperature was set at 160°C. Each tablet contained the same volume ratio of dutasteride, Lutrol F® 68 and Soluplus®, which was 1:10:89, respectively. The dimensions of these printlets were 5 × 2 mm.

The travel speed was 40 mm/s and the extrusion speed was 20 mm/s. The process was carried out under a pressure of 500 kPa. The temperature of the printing bed was 40°C. The diffractograms showed that after such co-processing, the crystalline dutasteride was amorphized and dispersed in the polymer bed at the molecular level. The drug release curves recorded at a pH of 6.8 with 1% of sodium lauryl sulfate (SLS) showed a significant increase in the percentage of dutasteride released from the printlets compared to tablets prepared by direct compression using the same PM in a laboratory single-punch tablet press. The authors also showed the suitability of copovidone, hydroxypropylcellulose (HPC) and Eudragit EPO in the formulation of tablets using single-step 3D printing. However, the proper selection of the matrix-forming polymer was crucial to control dutasteride release. When copovidone was used, immediate drug release was observed, but when HPC or Eudragit EPO was used, dutasteride was released in a controlled-release way. The performance of 3D-printed tablets made of copovidone or HPC prevailed over that of directly compressed tablets in the gastric environment. Different properties were found in tablets prepared using Eudragit EPO as a matrix-forming polymer. Their release profiles were similar regardless of technology.

Interestingly, the application of Soluplus® enabled the preparation of porous ASDs with carvedilol by freeze drying, which served as a semi-product in the final production of orodispersible tablets (ODT).⁵¹ These solid dispersions (1:10) were compacted with 3 directly compressed excipient systems, namely Pearlitol® Flash (Roquette, Les-trem, France), Pharmaburst® (SPI Polyols, Inc., Newcastle, USA), or Ludiflash® (BASF, Ludwigshafen, Germany). The 200-mg tablets measuring 10 mm in diameter were loaded with 6.25 mg of carvedilol in the form of the solid dispersion. The compression force was adjusted to form tablets with a hardness equal to 4 ± 0.5 kg. The immediate release of carvedilol was shown in tablets made of Pharmaburst® or Pearlitol® Flash. Their disintegration time was shorter than 1 min. In contrast, the disintegration time of tablets prepared with Ludiflash® was longer than 3 min, which could explain their sustained carvedilol release.

Several attempts have been made to create ASDs loaded with poorly soluble active ingredients of plant origin using Soluplus® as a carrier.^{52,53} Chowdhury et al. described the properties of complex ASDs loaded with 2 active ingredients that acted synergistically.⁵³ In this study, citrate of tamoxifen ($T_m = 144^\circ\text{C}$) and resveratrol ($T_m = 266^\circ\text{C}$) were combined in a 1:5 weight ratio. In addition to Soluplus®, 2 plasticizers, Cremophor RH 40 and Poloxamer 188, were applied to form the matrix. The proportion of drug, polymer and plasticizer was 1:9:1. A solid dispersion in the form of a thin film was prepared using a twin-screw hot-melt extruder. Despite using plasticizers, the extrusion was performed at a very high temperature (250°C). The rotational screw speed was set at 50 rpm and

the co-extrusion time was 3–5 min. After co-processing, the films were cooled and pulverized. After 24 h of dissolution studies, the percentage of tamoxifen released increased from 30% to 91% and from 9% to 37% in the gastric and intestinal environment, respectively. In terms of the amount of resveratrol released, even better results were obtained, especially in the intestinal environment. The percentage of resveratrol released increased from 7% to 60% and from 11% to 95% at a pH of 1.2 and 6.8, respectively.



Importantly, in vivo studies showed that the oral bioavailability of tamoxifen from this solid dispersion was significantly higher than that of the aqueous suspension of the drug. Furthermore, based on in vitro cytotoxicity studies performed using the human breast cancer cell line (MCF7), the synergy between tamoxifen and resveratrol was observed. All in all, this research study revealed that tamoxifen citrate co-processed with resveratrol in a solid dispersion system may considerably enhance the sensitivity of cancer cells to these active ingredients. This effect was most pronounced as the concentration of resveratrol was increased resulting in greater than a 3-fold decrease in the value of IC₅₀ compared to tamoxifen alone.

Conclusions

Both Soluplus® and Kollidon® VA 64 can be used in solvent- and melt-based methods to successfully produce ASDs. These polymers used as matrix-forming excipients are able to stabilize the amorphous drug and prevent recrystallization during storage. Their solubilizing effects translated into enhanced solubility and dissolution rates of poorly soluble drugs in vitro, which may result in a much higher bioavailability after oral administration in vivo. Such ASDs can be placed in hard gelatin capsules or can be compacted to form tablets of either immediate or controlled drug release. Importantly, they can be used to produce modern dosage forms, such as 3D-printed tablets or ODT.

To sum up, the choice between these polymers depends on drug properties, available equipment and preferable characteristics of the final dosage form.

ORCID iDs

Dominik Strojewski  <https://orcid.org/0000-0003-3283-8521>
Anna Krupa  <https://orcid.org/0000-0002-0603-512X>

References

1. Vasconcelos T, Sarmiento B, Costa P. Solid dispersions as strategy to improve oral bioavailability of poor water soluble drugs. *Drug Discov Today*. 2007;12(23–24):1068–1075. doi:10.1016/j.drudis.2007.09.005
2. Chiou WL, Riegelman S. Pharmaceutical applications of solid dispersion systems. *J Pharm Sci*. 1971;60(9):1281–1302. doi:10.1002/jps.2600600902
3. Sekiguchi K, Obi N. Studies on absorption of eutectic mixture. I. A comparison of the behavior of eutectic mixture of sulfathiazole and that of ordinary sulfathiazole in man. *Chem Pharm Bull*. 1961;9(11):866–872. doi:10.1248/cpb.9.866

4. Williams HD, Trevaskis NL, Charman SA, et al. Strategies to address low drug solubility in discovery and development. *Pharmacol Rev.* 2013;65(1):315–499. doi:10.1124/pr.112.005660
5. Bindhani S, Mohapatra S. Recent approaches of solid dispersion: A new concept toward oral bioavailability. *Asian J Pharm Clin Res.* 2018; 11(2):72. doi:10.22159/ajpcr.2018.v11i2.23161
6. Leuner C, Dressman J. Improving drug solubility for oral delivery using solid dispersions. *Eur J Pharm Biopharm.* 2000;50(1):47–60. doi:10.1016/S0939-6411(00)00076-X
7. Baird JA, Taylor LS. Evaluation of amorphous solid dispersion properties using thermal analysis techniques. *Adv Drug Deliv Rev.* 2012; 64(5):396–421. doi:10.1016/j.addr.2011.07.009
8. Van den Mooter G. The use of amorphous solid dispersions: A formulation strategy to overcome poor solubility and dissolution rate. *Drug Discov Today Technol.* 2012;9(2):e79–e174. doi:10.1016/j.ddtec.2011.10.002
9. Tekade AR, Yadav JN. A review on solid dispersion and carriers used therein for solubility enhancement of poorly water soluble drugs. *Adv Pharm Bull.* 2020;10(3):359–369. doi:10.34172/apb.2020.044
10. Vo CLN, Park C, Lee BJ. Current trends and future perspectives of solid dispersions containing poorly water-soluble drugs. *Eur J Pharm Biopharm.* 2013;85(3 Pt B):799–813. doi:10.1016/j.ejpb.2013.09.007
11. Descamps M, ed. *Disordered Pharmaceutical Materials.* Weinheim, Germany: Wiley-VCH Verlag GmbH & Co. KGaA; 2016. ISBN:978-3-527-33125-3.
12. Grzybowska K, Chmiel K, Knapik-Kowalczyk J, Grzybowski A, Jurkiewicz K, Paluch M. Molecular factors governing the liquid and glassy states recrystallization of celecoxib in binary mixtures with excipients of different molecular weights. *Mol Pharm.* 2017;14(4):1154–1168. doi:10.1021/acs.molpharmaceut.6b01056
13. Simonelli AP, Mehta SC, Higuchi WI. Dissolution rates of high energy polyvinylpyrrolidone (PVP)-sulfathiazole coprecipitates. *J Pharm Sci.* 1969;58(5):538–549. doi:10.1002/jps.2600580503
14. van Drooge DJ, Hinrichs WLJ, Visser MR, Frijlink HW. Characterization of the molecular distribution of drugs in glassy solid dispersions at the nano-meter scale, using differential scanning calorimetry and gravimetric water vapour sorption techniques. *Int J Pharm.* 2006;310(1–2):220–229. doi:10.1016/j.ijpharm.2005.12.007
15. Kempin W, Domsta V, Grathoff G, et al. Immediate release 3D-printed tablets produced via fused deposition modeling of a thermo-sensitive drug. *Pharm Res.* 2018;35(6):124. doi:10.1007/s11095-018-2405-6
16. Janssens S, de Armas HN, Roberts CJ, Van den Mooter G. Characterization of ternary solid dispersions of itraconazole, PEG 6000, and HPMC 2910 E5. *J Pharm Sci.* 2008;97(6):2110–2120. doi:10.1002/jps.21128
17. Paidi SK, Jena SK, Ahuja BK, Devasari N, Suresh S. Preparation, in-vitro and in-vivo evaluation of spray-dried ternary solid dispersion of biopharmaceutics classification system class II model drug. *J Pharm Pharmacol.* 2015;67(5):616–629. doi:10.1111/jphp.12358
18. Mahmah O, Tabbakh R, Kelly A, Paradkar A. A comparative study of the effect of spray drying and hot-melt extrusion on the properties of amorphous solid dispersions containing felodipine. *J Pharm Pharmacol.* 2014;66(2):275–284. doi:10.1111/jphp.12099
19. Gangurde AB, Kundaikar HS, Javeer SD, Jaiswar DR, Degani MS, Amin PD. Enhanced solubility and dissolution of curcumin by a hydrophilic polymer solid dispersion and its insilico molecular modeling studies. *J Drug Deliv Sci Technol.* 2015;29:226–237. doi:10.1016/j.jddst.2015.08.005
20. Bhujbal SV, Mitra B, Jain U, et al. Pharmaceutical amorphous solid dispersion: A review of manufacturing strategies. *Acta Pharm Sin B.* 2021;11(8):2505–2536. doi:10.1016/j.apsb.2021.05.014
21. Sarode AL, Sandhu H, Shah N, Malick W, Zia H. Hot melt extrusion for amorphous solid dispersions: Temperature and moisture activated drug–polymer interactions for enhanced stability. *Mol Pharm.* 2013;10(10):3665–3675. doi:10.1021/mp400165b
22. Söti PL, Bocz K, Pataki H, et al. Comparison of spray drying, electroblowing and electrospinning for preparation of Eudragit E and itraconazole solid dispersions. *Int J Pharm.* 2015;494(1):23–30. doi:10.1016/j.ijpharm.2015.07.076
23. Singh A, Van den Mooter G. Spray drying formulation of amorphous solid dispersions. *Adv Drug Deliv Rev.* 2016;100:27–50. doi:10.1016/j.addr.2015.12.010
24. Vasconcelos T, Marques S, das Neves J, Sarmiento B. Amorphous solid dispersions: Rational selection of a manufacturing process. *Adv Drug Deliv Rev.* 2016;100:85–101. doi:10.1016/j.addr.2016.01.012
25. Xu L, Li SM, Sunada H. Preparation and evaluation of Ibuprofen solid dispersion systems with kollidon particles using a pulse combustion dryer system. *Chem Pharm Bull (Tokyo).* 2007;55(11):1545–1550. doi:10.1248/cpb.55.1545
26. ASTM International. Additive manufacturing: General principles terminology (ASTM52900). *Rapid Manuf Assoc.* 2013:10–12. doi:10.1520/F2792-12A.2
27. Khaled SA, Burley JC, Alexander MR, Roberts CJ. Desktop 3D printing of controlled release pharmaceutical bilayer tablets. *Int J Pharm.* 2014;461(1–2):105–111. doi:10.1016/j.ijpharm.2013.11.021
28. Łyszczarz E, Brniak W, Szafraniec-Szczesny J, et al. The impact of the preparation method on the properties of orodispersible films with aripiprazole: Electrospinning vs. casting and 3D printing methods. *Pharmaceutics.* 2021;13(8):1122. doi:10.3390/pharmaceutics13081122
29. Goyanes A, Allahham N, Trenfield SJ, Stoyanov E, Gaisford S, Basit AW. Direct powder extrusion 3D printing: Fabrication of drug products using a novel single-step process. *Int J Pharm.* 2019;567:118471. doi:10.1016/j.ijpharm.2019.118471
30. Kim SJ, Lee JC, Ko JY, Lee SH, Kim NA, Jeong SH. 3D-printed tablets using a single-step hot-melt pneumatic process for poorly soluble drugs. *Int J Pharm.* 2021;595:120257. doi:10.1016/j.ijpharm.2021.120257
31. Patel NG, Serajuddin ATM. Moisture sorption by polymeric excipients commonly used in amorphous solid dispersion and its effect on glass transition temperature. I. Polyvinylpyrrolidone and related copolymers. *Int J Pharm.* 2022;616:121532. doi:10.1016/j.ijpharm.2022.121532
32. Buhler V. *Kollidon. Polyvinylpyrrolidone Excipients for the Pharmaceutical Industry.* Lampertheim, Germany: BASF SE Pharma Ingredients & Services; 2008.
33. Mehatha AK, Suryadevara V, Lankapalli SR, Deshmukh AM, Sambath LP. Formulation and optimization of ezetimibe containing solid dispersions using kollidon VA64. *Turkish J Pharm Sci.* 2014;11(2):113–126. https://cms.galenos.com.tr/Uploads/Article_12344/113-126.pdf
34. Aldawsari MF, Anwer MK, Ahmed MM, et al. Enhanced dissolution of sildenafil citrate using solid dispersion with hydrophilic polymers: Physicochemical characterization and in vivo sexual behavior studies in male rats. *Polymers (Basel).* 2021;13(20):3512. doi:10.3390/polym13203512
35. Wlodarski K, Sawicki W, Kozyra A, Tajber L. Physical stability of solid dispersions with respect to thermodynamic solubility of tadalafil in PVP-VA. *Eur J Pharm Biopharm.* 2015;96:237–246. doi:10.1016/j.ejpb.2015.07.026
36. Sobulska M, Zbicinski I. *Flame Spray Drying.* Boca Raton, USA: CRC Press; 2021. doi:10.1201/9781003100386
37. Nagy ZK, Balogh A, Démuth B, et al. High speed electrospinning for scaled-up production of amorphous solid dispersion of itraconazole. *Int J Pharm.* 2015;480(1–2):137–142. doi:10.1016/j.ijpharm.2015.01.025
38. Dong L, Mai Y, Liu Q, Zhang W, Yang J. Mechanism and improved dissolution of glycyrrhetic acid solid dispersion by alkalizers. *Pharmaceutics.* 2020;12(1):82. doi:10.3390/pharmaceutics12010082
39. Vasoya JM, Desai HH, Gumaste SG, et al. Development of solid dispersion by hot melt extrusion using mixtures of polyoxylglycerides with polymers as carriers for increasing dissolution rate of a poorly soluble drug model. *J Pharm Sci.* 2019;108(2):888–896. doi:10.1016/j.xphs.2018.09.019
40. Wang W, Kang Q, Liu N, et al. Enhanced dissolution rate and oral bioavailability of ginkgo biloba extract by preparing solid dispersion via hot-melt extrusion. *Fitoterapia.* 2015;102:189–197. doi:10.1016/j.fitote.2014.10.004
41. Reintjes T, ed. *Solubility Enhancement with BASF Pharma Polymers. Solubilizer Compendium.* Lampertheim, Germany: BASF SE Pharma Ingredients & Services; 2011.
42. Linn M, Collnot EM, Djuric D, et al. Soluplus® as an effective absorption enhancer of poorly soluble drugs in vitro and in vivo. *Eur J Pharm Sci.* 2012;45(3):336–343. doi:10.1016/j.ejps.2011.11.025
43. Cespi M, Casettari L, Palmieri GF, Perinelli DR, Bonacucina G. Rheological characterization of polyvinyl caprolactam–polyvinyl acetate–polyethylene glycol graft copolymer (Soluplus®) water dispersions. *Colloid Polym Sci.* 2014;292(1):235–241. doi:10.1007/s00396-013-3077-8

44. Anwer MK, Ahmed MM, Alshetaili A, et al. Preparation of spray dried amorphous solid dispersion of diosmin in soluplus with improved hepato-reno-protective activity: In vitro anti-oxidant and in-vivo safety studies. *J Drug Deliv Sci Technol.* 2020;60:102101. doi:10.1016/j.jddst.2020.102101
45. Homayouni A, Sadeghi F, Nokhodchi A, Varshosaz J, Garekani HA. Preparation and characterization of celecoxib dispersions in Soluplus®: Comparison of spray drying and conventional methods. *Iran J Pharm Res.* 2015;14(1):35–50. PMID:25561910. PMCID:PMC4277617.
46. Liu J, Zou M, Piao H, et al. Characterization and pharmacokinetic study of aprepitant solid dispersions with Soluplus®. *Molecules.* 2015; 20(6):11345–11356. doi:10.3390/molecules200611345
47. Krupa A, Descamps M, Willart JF, et al. High-energy ball milling as green process to vitrify tadalafil and improve bioavailability. *Mol Pharm.* 2016;13(11):3891–3902. doi:10.1021/acs.molpharmaceut.6b00688
48. Nowak P, Krupa A, Kubat K, et al. Water vapour sorption in tadalafil-soluplus co-milled amorphous solid dispersions. *Powder Technol.* 2019;346:373–384. doi:10.1016/j.powtec.2019.02.010
49. Krupa A, Cantin O, Strach B, et al. In vitro and in vivo behavior of ground tadalafil hot-melt extrudates: How the carrier material can effectively assure rapid or controlled drug release. *Int J Pharm.* 2017;528(1–2):498–510. doi:10.1016/j.ijpharm.2017.05.057
50. Lee JY, Kang WS, Piao J, Yoon IS, Kim DD, Cho HJ. Soluplus®/TPGS-based solid dispersions prepared by hot-melt extrusion equipped with twin-screw systems for enhancing oral bioavailability of valsartan. *Drug Des Devel Ther.* 2015;9:2745–2756. doi:10.2147/DDDT.S84070
51. Shamma RN, Basha M. Soluplus®: A novel polymeric solubilizer for optimization of carvedilol solid dispersions: Formulation design and effect of method of preparation. *Powder Technol.* 2013;237:406–414. doi:10.1016/j.powtec.2012.12.038
52. Vasconcelos T, Prezotti F, Araújo F, et al. Third-generation solid dispersion combining Soluplus and poloxamer 407 enhances the oral bioavailability of resveratrol. *Int J Pharm.* 2021;595:120245. doi:10.1016/j.ijpharm.2021.120245
53. Chowdhury N, Vhora I, Patel K, Bagde A, Kutlehria S, Singh M. Development of hot melt extruded solid dispersion of tamoxifen citrate and resveratrol for synergistic effects on breast cancer cells. *AAPS PharmSciTech.* 2018;19(7):3287–3297. doi:10.1208/s12249-018-1111-3

A critical review on the extraction and pharmacotherapeutic activity of piperine

Mohd Imran^{1,D}, Monalisha Samal^{1,A}, Abdul Qadir^{2,F}, Asad Ali^{3,E}, Showkat R. Mir^{1,F}

¹ Department of Pharmacognosy and Phytochemistry, School of Pharmaceutical Education and Research, New Delhi, India

² Herbalfarm Healthcare Pvt. Ltd., New Delhi, India

³ Department of Pharmaceutics, School of Pharmaceutical Education & Research, New Delhi, India

A – research concept and design; B – collection and/or assembly of data; C – data analysis and interpretation;

D – writing the article; E – critical revision of the article; F – final approval of the article

Polymers in Medicine, ISSN 0370-0747 (print), ISSN 2451-2699 (online)

Polim Med. 2022;52(1):29–34

Address for correspondence

Abdul Qadir

E-mail: aqkhan90@gmail.com

Funding sources

None declared

Conflict of interest

None declared

Acknowledgements

The authors would like to sincerely thank Jamia Hamdard, University of Delhi, for providing necessary facilities for writing this review.

Received on October 3, 2021

Reviewed on November 4, 2021

Accepted on January 3, 2022

Published online on February 23, 2022

Abstract

Black pepper (*Piper nigrum* L.) is a climbing perennial plant in the *Piperaceae* family. Pepper has been known since antiquity for its use both as a medicine and a spice. It is particularly valued for its pungency attributed to its principal constituent – piperine. This review summarizes the information on the biological source of piperine, its extraction and isolation strategies, physicochemical properties, and pharmacological activity – analgesic, immunomodulatory, anti-depressive, anti-diarrheal, hepatoprotective, etc. The effect of piperine on biotransformation of co-administered drugs is also presented in this review, along with the mechanisms involved in its bioavailability-enhancing effect. Its important medicinal uses, including anti-hepatotoxic, anti-diarrheal, anti-depressive, analgesic, and immunomodulatory effects, besides many other traditional uses, are compiled. Based on an exhaustive review of literature, it may be concluded that piperine is a very promising alkaloid found in members of the *Piperaceae* family.

Key words: piperine, pepper, extraction, *Piper nigrum*, bioavailability enhancement

Cite as

Imran M, Samal M, Qadir A, Ali A, Mir SR. A critical review on the extraction and pharmacotherapeutic activity of piperine. Polim Med. 2022;52(1):29–34. doi:10.17219/pim/145512

DOI

10.17219/pim/145512

Copyright

Copyright by Author(s)

This is an article distributed under the terms of the Creative Commons Attribution 3.0 Unported (CC BY 3.0) (<https://creativecommons.org/licenses/by/3.0/>)

Introduction

Since antiquity, plants have been used as a source of food, spices and medicines. Among all spices, pepper has been widely discussed and named accurately “the king of spices”, due to its characteristic pungency and flavor. Therefore, it is used as an important ingredient in food worldwide. The aroma of pepper is due to the presence of volatile oil, the content of which varies from 0.5% to 7%. Pepper is particularly valued for its pungency attributed to its principal alkaloidal constituent – piperine, the content of which varies among the members of the *Piperaceae* family. The highest content of piperine has been reported in black pepper (*Piper nigrum* L.; 9%), while moderate levels have been found in long pepper (*P. longum* L.; 4%) and Balinese pepper (*Piper retrofractum* Vahl; 4.5%).¹

Black pepper (*P. nigrum* L.) is a flowering woody perennial vine, which grows up to a maximum height of 4 m. It is native to southwestern India. It reached Egypt by 1200 BC and was extensively used by Greeks and Romans. Nowadays, major producers of black pepper include Vietnam, India, Indonesia, Malaysia, Sri Lanka, Brazil, and Costa Rica. Roots of this plant grow from the leaf nodes once vine touches the soil and its leaves are heart-shaped. Pepper fruits are small (approx. 3–4 mm in diameter) and are also known as drupes. Ripe fruits are dark brown to greyish. The plant starts bearing fruits from 4th or 5th year, and continues to bear fruits up till 7 years. Fruits are sessile, globular to subglobular in shape and have a strongly reticulated surface. They have an aromatic odor and are pungent in taste. The fruits are single-seeded. Each stem bears 20–30 spikes of fruits. Black and white pepper is made by sun-drying unripe green fruits and stony seeds, respectively. Traditionally these are used as aromatics, stomachics and stimulants.¹

Piper longum L., a plant native in South Asia, is a small shrub comprised of woody roots and various creeping, jointed stems, thickened at the nodes, commonly known as long pepper or Javanese, Indian or Indonesian long pepper. It is cultivated in the Assam, Tamil Nadu and Andhra Pradesh states of India and also grows wild in Malaysia, Singapore, Bhutan, and Myanmar. It is known and cultivated mainly for its fruits which are usually dried and used as a spice and seasoning. Long pepper is known to have a close relation with *P. nigrum* and comes in varieties such as black, green and white pepper. The fruits have characteristic aromatic, stimulant and carminative properties, and are used in the treatment of constipation, gonorrhoea, diarrhoea, cholera, chronic malaria, tongue paralysis, and viral hepatitis.² *Piper longum* is most commonly ingested to inhibit various respiratory infections such as bronchitis cough, tumors, asthma, and some diseases of the spleen. It is well known to reduce muscular pains and inflammation, and to provide a soothing effect when applied topically. The fruit and root of the plant are widely employed in Ayurvedic system of medicine for the prevention,

treatment and mitigation of various ailments. It is known as rejuvenator in Ayurveda, as it helps to enhance the appetite and dispel gas from the intestines. An infusion of *P. longum* root is used in promoting expulsion of the placenta after birth. It is used as sedative in insomnia and epilepsy, and as cholagogue in obstruction of bile duct and gallbladder.³ It is incorporated in essential Ayurvedic formulations such as Trikatu (composed of 3 pungent herbs, namely long pepper, black pepper and ginger). Reported research studies revealed that the consumption of Trikatu resulted in synergistic drug–drug interaction and enhanced bioavailability of the substances administered along with this formulation.^{4,5}

Chemistry of piperine

Piperine is the most abundant pungent alkaloid obtained from the fruits of *P. nigrum* L. and other peppers. It was first isolated by Hans Christian Ørsted in 1819 as yellow crystalline substance. Its structure was determined later. Its chemical formula is C₁₇H₁₉NO₃ and its IUPAC name is 1-[5-(1, 3-benzodioxol-5-yl)-1-oxo-2, 4-pentadienyl] piperidine. It is slightly soluble in water and has the melting point of 128–130°C. It has 3 other geometric isomers, namely *iso*-piperine, chavicine and *iso*-chavicine, but all these lack pungency. Piperine has good pungent taste but on hydrolysis it gets converted to piperidine and piperic acid, due to which it loses its pungent nature. Piperine accounts for about 98% of the total alkaloids in peppers.^{6,7}

Other alkaloids reported in peppers containing characteristic pungency include piperanine, piperlylin A, piperolein B, piperettine, and pipericine. However, these alkaloids make a small contribution to the total pungency of pepper. From the analysis of data obtained from gas chromatography-mass spectrometry (GC-MS) along with distillation–extraction of *P. nigrum*, it was concluded that vinylic volatile compounds are the predominant compounds present in pepper that are found in both white and black pepper.⁸ Jagella and Grosch concluded that compounds like α -pinene, β -pinene, limonene, α -phellandrene, myrcene, 2- and 3-methylbutanal, butyric acid, linalool, methyl propanol, and 3-methylbutyric acid are the predominant odorants present in *P. nigrum*.⁹ Figure 1 presents the chemical structure of piperine.

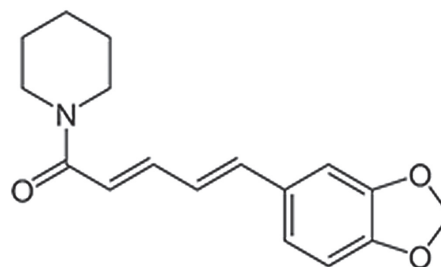


Fig. 1. Chemical structure of piperine

Extraction of piperine

Piperine is responsible for the pungency of many peppers such as black, white and long pepper. It is obtained essentially from the fruits of *P. nigrum* or *P. longum*, using various solvent extraction methods such as soaking, maceration and Soxhlet extraction. A wide range of solvents used for piperine extraction includes dichloromethane, petroleum ether, diethyl ether, alcoholic solvents like ethanol, hydrotropic solutions, and ionic-based solutions. Along with conventional extraction methods, the modern extraction techniques incorporated for piperine are supercritical carbon dioxide extraction, ultrasound-assisted extraction, pressurized liquid extraction, and microwave-assisted extraction. The dried fruits are pulverized and accurately weighed powder is used for extraction of piperine with dichloromethane at room temperature, with occasional stirring for 12 h, followed by filtration, vacuum concentration and then residue purification on an alumina column. Purified piperine can also be obtained by the crystallization from hydroalcoholic solutions and the treatment with aqueous alkali solutions.¹⁰ However, lesser amounts of piperine are attained from the crude residue by the aforementioned extraction with alcohol, filtration and then successive crystallization. Piperine can also be synthesized by the interaction of piperyl chloride (assembled from piperic acid and phosphorus pentachloride) and piperidine.

Medicinal use

Hepatoprotective activity

Piperine, when tested for treating acetaminophen-induced hepatotoxicity in mice, was found to decrease the levels of serums such as serum glutamic oxaloacetic transaminase (SGOT) and serum glutamic pyruvic transaminase (SGPT) in a dose-dependent manner.¹¹ The hepatoprotective activity of the methanolic extract of *P. nigrum* was determined in treatment of ethanol-CCl₄-induced hepatic damage in Wistar rats.¹² The results of other study, concerning D-glucosamine-induced hepatotoxicity in mice, indicated that piperine possess a vast therapeutic potential in the treatment of liver disorders.¹³

Anti-diarrheal activity

In another study, aqueous extract of black pepper was prepared in doses of 75 mg/kg, 150 mg/kg and 300 mg/kg for testing. Then, it was evaluated for its anti-motility, anti-secretory and anti-diarrheal activity in mice. Diarrhea was induced for the evaluation of anti-diarrheal activity and gastrointestinal motility by employing castor oil and magnesium sulfate in mice. The anti-motility and anti-secretory activities of *P. nigrum* were attributed to the presence of alkaloids, mainly piperine.¹⁴

Antidepressant activity

The corticosterone-induced model of depression in mice was used to study the effects of piperine as antidepressant and its possible mechanism of action. In this study, corticosterone injections were given to mice for 3 weeks to induce depression, and the mice were observed for the decreased brain-derived neurotrophic factor protein and mRNA levels in the hippocampus. These changes disappeared after the mice had been treated with piperine. These results demonstrated that piperine has potential anti-depressive activity in the corticosterone-induced depression model in mice.¹⁵ Piperine also showed anti-depressive-like effects in mice with chronic mild stress.¹⁶

Immunomodulatory activity

Piperine was evaluated for its immunomodulatory and antitumor activities. It was found to be cytotoxic to Ehrlich ascites carcinoma (EAC) cells, known widely as Ehrlich cells and Dalton's lymphoma ascites. Increased white blood cells (WBC), bone marrow cells and alpha esterase-positive cells count was observed in mice after treatment with piperine.¹⁷

Analgesic activity

In vivo evaluation of piperine was performed to determine the analgesic effects in acetic-acid induced writhing and tail flick assay models in mice. The acetic-acid induced writhing model showed a significant reduction after intraperitoneal administration of piperine in mice at dose of 30 mg/kg, 50 mg/kg and 70 mg/kg. Piperine showed greater inhibition when compared with indomethacin at a dose of 30 mg/kg administered intraperitoneally (ip.). In the tail flick assay, an ip. injection of piperine and morphine at doses of 30 mg/kg and 5 mg/kg, respectively, resulted in remarkable increase in reaction time.¹⁸

Anti-tubercular activity

In vitro evaluation of piperine was determined in a murine model of *Mycobacterium tuberculosis* infection. The results showed an increase in the secretion of Th1 cytokines (interferon gamma (IFN- γ) and interleukin 2 (IL-2)) and in macrophage activation.¹⁹

Effect of piperine on metabolism

Piperine regulates the metabolic pathway of many components inside the body and is also involved in altering the bioavailability of many therapeutically crucial drugs and nutrients. Through various mechanisms, it stimulates the absorption of drugs and other nutrients from the gastrointestinal tract. It works by changing the membrane dynamics, thus enhancing the permeability at the site of drug

absorption. It is also responsible for extending the serum half-life of substances such as β -carotene and coenzyme Q10, and declining the metabolism of many drugs by handicapping metabolizing enzymes like cytochrome BS, uridine 5'-diphospho (UDP)-glucuronyltransferase, UDP-glucose dehydrogenase (UDP-GDH), CYP3A4, aryl hydrocarbon hydroxylase, and nicotinamide adenine dinucleotide phosphate (NADPH) cytochrome.²⁰ Piperine has been reported to influence the bioavailability of many drugs such as amoxicillin, acefotaxime, norfloxacin,²¹ metronidazole, carbamazepine,²² oxytetracycline, pentobarbitone, phenytoin,²³ resveratrol,²⁴ β -carotene,²⁵ curcumin, tiferron, nevirapine, docetaxel,²⁶ theophylline, and propranolol.²⁷ Hence, piperine is also known as bioavailability enhancer. The other uses of piperine are summarized in Table 1.

Antibacterial activity

Piperine and black pepper oil are powerful antibacterial agents – especially piperine, which is active against both Gram-positive and Gram-negative microorganisms.⁶⁴

Table 1. Uses of piperine and health benefits

Category	Activity	References
Traditional uses	flavor, cough, diuretic, antispasmodic, increases saliva flow, antiseptic, dyspepsia, central nervous system (CNS) stimulant, digestive tonic, aroma, flatulence, indigestion, strep throat, germicide, blood purifier, bactericide, analgesic, antitoxic, religious ceremony, aphrodisiac, pain, antipyretic, insecticide, rheumatism, diabetes, muscle aches	3, 9, 28–34
Modern uses	anti-diarrheal	35
	antihypertensive	36
	antihyperlipidemic	37
	increased hypersensitivity response	38
	cognitive improvement	39, 40
	anti-asthmatic	41
	anti-oxidant	42, 43
	reduce high fat induce oxidative stress	44, 45
	antiepileptic	46
	anti-fertility	47
	lipid metabolism acceleration	48
	increased food absorption rate	49–51
	anti-inflammatory	52, 53
	anticancer	54, 55
	synergic nociceptive effect	56
	anti-ulcer	57
	hepatoprotective activity	58
	increased bile secretion	59, 60
	drug metabolism	61
hepatic enzyme activity	62	
inhibit lung metastatic	63	

Appetite suppressant

The findings indicated that preloading with BPB (black pepper-based beverage) reduced hunger, desire to eat and prospective intake, while increasing satiety and a feeling of fullness. Thus, this demonstrates appetite suppressing action of piperine.⁶⁵

Piperine enhances body efficiency

Piperine is an alkaloid present in black pepper (*P. nigrum*), long pepper (*P. longum*) and other species belonging to the *Piperaceae* family. It is responsible for the black pepper distinct biting quality. Piperine has many pharmacological effects, especially against chronic diseases, such as reducing insulin-resistance and anti-inflammatory effects, and mitigating hepatic steatosis.

Side effects

Major side effects of piperine include loss of potassium, acid reflux, constipation, and nausea. Pepper can cause allergic reactions like sneezing, hives, rashes, and swelling of the tongue and mouth, and even profound respiratory reactions in cases of severe allergic reactions.

Isolation of piperine

Several methods have been developed for the isolation of piperine from black pepper, namely Soxhlet extraction, hydrotropic extraction, supercritical fluid extraction, ionic liquid-based extraction, and microwave-assisted extraction. However, in one study, bulk isolation of piperine from black pepper and white pepper fruits was performed using Soxhlet extraction with 95% ethanol, and from the concentrated extracts, the yellow-colored needles were obtained, which were isolated by precipitation with 10% alcoholic potassium hydroxide (KOH) solution. It was then followed by purification by recrystallizing the obtained crystals with dichloromethane followed by few drops of n-Hexane that will lead to the formation of rod-like, pale yellow crystals of piperine.⁶⁶

Conclusion

Based on an exhaustive review of literature, it may be concluded that piperine is a very promising alkaloid found in members of *Piperaceae* family. This review aimed to gather information about the biological source of piperine, its extraction and isolation strategies, physicochemical properties, and pharmacological activity. The effect of piperine on biotransformation of co-administered drugs is also presented in this review. The major mechanisms involved in its bioavailability-enhancing activity

are: a) acting on drug metabolizing enzyme; b) disrupting the supply of blood to gastrointestinal tract and the membrane fluidity; c) affecting drug transport; and d) disturbing drug absorption.

ORCID iDs

Mohd Imran  <https://orcid.org/0000-0002-7465-4619>
 Monalisha Samal  <https://orcid.org/0000-0001-8822-1104>
 Dr. Abdul Qadir  <https://orcid.org/0000-0002-7119-0847>
 Asad Ali  <https://orcid.org/0000-0002-1801-9207>
 Showkat R. Mir  <https://orcid.org/0000-0001-7292-8519>

References

1. *The Wealth of India. A Dictionary of Indian Raw Materials and Industrial Products. First Supplementary Series: Raw Materials.* New Delhi, India: Publications and Information Directorate (PID); 2003:318–319.
2. Satyavati GV, Gupta AK, Tandon N, eds. *Medicinal Plants of India.* New Delhi, India: Indian Council of Medical Research (ICMR); 1987:426–456.
3. Pei YQ. A review of pharmacology and clinical use of piperine and its derivatives and uses. *Epilepsia.* 1983;24(2):177–181. doi:10.1111/j.1528-1157.1983.tb04877.x
4. *Handbook of Domestic Medicine and Common Ayurvedic Remedies.* New Delhi, India: Central Council for Research in Indian Medicine and Homeopathy; 1979:91–112.
5. Antarkar DS, Vaidya AB. Therapeutic approach to malaria in Ayurveda. In: Subrahmanyam D, Radhakrishna V, eds. *Symposium on Recent Advances in Protozoan Diseases.* Bombay, India: Hindustan Ciba-Geigy Research Centre Goregaon; 1983:96–101.
6. Hirasa K, Takemasa M. *Spice Science and Technology.* Boca Raton, USA: CRC Press; 1998:98–107.
7. Parmar VS, Jain SC, Bisht KS, Jain R, Taneja P, Jha A. Phytochemistry of the genus *Piper*. *Phytochemistry.* 1997;46(4):597–673. doi:10.1016/S0031-9422(97)00328-2
8. Chen W, Dou H, Ge C. Comparison of volatile compounds in pepper (*P. nigrum* L.) by simultaneous distillation extraction (SDE) and GC-MS. *Adv Mater Res.* 2011;236–238:2643–2646. doi:10.4028/www.scientific.net/AMR.236-238.2643
9. Jagella T, Grosch W. Flavour and off-flavour compounds of black and white pepper (*Piper nigrum* L.). II. Odour activity values of desirable and undesirable odorants of black pepper. *Eur Food Res Technol.* 1999;209:22–26. doi:10.1007/s002170050450
10. Gorgani L, Mohammadi M, Najafpour GD, Nikzad M. Piperine, the bioactive compound of black pepper: From isolation to medicinal formulations. *Compr Rev Food Sci Food Saf.* 2017;16(1):124–140. doi:10.1111/1541-4337.12246
11. Sabina EP, Souriyana ADH, Jackline D, Rasool MK. Piperine, an active ingredient of black pepper attenuates acetaminophen-induced hepatotoxicity in mice. *Asian Pac Trop Dis.* 2010;3(12):971–976. doi:10.1016/S1995-7645(11)60011-4
12. Nirwane AM, Bapat AR. Effect of methanolic extract of *Piper nigrum* fruits in ethanol-CCl₄-induced hepatotoxicity in Wistar rats. *Der Pharmacia Letter.* 2012;4:795–802.
13. Matsuda H, Ninomiya K, Morikawa T, Yasuda D, Yamaguchi I. Protective effects of amide constituents from the fruit of *Piper chaba* on D-galactosamine/TNF- α -induced cell death in mouse hepatocytes. *Bioorg Med Chem Lett.* 2008;18(6):2038–2042. doi:10.1016/j.bmcl.2008.01.101
14. Shamkuwar PB, Shahi SR, Jadhav ST. Evaluation of anti-diarrheal effect of black pepper (*Piper nigrum* L.). *Asian J Plant Sci Res.* 2012;2:48–53. <https://naturalingredient.org/wp/wp-content/uploads/AJPSR-2012-2-1-48-53.pdf>
15. Mao QQ, Huang Z, Zhong XM, Xian YF, Ip SP. Piperine reverses the effects of corticosterone on behavior and hippocampal BDNF expression in mice. *Neurochem Int.* 2014;74:36–41. doi:10.1016/j.neuint.2014.04.017
16. Li S, Wang C, Wang M, Li W, Matsumoto K. Antidepressant like effects of piperine in chronic mild stress treated mice and its possible mechanisms. *Life Sci.* 2007;80(15):1373–1381. doi:10.1016/j.lfs.2006.12.027
17. Sunila ES, Kuttan G. Immunomodulatory and antitumor activity of *Piper longum* Linn. and piperine. *J Ethnopharmacol.* 2004;90(2–3):339–346. doi:10.1016/j.jep.2003.10.016
18. Bukhari IA, Pivac N, Alhumayyd MS, Mahesar AL, Gilani AH. The analgesic and anticonvulsant effects of piperine in mice. *J Physiol Pharmacol.* 2013;64(6):789–794. PMID:24388894
19. Sharma S, Kalia NP, Suden P, Chauhan PS, Kumar M. Protective efficacy of piperine against *Mycobacterium tuberculosis*. *Tuberculosis (Edinb).* 2014;94(4):389–396. doi:10.1016/j.tube.2014.04.007
20. Badmaev V, Majeed M, Prakash L. Piperine derived from black pepper increases plasma levels of coenzyme Q10 following oral supplementation. *J Nutr Biochem.* 2000;11(2):109–113. doi:10.1016/s0955-2863(99)00074-1
21. Hiwale AR. Effect of coadministration of piperine on pharmacokinetics of b-lactam antibiotics in rats. *Indian J Exp Biol.* 2002;40(3):277–281. PMID:12635696
22. Pattanaik S, Hota D, Prabhakar S. Pharmacokinetic interaction of single dose of piperine with steady state carbamazepine in epilepsy patient. *Phytother Res.* 2009;23(9):1281–1286. doi:10.1002/ptr.2676
23. Pattanaik S, Hota D, Prabhakar S. Effect of piperine on the steady-state pharmacokinetics of phenytoin in patients with epilepsy. *Phytother Res.* 2006;20(8):683–686. doi:10.1002/ptr.1937
24. Johnson JJ, Nihal M, Siddiqui IA, Scarlett CO, Bailey HH. Enhancing the bioavailability of resveratrol by combining it with piperine. *Mol Nutr Food Res.* 2011;55(8):1169–1176. doi:10.1002/mnfr.201100117
25. Badmaev V, Majeed M, Norkus EP. Piperine, an alkaloid derived from black pepper increases serum response of β -carotene during 14 days of oral β -carotene supplementation. *Nutr Res.* 1999;19(3):381–388. doi:10.1016/S0271-5317(99)00007-X
26. Makhov P, Golovine K, Canter D, Kutikov A, Simhan J. Co-administration of piperine and docetaxel results in improved anti-tumor efficacy via inhibition of CYP3A4 activity. *Prostate.* 2012;72(6):661–667. doi:10.1002/pros.21469
27. Bano G, Raina RK, Zutshi U. Effect of piperine on bioavailability and pharmacokinetics of propranolol and theophylline in healthy volunteers. *Eur J Clin Pharmacol.* 1991;41(6):615–617. doi:10.1007/BF00314996
28. Ahmad N, Fazal H, Abbasi BH, Farooq S, Ali M. Biological role of *Piper nigrum* L. (black pepper): A review. *Asian Pac J Trop Biomed.* 2012;2(3 Suppl):S1945–S1953. doi:10.1016/S2221-1691(12)60524-3
29. Db M, Sreedharan S, Mahadik KR. Role of piperine as an effective bioenhancer in drug absorption. *Pharm Anal Acta.* 2018;9(7):1–4. doi:10.4172/2153-2435.1000591
30. Srinivasan K. Black pepper and its pungent principle-piperine: A review of diverse physiological effects. *Crit Rev Food Sci Nutr.* 2007;47(8):735–748. doi:10.1080/10408390601062054
31. Capasso R, Izzo AA, Borrelli F. Effect of piperine, the active ingredient of black pepper on intestinal secretion in mice. *Life Sci.* 2002;71(19):2311–2317. doi:10.1016/s0024-3205(02)02019-2
32. Myers BM, Smith JL, Graham DY. Effect of red pepper and black pepper on the stomach. *Am J Gastroenterol.* 1987;82(3):211–214. PMID:3103424
33. Khan M, Siddiqui M. Antimicrobial activity of *Piper* fruits. *Natural Product Radiance.* 2007;6(2):111–113. <http://nopr.niscair.res.in/bitstream/123456789/7845/1/NPR%206%282%29%20111-113.pdf>
34. Doucette CD, Hilchie AL, Liwski R, Hoskin DW. Piperine, a dietary phytochemical, inhibits angiogenesis. *J Nutr Biochem.* 2013;24(1):231–239. doi:10.1016/j.jnutbio.2012.05.009
35. Atal CK, Dubey RK, Singh J. Biochemical basis of enhanced drug bioavailability of piperine: Evidence that piperine is a potent inhibitor of drug metabolism. *J Pharmacol Exp Ther.* 1985;232(1):258–262. PMID:3917507
36. Taqvi SI, Shah AJ, Gilani AH. Blood pressure lowering and vasomodulator effects of piperine. *J Cardiovasc Pharmacol.* 2008;52(5):452–458. doi:10.1097/FJC.0b013e31818d07c0
37. Agbor GA, Akinfiesoye L, Sortino J, Johnson R, Vinson JA. *Piper* species protect cardiac, hepatic and renal antioxidant status of atherogenic diet fed hamsters. *Food Chem.* 2012;134(3):1354–1359. doi:10.1016/j.foodchem.2012.03.030
38. Dogra RKS, Khanna S, Shanker R. Immunotoxicological effects of piperine in mice. *Toxicology.* 2004;196(3):229–236. doi:10.1016/j.tox.2003.10.006
39. Hritcu L, Noumedem JA, Cioanca O, Hancianu M, Kuete V. Methanolic extract of *Piper nigrum* fruits improves memory impairment by decreasing brain oxidative stress in amyloid beta(1-42) rat model of Alzheimer's disease. *Cell Mol Neurobiol.* 2014;34(3):437–449. doi:10.1007/s10571-014-0028-y

40. Chonpathompikunlert P, Wattanathorn J, Muchimapura S. Piperine, the main alkaloid of Thai black pepper, protects against neurodegeneration and cognitive impairment in animal model of cognitive deficit like condition of Alzheimer's disease. *Food Chem Toxicol.* 2010;48(3):798–802. doi:10.1016/j.fct.2009.12.009
41. Kaushik D, Rani R, Kaushik P, Sacher D, Yadav J. In vivo and in vitro antiasthmatic studies of plant *Piper longum* Linn. *Int J Pharmacol.* 2012;8(3):192–197. doi:10.3923/ijp.2012.192.197
42. Khajuria A, Thusu N, Zutshi U, Bedi KL. Piperine modulation of carcinogen induced oxidative stress in intestinal mucosa. *Mol Cell Biochem.* 1998;189(1–2):113–118. doi:10.1023/a:1006877614411
43. Mittal R, Gupta RL. In vitro antioxidant activity of piperine. *Exp Clin Psychopharmacol.* 2000;22(5):271–274. doi:10.1358/mf.2000.22.5.796644
44. Vijayakumar RS, Surya D, Nalini N. Antioxidant efficacy of black pepper (*Piper nigrum* L.) and piperine in rats with high fat diet induced oxidative stress. *Redox Rep.* 2004;9(2):105–110. doi:10.1179/135100004225004742
45. Naidu KA, Thippeswamy NB. Inhibition of human low density lipoprotein oxidation by active principles from spices. *Mol Cell Biochem.* 2002;229(1–2):19–23. doi:10.1023/a:1017930708099
46. Chen CY, Li W, Qu KP, Chen CR. Piperine exerts anti-seizure effects via the TRPV1 receptor in mice. *Eur J Pharmacol.* 2013;714(1–3):288–294. doi:10.1016/j.ejphar.2013.07.041
47. Lakshmi V, Kumar R, Agarwal SK, Dhar JD. Antifertility activity of *Piper longum* L. in female rats. *Nat Prod Res.* 2006;20(3):235–239. doi:10.1080/14786410500045465
48. Duangjai A, Ingkaninan K, Praputbut S, Limpeanchob N. Black pepper and piperine reduce cholesterol uptake and enhance translocation of cholesterol transporter proteins. *J Nat Med.* 2013;67(2):303–310. doi:10.1007/s11418-012-0682-7
49. Platel K, Srinivasan K. Influence of dietary spices or their active principles on digestive enzymes of small intestinal mucosa in rats. *Int J Food Sci Nutr.* 1996;47(1):55–59. doi:10.3109/09637489609028561
50. Platel K, Srinivasan K. Influence of dietary spices and their active principles on pancreatic digestive enzymes in albino rats. *Nahrung.* 2000;44(1):42–46. doi:10.1002/(SICI)1521-3803(20000101)44:1<42::AID-FOOD42>3.0.CO;2-D
51. Platel K, Srinivasan K. Studies on the influence of dietary spices on food transit time in experimental rats. *Nutr Res.* 2001;21(9):1309–1314. doi:10.1016/S0271-5317(01)00331-1
52. Mujumdar AM, Dhuley JN, Deshmukh VK. Anti-inflammatory activity of piperine. *Jap J Med Sci Biol.* 1990;43(3):95–100. doi:10.7883/yoken1952.43.95
53. Bang JS, Oh da H, Choi HM, Sur BJ, Lim SJ. Anti-inflammatory and antiarthritic effects of piperine in human interleukin 1beta-stimulated fibroblast-like synoviocytes and in rat arthritis models. *Arthritis Res Ther.* 2009;11(2):R49. doi:10.1186/ar2662
54. Samykutty A, Shetty AV, Dakshinamoorthy G, Bartik MM, Johnson GL, Webb B. Piperine, a bioactive component of pepper spice, exerts therapeutic effects on androgen dependent and androgen independent prostate cancer cells. *PLoS One.* 2013;8(6):e65889. doi:10.1371/journal.pone.0065889
55. Manoharan S, Balakrishnan S, Menon V, Alias L, Reena A. Chemopreventive efficacy of curcumin and piperine during 7,12-dimethylbenz[a]anthracene-induced hamster buccal pouch carcinogenesis. *Singapore Med J.* 2009;50(2):139–146. PMID:19296028
56. Gupta SK, Velpandian T, Sengupta S. Influence of piperine on nimesulide induced antinociception. *Phytother Res.* 1998;12(4):266–269. doi:10.1002/(SICI)1099-1573(199806)12:4<266::AID-PTR291>3.0.CO;2-S
57. Bai YF, Xu H. Protective action of piperine against experimental gastric ulcer. *Acta Pharmacol Sin.* 2000;21(4):357–359. PMID:11324467
58. Piyachaturawat P, Kingkaehoi S, Tosulkao C. Potentiation of carbon tetrachloride hepatotoxicity by piperine. *Drug Chem Toxicol.* 1995;18(4):333–344. doi:10.3109/01480549509014327
59. Bhat GB, Chandrasekhara N. Effect of black pepper and piperine on bile secretion and composition in rats. *Nahrung.* 1987;31(9):913–916. doi:10.1002/food.19870310916
60. Ononiwu IM, Ibeneme CE, Ebong OO. Effects of piperine on gastric acid secretion in albino rats. *Afr J Med Sci.* 2002;31(4):293–295. PMID:15027765
61. Dalvi RR, Dalvi PS. Differences in the effects of piperine and piperonylbutoxide on hepatic drug-metabolizing enzyme system in rats. *Drug Chem Toxicol.* 1991a;14(1–2):219–229. doi:10.3109/01480549109017878
62. Dalvi RR, Dalvi PS. Comparison of the effects of piperine administered intragastrically and intraperitoneally on the liver and liver mixed function oxidases in rats. *Drug Metabol Drug Interaction.* 1991b;9(1):23–30. doi:10.1515/dmdi.1991.9.1.23
63. Selvendiran K, Sakthisekaran D. Chemopreventive effect of piperine on modulating lipid peroxidation and membrane bound enzymes in benzo(a) pyrene induced lung carcinogenesis. *Biomed Pharmacother.* 2004;58(4):264–267. doi:10.1016/j.biopha.2003.08.027
64. Hikal DM. Antibacterial activity of piperine and black pepper oil. *Biosci Biotechnol Res Asia.* 2018;15(4):877–880. doi:10.13005/bbra/2697
65. Zanzer YC, Plaza M, Dougkas A, Turner C, Östman E. Black pepper-based beverage induced appetite-suppressing effects without altering postprandial glycaemia, gut and thyroid hormones or gastrointestinal well-being: A randomized crossover study in healthy subjects. *Food Function.* 2018;9(5):2774–2786. doi:10.1039/c7fo01715d
66. Khan ZR, Moni F, Sharmin S, et al. Isolation of bulk amount of piperine as active pharmaceutical ingredient (API) from black pepper and white pepper (*Piper nigrum* L.). *Pharmacol Pharm.* 2017;8(7):253–262. doi:10.4236/pp.2017.87018

Polymeric capsules and micelles as promising carriers of anticancer drugs

Kapsułki i micelle polimerowe jako nośniki leków przeciwnowotworowych

Tomasz Kubiak^{A–F}

Chair of Acoustics, Faculty of Physics, Adam Mickiewicz University in Poznań, Poland

A – research concept and design; B – collection and/or assembly of data; C – data analysis and interpretation; D – writing the article; E – critical revision of the article; F – final approval of the article

Polymers in Medicine, ISSN 0370-0747 (print), ISSN 2451-2699 (online)

Polim Med. 2022;52(1):35–48

Address for correspondence

Tomasz Kubiak
E-mail: tomekbiofizyk@wp.pl

Funding sources

None declared

Conflict of interest

None declared

Received on September 3, 2021
Reviewed on December 10, 2021
Accepted on January 3, 2022

Published online on February 23, 2022

Abstract

Polymeric micelles and capsules are promising candidates for carriers of antineoplastic medications. Biodegradability and broadly defined biocompatibility are the key features that should always characterize polymers intended for medical applications. A well-designed delivery system ought to ensure the safe transport of chemotherapeutic agents to the target area and thus minimize systemic exposure to these drugs, limiting their toxic effect, preferably to the cancer cells. Polymeric micelles are often tailored for encapsulation of water-insoluble drugs. Micellar structures are usually fabricated as a result of self-assembly of various amphiphilic block copolymers in aqueous environment. More advanced methods are used to form capsules with a liquid core and a shell made of fused polymer nano- or microparticles. Such a coating can have homogeneous or heterogeneous composition. Janus and patchy capsules are usually characterized by more useful and advanced properties. Although some polymeric carriers are designed for a sustained release of the cargo, more sophisticated approaches involve payload liberation on demand under the influence of selected chemical or physical stimuli. The variety of available polymers and a wide range of possibilities of forming copolymers from different kind of monomers make polymeric materials ideal for the production of drug delivery systems with the desired properties. The aim of the present review is to sum up selected aspects of the use of polymeric micelles as carriers of cytostatic drugs, taking into account clinical applications. The additional objective is to show the studies on creating alternative systems based on stimuli-responsive capsules with shells made of polymeric particles.

Key words: controlled release, block copolymers, drug carriers, microcapsules, polymeric micelles

Cite as

Kubiak T. Polymeric capsules and micelles as promising carriers of anticancer drugs. *Polim Med.* 2022;52(1):35–48. doi:10.17219/pim/145513

DOI

10.17219/pim/145513

Copyright

Copyright by Author(s)

This is an article distributed under the terms of the Creative Commons Attribution 3.0 Unported (CC BY 3.0) (<https://creativecommons.org/licenses/by/3.0/>)

Streszczenie

Micelle i kapsułki polimerowe to dobrze zapowiadający się kandydaci na nośniki leków przeciwnowotworowych. Biodegradowalność i szeroko pojęta biokompatybilność zawsze stanowią kluczowe cechy, jakimi muszą charakteryzować się polimery przeznaczone do zastosowań medycznych. Poprawnie zaprojektowany system dostarczania powinien zapewniać bezpieczny transport chemioterapeutyków do obszaru docelowego, a tym samym minimalizować ogólnoustrojową ekspozycję na te leki, ograniczając ich toksyczne działanie (najlepiej tylko do komórek nowotworowych). Micelle polimerowe są często przystosowane do enkapsulacji leków słabo rozpuszczalnych w wodzie. Struktury micelarne powstają zwykle w wyniku samoorganizacji różnego typu amfifilowych kopolimerów blokowych w środowisku wodnym. Bardziej zaawansowane metody wykorzystuje się do formowania kapsułek z ciekłym rdzeniem i powłoką złożoną z połączonych nano- bądź mikrocząstek polimerowych. Taka powłoka może być jedno- bądź niejednorodna. Kapsułki Janusa i niejednorodne charakteryzują się zazwyczaj bardziej użytecznymi i złożonymi właściwościami. Chociaż niektóre nośniki polimerowe są zaprojektowane do przedłużonego uwalniania leku, bardziej zaawansowane podejścia obejmują uwalnianie ładunku na żądanie pod wpływem wybranego bodźca chemicznego lub fizycznego. Bogaty wybór dostępnych polimerów oraz szeroki wachlarz możliwości formowania kopolimerów z różnego rodzaju monomerów sprawiają, że materiały polimerowe idealnie nadają się do wytwarzania systemów dostarczania leków o odpowiednich własnościach. Celem niniejszego przeglądu jest podsumowanie wybranych aspektów wykorzystania miceli polimerowych jako nośników leków cytostatycznych, z uwzględnieniem zastosowań klinicznych. Dodatkowym celem jest pokazanie badań nad alternatywnymi systemami opartymi na kapsułkach z powłokami utworzonymi z cząstek polimerowych.

Słowa kluczowe: kontrolowane uwalnianie, mikrokapsułki, micelle polimerowe, nośniki leków, kopolimery blokowe

Introduction

Although microencapsulation is useful in many branches of economy, the greatest hope lies in its application in pharmacy and medicine. On the one hand, capsules can protect various payloads from contamination, deactivation or oxidation caused by the reaction with the surrounding medium, but on the other hand, they may preserve the environment from toxic or harmful effect of the transported substance.^{1,2} Delivery of drugs, proteins, enzymes, nucleic acids, microorganisms (e.g., probiotics), or implantation of living cells (e.g., stem or hepatic cells) are just some of the tasks that scientists assign to polymer capsules.³ Most of the research is focused on their use in cancer therapy. The primary goal of the employment of polymeric carriers in this field is to deliver chemotherapy medications directly to the target area and thus, to minimize systemic exposure to these drugs, confining their action only to malignant tissues and cells. In general, the drug can be physically entrapped inside the shell, conjugated or complexed with the polymer, alternatively dissolved or dispersed in the liquid core.^{4,5} Capsules are often vesicular systems with liquid core (consisting of water or oil) acting as a drug reservoir, surrounded by a protecting shell.⁶ Polymeric micelles are self-assembled structures built out of amphiphilic copolymers. In aqueous media, hydrophilic groups form an outer shell and hydrophobic fragments face the core in which the lipophilic drug can be encapsulated.^{6,7} Polymeric micelles are typically more stable compared to traditional surfactant-based micelles.^{6,8} They also have an advantage over liposomes, because hydrophobic medications incorporated into the lipid bilayer tend to be released quite rapidly after systemic administration.⁹ Polymer structures do not only retain the drug longer, but also have better loading capacity than micelles and liposomes.⁴

The most commonly encapsulated anticancer drugs are: paclitaxel (chemotherapy medication originally isolated from the bark of the Pacific yew tree *Taxus brevifolia*),¹⁰ docetaxel (semisynthetic taxane obtained by chemical modification of 10-deacetylbaccatin III, isolated from needles of European yew tree *Taxus baccata*)¹¹ and doxorubicin (anthracycline antibiotic obtained from the *Streptomyces peucetius* bacterium species).^{9,12–14} Serious side effects caused by the standard formulations of the aforementioned drugs motivate scientists to search for efficient and safe intravenous delivery systems. Another significant problem is very poor water solubility of taxanes.¹⁵ However, the efficient delivery of small hydrophilic drugs is also complicated due to their rapid clearance from the bloodstream and the tendency to spread in the aqueous environment of the human body.¹⁶ Unplanned local aggregation of anticancer agents after intravenous injection may increase their toxic effect on healthy tissues and even be the cause of embolism.¹⁷ Therefore, targeted delivery of cytotoxic medications is needed to considerably increase their efficacy and significantly reduce their total concentration in the body.¹⁸ Thanks to the protective shell, the drug can be safely transported, because its release is delayed or completely prevented until the coverage is ruptured.¹⁹

The distribution and behavior of polymeric carriers in biological environment primarily depend on their size and surface properties.²⁰ Polymeric capsules with a size that does not exceed 200 nm may enter the tumor region through leaky vessels, which is related to the enhanced permeability and retention (EPR) effect.^{21,22} Proper composition of nanocarriers or chemical modification of their surface may contribute to the extension of their circulation time and thus the tumor site exposure to the drug formulation. Capsules should preferentially amass within neoplasm and should not accumulate in healthy tissues. However, many studies indicate that the role of passive

accumulation of nanomedications is overestimated, and the delivery strategy based merely on EPR effect can only be sufficient for a narrow subset of clinical tumors.²³ Therefore, more advanced solutions are needed. For example, active targeting utilizes surface-modified capsules with bioactive ligands (peptides, antibodies, etc.) that are recognized by receptors overexpressed in the tumor region.²⁴ There is still an issue of insufficient penetration of cytostatic drugs into the inner cell layers of solid tumors.²⁵ Nanocarriers after extravasation from tumor vessels still have to break through a series of obstacles including interstitial extracellular matrix, cellular membranes and nuclear envelope.²⁶ The strategies for promoting drug release from polymeric capsules and micelles are discussed in a separate section of this paper.

In the context of the functionality of polymeric carriers, it should be emphasized that the most important matter is their broadly defined biocompatibility. It means that structures administered to the body not only cannot be toxic and cause immune response, but they should also fulfill planned role in the biological environment.^{27,28} In case of core-shell type nanostructures, biocompatibility can be obtained by using appropriate polymer coating made of chitosan and poly(ethylene glycol) (PEG).²⁷ For example, one can mention chitosan or PEG-coated magnetite nanoparticles investigated by means of electron paramagnetic resonance technique,²⁹ also in human whole blood,³⁰ and polymer-coated gadolinium, platinum and gold nanoparticles designed as radiosensitizers in cancer treatment.³¹ In the case of nanoparticles, “stealth” polymers typically modify the surface of the solid core. For capsules which are hollow or liquid-filled structures, PEG chains are the integral part of the shell or are grafted on it. One can cite the examples of PEG-coated hollow polyelectrolyte microcapsules injected into the bloodstream of zebrafish,³² PEGylated poly(D,L-lactide) nanocapsules with aqueous-core containing hydrophilic anticancer drug – gemcitabine hydrochloride,³³ or even nanocapsules with the whole shell made of chitosan, chemically modified with PEG.³⁴ Nevertheless, the research on PEG-terminated multilayer polyelectrolyte nanocapsules indicated the necessity of checking the long-term immune response stimulated by PEGylated structures.³⁵ Poly(2-ethyl-2-oxazoline) (PEtOz) is considered as an alternative to PEG because of biocompatibility, biodegradability and ability to prolong the circulation time of nanocarriers.³⁶ Both PEG and PEtOz can constitute hydrophilic segments of copolymers forming polymeric micelles.

Copolymer micelles

Block copolymer micelles (Fig. 1A) are often tailored for encapsulation of water-insoluble drugs. Such artificial vesicles can mimic the structure and function of natural biological transport systems.⁵ In aquatic environment, amphiphilic properties of block copolymers favor

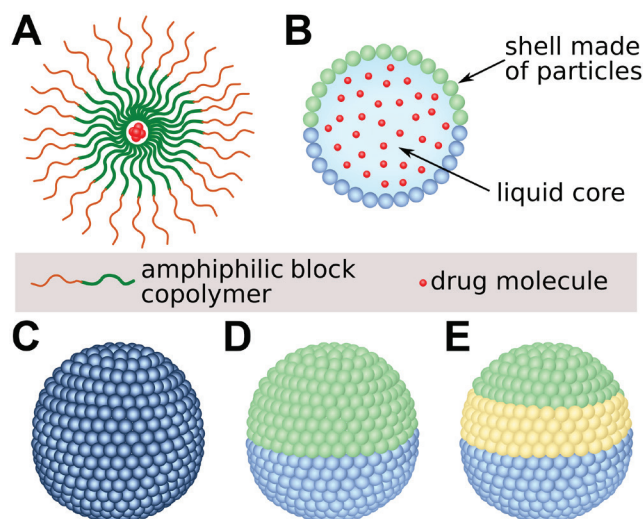


Fig. 1. Examples of polymer drug carriers. A. Amphiphilic copolymer micelle; B. Capsule with the shell composed of polymer particles; C. Capsule with homogeneous shell; D. Capsule with Janus shell; E. Capsule with patchy shell

self-organization into micelles, in which hydrophilic regions face outwards and hydrophobic inwards.³⁷ The decrease in free energy of the system due to the removal of hydrophobic regions from water neighborhood is the main driving force responsible for this process.¹⁷ In general, hydrophilic block is usually PEG or PEtOz, while hydrophobic block can be a polyester, e.g., poly(caprolactone) (PCL) or poly(DL-lactide) (PDLA); a polyamino acid, e.g., poly(β -benzyl-L-aspartate) (PBLA), poly(lactic-co-glycolic acid) (PLGA); or a polyether, e.g., poly(propylene oxide) (PPO).^{9,13} As previously mentioned, the hydrophobic segments form a compartment in which the lipophilic payload is enclosed, while the hydrophilic parts are in contact with the biological environment. The great advantage of encapsulating drugs in polymer micelles is the ability to eliminate toxic solubilizers, including Cremophor EL or dimethyl sulfoxide (DMSO).³⁸ Drug preparations free of harmful surfactants and organic cosolvents are safer for patients and do not cause so many adverse side effects as traditional formulations.³⁹ It is worth presenting selected examples of utilizing various types of block copolymers for the formation of micelles designed as carriers of cytostatic drugs.

Self-assembled poly(ethylene oxide)-block-poly(L-amino acid) (PEO-b-PLAA) micelles, thanks to free functional groups of the PLAA block, easily form drug-polymer conjugates.⁵ In aqueous environment, amphiphilic PEO-PPO block copolymers also aggregate into stable micelles capable of transporting water-insoluble medications inside their hydrophobic cores.⁸ Pluronic P123 (PEO-PPO-PEO synthetic triblock copolymer) micelles loaded with paclitaxel were administered to rats and mice in order to check the pharmacokinetics and tissue distribution of this formulation.¹⁰ Study proved the prolonged circulation time of vehicles due to the presence of hydrophilic

PEO shell additionally protecting against the recognition by reticuloendothelial system.¹⁰ In vivo studies were also performed with spherical Pluronic P123 micelles containing docetaxel.^{40–42} It is worth mentioning that the thermodynamics of spontaneous Pluronic P123 micellization in water can be influenced by temperature changes and the addition of different solvents, e.g., ethanol, 1-propanol, glycerol, or protic ionic liquid ethylammonium nitrate.⁴³ Therefore, the self-assembly process of Pluronic drug carriers is adjustable.

Grafted polyphosphazenes are also promising candidates for microsphere and micelle forming materials due to biodegradability, tunable properties and flexibility in structural design.⁴⁴ The thermosensitive polyphosphazene micelles containing hydrophilic segments of oligo-poly(*N*-isopropylacrylamide) and hydrophobic groups of ethyl 4-aminobenzoate may be useful as carriers of hydrophobic medications.⁴⁵ Polymeric micelles built of amphiphilic graft polyphosphazenes with hydrophilic poly(*N*-isopropylacrylamide-co-*N,N*-dimethylacrylamide) (Poly(NIPAm-co-DMAA)) and hydrophobic ethyl glycinate as side groups have already been tested as doxorubicin carriers.⁴⁶ It is believed that desirable features of polyphosphazene-based polymers, in particular the self-neutralizing properties of their degradation products and the possibility of smooth integration of the polyphosphazene skeleton with the substituent groups, open up new prospects for the design of next-generation drug delivery systems.⁴⁷

The stability of vehicles composed of methoxy poly(ethylene oxide)-poly(L-lactide) (MePEO-PLLA) block copolymer depends on the polymerization method. Research showed that structures prepared with solution polymerization were kinetically more stable than those obtained using bulk polymerization.⁴⁸ The capability of (m)PEG-PDLLA micelles to be efficiently loaded with hydrophobic drugs can be qualitatively predicted based on calculated solubility parameters.⁴⁹ The PEG-PDLLA nanocarriers have already been tested with paclitaxel,⁵⁰ doxorubicin⁵¹ and tanespimycin.³⁹

One of the most studied drugs – doxorubicin – was also encapsulated in vehicles prepared using biocompatible copolymer composed of PEO and poly(γ -benzyl l-glutamate) (PBLG), which is synthetic polypeptide with the ability to form secondary structures such as α -helices or β -strands.³⁷ These PEO-PBLG diblock and PBLG-PEO-PBLG triblock copolymer micelles were effectively internalized by human head and neck squamous carcinoma cells in vitro.³⁷

Biodegradable diblock mPEG-PCL micelles were used for encapsulation of doxorubicin⁵² and paclitaxel.⁵³ The PEG-PCL copolymer and its modified version containing benzylcarboxylate side chain were also used for producing nanomicelles loaded with silibinin – a poorly water-soluble antioxidant and antineoplastic agent.²² A study showed that micelles provided high encapsulation efficiency and sustained release of this active substance, and also

contributed to its increased cytotoxicity against melanoma cells.²² Improved targeting ability was reported for rituximab-conjugated PEO-poly(ester) micelles of different structures prepared for treatment of lymphoma cells.⁷

Self-assembled nanocarriers composed of D- α -tocopheryl poly(ethylene glycol) succinate-block-poly(ϵ -caprolactone) (TPGS-b-PCL) and loaded with paclitaxel owe their properties to PEG, which extends their circulation time, and vitamin E, that enhances the cellular uptake of the medication.⁵⁴ The TPGS, which is a derivative of the natural vitamin E (α -tocopherol) conjugated with PEG, was also used as a component for the production of micelles containing docetaxel.⁵⁵ Among the advanced delivery systems, tested both in vitro and in vivo, one can mention pH-sensitive, multidrug (α -tocopherol and doxorubicin) grafted O-carboxymethyl chitosan polymeric micelles with chemically conjugated targeting ligand (anti-HER2/neu peptide-PEG).⁵⁶

In contemporary oncology, synergistic drug combinations are often used in order to increase the effectiveness of the therapy. The PEG-b-PDLLA micelles are capable of encapsulating up to 3 poorly water-soluble chemotherapeutic agents at the same time, which was proven in experiments with paclitaxel, etoposide, docetaxel, and tanespimycin.⁵⁷ The formulation of paclitaxel and tanespimycin, which utilized 1,2-distearoyl-*sn*-glycero-3-phosphoethanolamine-*N*-methoxy(polyethylene glycol) ((m)PEG-DSPE) and TPGS copolymers, significantly extended the circulation time and increased the intratumoral accumulation of these synergistic drugs.³⁸ The co-encapsulation of sorafenib and all-trans retinoic acid in PEG-PLGA copolymer micelles allowed for obtaining prolonged release and effective cell uptake of both agents in thyroid cancer-bearing mice.⁵⁸ The co-encapsulation does not have to be limited to pharmaceuticals. Doxorubicin and microRNA-34a (tumor suppressor RNA) were trapped in hybrid nanomicelles containing 2 amphiphilic diblock copolymers PEG-PCL and polyethylenimine-PCL in order to combine the effects of chemotherapy and gene therapy.⁵⁹ The summary of different types of polymeric micelles used as drug carriers and their basic properties is presented in Table 1.

Micellar drug formulations designed by scientists are increasingly used in clinical trials and cancer treatment. One can mention commercially available delivery systems such as Genexol PM[®] (paclitaxel loaded mPEG-PDLLA diblock copolymer micelles),⁶⁰ Nanoxel – PM[®] (docetaxel loaded mPEG-PDLLA micelles),^{61,62} Apealea[®]/Paclical[®] (micellar paclitaxel),^{6,63} and Paxceed[®] (mPEG-PDLLA micellar formulation of paclitaxel, originally tested for the treatment of rheumatoid arthritis).⁶² Although more and more micellar drug formulations are approved for clinical trials, some of the products do not live up to expectations. Phase I clinical trial and pharmacokinetics evaluation of NK911 PEG-poly(aspartic acid) block copolymer micelles containing doxorubicin showed that these structures were less stable in plasma and less efficient at drug delivery to solid tumors

Table 1. Summary of different types of polymeric micelles and their basic properties

Polymer/ copolymer type	Cargo	Size	Basic properties	Reference
PEO-PCL	rituximab, paclitaxel	95 ±20.6 nm	CMC = 18.2 ±2.5 µg/m PDI = 0.284 ±0.068 kinetically stable <6 h in SDS drug release = 40.7 ±4.5% within 48 h improved tumor targeting efficiency	7
	silibinin	54.73 ±1.82 nm	PDI = 0.31 ±0.06 zeta potential of -2.23 ±0.14 mV drug release = 91.7 ±0.81% within 24 h	22
PEG-PCL/PEI-PCL	doxorubicin, miRNA-34a	≈64.34 nm ≈105.4 nm ≈160.7 nm	hybrid micelles CMC ≈ 8.57 µg/mL PDI of 0.24–0.28 zeta potential of 5.43; 19.3; 32.6 mV (for different molar ratios of copolymers) pH dependent drug release: ≈78.2% (pH 7.4) and 88.6% (pH 5.5) within 24 h in PBS	59
mPEG-PCL	doxorubicin	25.4 ±0.2 nm 22.9 ±0.2 nm 37.3 ±0.2 nm 84.0 ±0.3 nm 104.9 ±0.2 nm	CMC ≈ 20 µg/mL or ≈12 µg/mL size of micelles determined by PCL block length hemocompatibility pH dependent drug release influence on cellular distribution of drug	52
	paclitaxel	<124 nm (before core cross-linking) <202 nm (core- cross-linked)	size of micelles determined by PCL block length drug encapsulation dependent on the PCL length and cross-linking enhanced loading efficiency after cross-linking of micelle core stability against dilution in water weak stability in the presence of serum protein (BSA, 2.5%)	53
PEO-PBCL	rituximab, paclitaxel	110 ±11.6 nm	CMC = 12.3 ±3.1 µg/mL PDI = 0.216 ±0.010 kinetically stable >24 h in SDS drug release = 60.75 ±3.70% within 48 h improved tumor targeting efficiency	7
	silibinin	46.9 ±0.33 nm	PDI = 0.33 ±0.01 zeta potential of -3.23 ±0.32 mV sustained release of cargo 30.5 ±1.5% within 24 h	22
TPGS-PCL	paclitaxel	60.6–209.4 nm (depending on MW of PEG and TPGS)	self-assembly only for copolymers with PEG molecular weights ≥2 kDa PDI of 0.16–0.53 (depending on MW of PEG and TPGS) CMC of 5.44–41.00 µM (depending on MW of hydrophobic block) extended circulation time sustained release of drug, e.g., 10% within 12 h and 36% within 72 h in PBS (pH 7.4)	54
TPGS	docetaxel	12.4–14.4 nm	CMC < 2.2 mM PDI of 0.166–0.290 drug release ≈50% (pH 7.4) within 16 h, 24 h or 90 h in PBS depending on TPGS content influence on drug biodistribution	55
PEtOz-PU-PEtOz	doxorubicin	175.9 ±6.6 nm	CMC ≈ 0.43 mg/L PDI ≈ 0.11 zeta potential of -20.6 mV high stability; "stealth" property pH dependent drug release ≈29% (pH 7.4); 92% (pH 5.0) within 24 h in acetate buffer	36
Pluronic P123 (PEO-PPO-PEO)	paclitaxel	25.2 ±2.9 nm (freshly prepared) 28.5 ±2.1 nm (freeze-dried)	CMC ≈ 4.4 × 10 ⁻⁶ mol/L drug release ≈ 41.2% within 4 h and 87.8% within 24 h in sodium salicylate solution "stealth" property – prolonged circulation time in plasma influence on drug pharmacokinetics and biodistribution	10
	docetaxel	9–55 nm (freshly prepared) 22–84 nm (freeze-dried)	physically entrapped drug zeta potential of -10.56 ±2.34 mV (fresh) and -12.45 ±3.24 mV (freeze-dried) remarkable antitumor activity high encapsulation efficacy drug release ≈84.05% within 24 h (in PBS, pH 7.4, 37 ±0.5°C)	40
		85.30 ±1.59 nm	covalently conjugated drug CMC = 1.34 ±0.05 × 10 ⁻⁵ mol/L PDI ≈ 0.267 zeta potential of -19.34 ±3.25 mV pH dependent drug release ≈1.83% (pH 7.4); 4.23% (pH 5.0); 8.67% (pH 1.2) within 24 h in PBS significant antitumor activity	41
	≈138 nm (average)	covalently conjugated drug (hydrazone bonds) CMC ≈ 7.232 × 10 ⁻⁵ mol/L pH dependent drug release ≈13.4% (pH 7.4); 84.9% (pH 5.0) within 48 h in PBS at 37 ±0.5°C	42	

Table 1. Summary of different types of polymeric micelles and their basic properties – cont

Polymer/copolymer type	Cargo	Size	Basic properties	Reference
PNIPAm/EAB-PPP	–	≈80 nm (average)	CMC ≈ 0.1 mg/mL LCST ≈ 32.6°C	45
P (NIPAm-DMAA)	doxorubicin	<150 nm	CMC ≈ 0.281; 0.178; 0.0324 g/L (depending on the content of hydrophobic ethyl glycinate) LCST ≈ 39.2°C physically loaded drug pH dependent drug release: ≈8.5% (pH 7.4), ≈21% (pH 6.5), ≈28% (pH 5.5) within 24 h in PBS good biocompatibility	46
mPEG-PDLLA	doxorubicin, SPIO	45 ±4 nm	multifunctional micelles (can incorporate lung cancer targeting peptide, drug and contrast agent) significantly increased cell targeting	51
PEO-PDLLA	tanespimycin	257 ±2 nm	CMC ≈ 350 nM release half-life ≈4 h (37°C, in water) lack of substantial sustained release prolonged circulation time in blood low toxicity (micelles well tolerated by rats)	39
	paclitaxel, etoposide, docetaxel, tanespimycin	30–40 nm	encapsulating up to 3 drugs high loading capacity PDI < 0.2 drug release profile dependent on drug combination	57
PEG-PLGA	sorafenib, all-trans retinoic acid	<200 nm	sustained release ≈56–62% within 72 h (pH 7.4) in PBS at 37°C effective cell uptake minimal systemic toxicity (mouse model)	58
OCMCh	α-tocopherol, doxorubicin	124.7–244.9 nm, 151.9–311.2 nm	functionalized with targeting ligand (anti-HER2/neu peptide-PEG) stable in blood plasma pH dependent drug release ≈0% (pH 7.4) and 90% (pH 5.2) within 6 h in PBS	56

CMC – critical micelle concentration; PDI – polydispersity index; LCST – lower critical solution temperature; MW – molecular weight; PBS – phosphate-buffered saline; PEO – poly(ethylene oxide); PCL – poly(ϵ -caprolactone); PBCL – poly(ϵ -benzylcarboxylate- ϵ -caprolactone); PEI – polyethylenimine; PEtOz – poly(2-ethyl-2-oxazoline); PU – polyurethane; PPO – poly(propylene oxide); PNIPAm – poly(N-isopropylacrylamide); EAB – ethyl 4-aminobenzoate; PPP – polyphosphazene; DMAA – dimethylacrylamide; PDLLA – poly(D, L-lactide); PLGA – poly(lactic-co-glycolic acid); SPIO – superparamagnetic iron oxide; TPGS – D- α -tocopheryl poly(ethylene glycol) succinate; OCMCh – O-carboxymethyl chitosan.

than PEGylated liposomal doxorubicin known as Doxil[®].⁶⁴ Table 2 summarizes clinical applications of polymeric micelles as carriers of anticancer drugs. Clinical trials with published results have been already performed for formulations with names: Genexol-PM[®],^{65–76} Nanoxel M[®],⁷⁷ NK 911,⁶⁴ NK 105,^{78–82} NK 012,^{83–87} NC-6004,^{88–91} NC-6300,^{92–94} BIND-014,^{95–97} and Sp1049C.^{98–100}

The behavior of polymeric micelles after administration is related to several stress factors acting on these carriers. The major problems are: immediate dilution of the formulation following injection, biophysical interactions with corpuscular blood components, serum proteins, enzymes, etc., and immunological response of the body.¹⁰¹ If the shell of micelles fails to provide them “stealth” properties, they will be covered with opsonins and quickly removed by the mononuclear phagocyte system.^{24,101} Another issue associated with in vivo applications of some polymeric micelles is the premature release of the encapsulated drug due to the loss of integrity of these carriers in circulating blood.⁴⁸ As an example, it is worth mentioning the rapid separation of hydrophobic drug from the PEG-PDLLA micelles injected into the bloodstream of the tumor bearing mice.¹⁰² One approach to limiting the uncontrolled leakage of active content is the formation of multilayer

micelles. Each layer can be made of a different material and perform distinct function. This is the case for ABC triblock copolymer micelles, where A block (PEO) provides an outer covering, B block (PLA) forms a barrier against drug release, and C block (PCL) builds an inner core and a reservoir for the medication.¹⁰³ However, the properties of such structures in terms of kinetic stability and cargo release profile are still not optimal. Drug delivery systems based on polymeric micelles are constantly developed and improved to better protect the payload and meet the high safety standards set by modern medicine.

Capsules with the shell composed of polymer particles

Another group of capsules encompasses the structures with the shell built of many polymer particles (Fig. 1B). Such nano- or microparticles are usually fused, which ensures the integrity of the entire coating. One of the methods of fabricating particle capsules utilizes so called Pickering droplets. These liquid drops are covered with densely packed particles adsorbed on their surface.¹⁰⁴ The electric field-assisted mechanisms of assembling colloidal particles

Table 2. Clinical applications of polymeric micelles as carriers of anticancer drugs. Data based on the results of clinical trials published in journal articles

Name/trade name	Copolymer type	Cargo	Applications (clinical trials with published results)			
			cancer type	combination	phase of clinical trial	reference
Genexol-PM®	mPEG-PDLLA	paclitaxel	advanced malignancies (lung, colorectal, renal, ovarian and breast cancers)	–	phase I	65
			lung, nasopharyngeal and breast cancers	–	phase I	66
			epithelial ovarian cancer	+ carboplatin	phase I	67
			epithelial ovarian cancer	+ carboplatin	phase II	68
			non-small cell lung cancer	+ cisplatin	phase II	69
			head and neck squamous cell carcinoma	+ cisplatin	phase II	70
			non-small cell lung cancer	+ gemcitabine	phase II	71
			biliary tract cancer	+ gemcitabine	phase II	72
			thymic epithelial tumors	+ cisplatin	phase II	73
			metastatic breast cancer	–	phase II	74
			urothelial carcinoma	–	phase II	75
			HER2-negative breast cancer	–	phase III	76
Nanoxel M®	PVP-b-PDLLA	docetaxel	breast cancer	+ cyclophosphamide	phase IV	77
NK 911	PEG-PASP	doxorubicin	pancreatic cancer	–	phase I	64
NK 105	PEG-PPBA	paclitaxel	breast, gastric, esophageal, renal pelvis, prostate and bladder tumors	–	phase I	78
			pancreatic, bile duct, gastric and colon cancers	–	phase I	79
			advanced gastric cancer	–	phase II	80
			breast cancer	–	phase III	81
			breast cancer	–	phase III	82
NK 012	PEG-b-P(Glu)	SN-38 (active metabolite of irinotecan)	advanced solid tumors (lung, breast, ovarian, esophageal, gastric, colon, and endometrial cancers)	–	phase I	83
			solid tumors (colorectal, pancreatic, esophageal, and small and non-small cell lung cancers)	–	phase I	84
			gastrointestinal malignancies	+ 5-fluorouracil	phase I	85
			multiple myeloma	–	phase I/II	86
			colorectal cancer	–	phase II	87
NC-6004	PEG-P(Glu)	cisplatin	advanced solid tumors (lung, colon, pancreatic, esophageal, and renal cancers)	–	phase I	88
			advanced solid tumors (carcinoma, neuroendocrine tumors)	+ gemcitabine	phase I	89
			advanced solid tumors (lung, colorectal, endocrine, squamous cell head and neck, breast, and gastro/esophageal cancers)	+ gemcitabine	phase I b/II	90
			squamous non-small cell lung carcinoma, biliary tract and bladder cancers	+ gemcitabine	phase II	91
NC-6300	PEG-b-PASP	epirubicin	advanced solid tumors (urothelial, breast and other cancers)	–	phase I	92
			cutaneous and non-cutaneous angiosarcoma	–	phase I b	93
			sarcoma, osteosarcoma and other tumors	–	phase I b	94
BIND-014	PEG-PLA	docetaxel	advanced solid tumors (lung, head and neck, ovarian, prostate, rectal, and other cancers)	–	phase I	95
			metastatic castration-resistant prostate cancer	+ prednisone	phase II	96
			metastatic castration-resistant prostate cancer	+ prednisone	phase II	97

Table 2. Clinical applications of polymeric micelles as carriers of anticancer drugs. Data based on the results of clinical trials published in a journal article – cont.

Name/trade name	Copolymer type	Cargo	Applications (clinical trials with published results)			
			cancer type	combination	phase of clinical trial	reference
Sp1049C	Pluronic F127 and Pluronic L61®	doxorubicin	colorectal, esophageal and lung cancer, soft-tissue sarcoma, mesothelioma and other cancers	–	phase I	98
			esophageal adenocarcinoma	–	phase II	99
			adenocarcinoma of the esophagus and gastroesophageal junction	–	phase II	100

mPEG – methoxy poly(ethylene glycol); PDLLA – poly(D, L-lactide); PVP – poly(N-vinylpyrrolidone); PASP – poly(aspartic acid); PPBA – poly(4-phenyl-1-butanoate-L-aspartamide); P(Glu) – poly(glutamic acid); PLA – poly(lactic acid).

at the fluid interfaces are described in details in a study dedicated specifically to this subject.¹⁰⁵ Microwave heating of highly ordered jammed Pickering droplets allows for fusing (to a certain extent) and interlocking the shell particles, and thus creating capsules with the cohesive shells.¹⁰⁶ However, the electroformation method is used not only for the production of homogeneous capsules (Fig. 1C), but also for the fabrication of heterogeneous structures. Janus and patchy particle shells can be formed using the joint action of electrohydrodynamic flows and electrocoalescence of 2 or several leaky dielectric droplets partially covered with different kind of particles and embedded in another leaky dielectric medium.¹⁰⁷ It is worth recalling that the shell of the Janus capsule is composed of 2 similarly sized hemispheres, each made of separate material (Fig. 1D). The covering of patchy capsule (Fig. 1E) can comprise more regions with various shares in the total area of the sphere. When the patches are characterized by distinct chemical or physical properties, the functionality of the whole structure might be considerably extended.¹⁰⁸ The use of electroformation method followed by the thermal strengthening allowed to produce liquid-containing, ultrasound-sensitive capsules with a shell made of a monolayer of polyethylene and polystyrene microparticles.¹⁰⁶ An analogous preparation technique was used to fabricate Janus structures combining polystyrene particles with turmeric granules.¹⁰⁹

Elastic shells with adjustable permeability (dependent on the size of pores) are also produced through self-assembly of colloidal particles at the interface of emulsified droplets.¹¹⁰ The process of locking of the adsorbed particles can be performed in several ways, e.g., by sintering, the addition of polyelectrolyte molecules that bridge neighboring particles, or by inducing the van der Waals interaction between particles.¹¹⁰ For colloidal capsules with incorporated magnetite particles, the polymer shell strengthening was successfully performed with heating in the alternating magnetic field.¹¹¹ In case of submicron capsules prepared on the basis of the emulsion droplets stabilized by surface-modified gold nanoparticles, the shell reinforcement was carried out by chemical cross-linking (polymerization of olefinic bonds) induced by ultraviolet radiation.¹¹² Poly(methyl methacrylate) (PMMA) colloidal

particles adsorbed onto the surface of water droplets were held together by van der Waals forces.¹¹⁰

In the literature, the term “colloidosomes” often appears in reference to the structures having a shell comprising colloidal particles. This kind of capsules may be fabricated through Pickering emulsion interface-initiated atom transfer radical polymerization,¹¹³ using a double emulsification technique in a microfluidic device,¹¹⁴ and by extraction or dissolving of the template core of coated particles.^{115–117} Details about the techniques for preparing various sorts of colloidosomes can be found in a dedicated review.¹¹⁸ However, methods for producing colloidosomes are still being developed. Recently, emulsion droplets have been used as templates for interfacial polymerization of the monomers and thus, contributed to hierarchical assembly of two-dimensional polymers into colloidosomes and microcapsules.¹¹⁹

The majority of colloidosomes designed and manufactured so far had homogeneous shells, including those composed of charge-stabilized fluorescent polystyrene beads,¹²⁰ poly(vinyl difluoride) nanoparticles,¹¹⁴ polymeric microrods,¹²¹ or chitosan-modified silica nanoparticles.¹²² Due to the fact that capsules with particle shells are mainly intended for biomedical use, they are often tested in the role of anticancer drugs carriers. As an example, one can mention doxorubicin hydrochloride-loaded, poly(methyl methacrylate-co-butyl acrylate) colloidosomes protected with an additional silver shell¹²³ and their gold-coated counterparts with attached immunoglobulin G.¹²⁴ The second outer coating, comprising metal particles, was introduced in order to make the capsules impermeable, because pure polymer coverage was inherently porous and thus leaky to low-molecular-weight substances.^{123,125,126} Treatments such as cross-linking or increasing the thickness of the polymer coating may reduce the diffusion of small molecules through the shell, but cannot stop this process completely over a longer period of time.¹²⁶ Therefore, the additional protective layer made of interlocked solid particles seems to be an effective solution. Such a double casing was used in case of polyacrylamide/silica composite capsules¹²⁷ and gold-coated PMMA microcapsules.¹²⁸ In the latter, the growth of a secondary metallic film was catalyzed by metallic nanoparticles adsorbed onto polymeric shells.¹²⁸ Well-designed capsules

should prevent the leakage of active substances, and thus provide the long-term protection of the cargo during its storage and transport to the predefined destination.

Payload liberation strategies

The liberation of encapsulated anticancer drug can be sustained owing to the certain permeability of the shell or may result from the rupture of capsules. This disintegration must be triggered and take place near the predefined destination, i.e., tumor region. In general, factors provoking payload release can be divided into 3 groups: biological (mainly enzymes present at the target site), chemical (change in pH of a medium or salt effect on the coating) and physical (ultraviolet or infrared light, electric and magnetic field, temperature, mechanical force, and ultrasonic waves).¹²⁹

It is expected that faster release of the drug will take place within the solid tumor, where pH is lower in comparison with normal tissue and the bloodstream.^{52,130} Hence, the fabrication of pH responsive capsules is a very common practice – for example regarding doxorubicin-loaded polyelectrolyte microcapsules built of sodium poly(styrene sulfonate) and poly(allylamine hydrochloride),¹³¹ micelles made of mPEG-*b*-PCL,⁵² PEG-PBLA,^{20,130} and PEO-*b*-polyurethane-SS-*b*-PEtOz.^{36,132} In the abovementioned cases, the release of cytostatic drug was intensified as the pH decreased, because a slightly acidic conditions contributed to the rapid disassembling of polymer micelles.

Local heating of the target region to the temperature slightly higher than the normal human body temperature in order to induce breakage of polymer carriers is also considered as one of the controlled release strategies. The proper adjustment of the properties of comonomers, which allows to optimally tune a lower critical solution temperature (LCST), is crucial for thermosensitive polymers.¹³³ When the temperature of aqueous environment is below the LCST, hydrogen bonds between water molecules and polar groups of the polymer facilitate its solubility. When the temperature is above LCST, the network of hydrogen bonds breaks up and phase separation is observed.¹³⁴ The collapse of polymer chains followed by their aggregation cause the degradation of the entire vehicle. For polymeric drug carriers designed for medical applications, the LCST in which the material exhibits reversible thermo-responsive phase transition should be in a range of 37–42°C.^{133,135} Copolymers based on poly(*N*-isopropylacrylamide) are frequently used for preparation of thermo-triggered vehicles.²¹ Thermally sensitive micelles containing doxorubicin were produced using poly(*N*-isopropylacrylamide-co-*N*, *N*-dimethylacrylamide)-*b*-PLGA (P(NIPAAm-co-DMAAm)-*b*-PLGA) copolymer with various lengths of PLGA block.¹³⁶ The anticancer activity of methotrexate-loaded poly(*N*-isopropylacrylamide-co-acrylamide)-*b*-poly(*n*-butyl methacrylate) (P(NIPAAm-co-AAm)-*b*-PBMA) micelles was significantly improved

by local hyperthermia.¹³³ A similar situation was observed for docetaxel loaded poly(*N*-isopropylacrylamide-co-acrylamide)-*b*-PDLLA (Poly(IPAAm-co-AAm)-*b*-PDLLA) micelles.¹³⁵ Overall, well-designed thermoresponsive carriers should protect the whole organism against the toxic effect of the drug at physiological temperature and be able to release the payload on demand in the heated region.

It is well known that an alternating magnetic field acting on magnetic nanoparticles can induce hyperthermia.¹³⁷ Therefore, such nanoparticles are sometimes incorporated into capsules or micelles made of thermosensitive polymers. Thus, due to the magnetic hyperthermia, drug release can be remotely triggered. The enhanced hyperthermic release of doxorubicin was observed for poly(ethylene glycol)-poly(lactide) (PEG-PLA) micelles conjugated with iron oxide nanoparticles coated with citric acid.¹³⁸

In case of capsules with a liquid core, the radio-frequency magnetic heating of suspended nanoparticles can cause the local rise in liquid temperature. The temperature gradient between the inside and the outside of the shell promotes the increased diffusion of the drug.²⁵ Electromagnetic field easily penetrates human body, so it can be successfully used for deep tissue targeting. The latest trend is the fabrication of nanotransporters, which exhibit multiple magnetic-responsive behaviors under the influence of various electromagnetic frequencies, e.g., magnetophoresis in the range of 30–500 Hz and magneto-thermal effect in the range of 100–500 kHz.²⁶ The former of the mentioned physicochemical effects facilitates the mobility of the carrier through cellular barriers and the latter aids in burst release of a drug in the target. Such frequency-programmed operations were successfully performed for doxorubicin-loaded nanovehicles comprising ferrimagnetic iron oxide ring coated with a thermoresponsive polyethylenimine terminated with isobutyramide groups.²⁶

The inclusion of nanoparticles into polymeric carriers may also facilitate the ultrasound-triggered release of the drug. The study of microcapsules with polyelectrolyte: cationic poly(allylamine hydrochloride) and anionic poly(sodium styrene sulfonate) multilayer shells showed that the incorporation of iron oxide nanoparticles into these shells considerably enhanced their sensitivity to ultrasound.¹⁸ The addition of gold nanoparticles into the shells of polypyrrole capsules increased their sensitivity to ultrasound.¹³⁹ Capsules with the coating made of polymer particles can be inherently sensitive to ultrasound. The cargo from submillimeter- and millimeter-sized capsules with homogeneous, Janus and patchy shells was released in specific direction in fully controllable manner, under the influence of MHz-frequency acoustic waves.^{106,109} Other physical mechanisms were responsible for the ultrasound-induced doxorubicin liberation from polyelectrolyte microcapsules made of poly(allylamine hydrochloride)/polystyrene sulfonate,¹⁴⁰ microspheres composed of multilayers of tannic acid and poly(*N*-vinylpyrrolidone),¹⁴¹ or PLGA-based nanodroplets.¹⁴² In general,

ultrasonic waves show great potential as triggering factor, because they are harmless, easy to focus, and widely used thanks to the availability of commercial medical devices.¹⁴³

When discussing the physical factors that are capable of releasing active substances from polymer capsules, it is also worth mentioning ultraviolet (UV) radiation. Among the advantages of using UV light as a trigger, one can highlight the possibility of precise temporal and spatial control of this stimulus.¹⁴⁴ Micelles can be molded from amphiphilic block copolymers with photodegradable linker, acting as a junction between hydrophilic and hydrophobic chains.^{144,145} Polyurea microcapsules with liquid cores,¹⁴⁶ unimolecular micelles containing PMMA and poly(poly(ethylene glycol) methyl ether methacrylate)¹⁴⁷ and nanomicelles composed of PEG connected with doxorubicin via UV-sensitive amide linkage¹⁴⁸ are just a few examples of photocleavable polymeric structures.

Some drug delivery systems are sensitive to a variety of factors that allow to trigger the payload liberation at different timescales. For example, polyurethane nanocapsules released their payload under the action of UV light, temperature and pH change within minutes, hours and days, respectively.¹⁴⁹ Dual-responsive doxorubicin loaded poly(methacrylic acid)–poly(ϵ -caprolactone) micelles owe their properties to the linker containing adjacent photo- and redox-sensitive sites.¹⁴⁵

There is no doubt that stimuli-responsive polymer micelles and capsules will gain more and more applications, in particular in medicine. The fabrication of biocompatible and biodegradable drug carriers is especially important for contemporary oncology. The safe delivery of cytostatic medications to the tumor region and their controlled release on demand will allow to minimize the adverse effects of chemotherapy treatment.

ORCID iDs

Tomasz Kubiak  <https://orcid.org/0000-0002-6991-6127>

References

- Chen H, Li J, Wan J, Weitz DA, Stone HA. Gas-core triple emulsions for ultrasound triggered release. *Soft Matter*. 2013;9(1):38–42. doi:10.1039/C2SM26992A
- Urbas R, Milošević R, Kašiković N, Pavlović Ž, Elesini US. Microcapsules application in graphic arts industry: A review on the state-of-the-art. *Iranian Polym J (Eng Ed)*. 2017;26(7):541–561. doi:10.1007/s13726-017-0541-1
- Tomaro-Duchesneau C, Saha S, Malhotra M, Kahouli I, Prakash S. Microencapsulation for the therapeutic delivery of drugs, live mammalian and bacterial cells, and other biopharmaceuticals: Current status and future directions. *J Pharm (Cairo)*. 2013;2013:103527. doi:10.1155/2013/103527
- Szafraniec-Szczęsny J, Janik-Hazuka M, Odrobińska J, Zapotoczny S. Polymer capsules with hydrophobic liquid cores as functional nanocarriers. *Polymers (Basel)*. 2020;12(9):1999. doi:10.3390/polym12091999
- Lavasanifar A, Samuel J, Kwon GS. Poly(ethylene oxide)-block-poly(L-amino acid) micelles for drug delivery. *Adv Drug Deliv Rev*. 2002;54(2):169–190. doi:10.1016/s0169-409x(02)00015-7
- García MC, Aloisio C, Onnainty R, Ullio-Gamboa G. Part 3. Self-assembled nanomaterials. In: Narayan R, ed. *Nanobiomaterials*. Sawston, UK: Woodhead Publishing; 2018:41–94.
- Saqr A, Vakili MR, Huang YH, Lai R, Lavasanifar A. Development of traceable rituximab-modified PEO-polyester micelles by postinsertion of PEG-phospholipids for targeting of B-cell lymphoma. *ACS Omega*. 2019;4(20):18867–18879. doi:10.1021/acsomega.9b02910
- Chiappetta DA, Sosnik A. Poly(ethylene oxide)–poly(propylene oxide) block copolymer micelles as drug delivery agents: Improved hydro-solubility, stability and bioavailability of drugs. *Eur J Pharm Biopharm*. 2007;66(3):303–317. doi:10.1016/j.ejpb.2007.03.022
- Liu J, Lee H, Allen C. Formulation of drugs in block copolymer micelles: Drug loading and release. *Curr Pharm Des*. 2006;12:4685–4701. doi:10.2174/138161206779026263
- Han LM, Guo J, Zhang LJ, Wang QS, Fang XL. Pharmacokinetics and biodistribution of polymeric micelles of paclitaxel with Pluronic P123. *Acta Pharmacol Sin*. 2006;27(6):747–753. doi:10.1111/j.1745-7254.2006.00340.x
- Engels F, Mathot R, Verweij J. Alternative drug formulations of docetaxel: A review. *Anticancer Drugs*. 2007;18(2):95–103. doi:10.1097/CAD.0b013e3280113338
- Meredith AM, Dass CR. Increasing role of the cancer chemotherapeutic doxorubicin in cellular metabolism. *J Pharm Pharmacol*. 2016; 68(6):729–741. doi:10.1111/jphp.12539
- Yang F, Xu J, Fu M, Ji J, Chi L, Zhai G. Development of stimuli-responsive intelligent polymer micelles for the delivery of doxorubicin. *J Drug Targeting*. 2020;28(10):993–1011. doi:10.1080/1061186X.2020.1766474
- Situ JQ, Wang XJ, Zhu XL, et al. Multifunctional SPIO/DOX-loaded A54 homing peptide functionalized dextran-g-PLGA micelles for tumor therapy and MR imaging. *Sci Rep*. 2016;6(1):35910. doi:10.1038/srep35910
- Nakamura J, Nakajima N, Matsumura K, Hyon SH. Water-soluble taxol conjugates with dextran and targets tumor cells by folic acid immobilization. *Anticancer Res*. 2010;30(3):903. PMID:20393013.
- Li Q, Li X, Zhao C. Strategies to obtain encapsulation and controlled release of small hydrophilic molecules. *Front Bioeng Biotechnol*. 2020; 8:437. doi:10.3389/fbioe.2020.00437
- Torchilin VP. Micellar nanocarriers: Pharmaceutical perspectives. *Pharm Res*. 2006;24(1):1–16. doi:10.1007/s11095-006-9132-0
- Kolesnikova TA, Khlebtsov BN, Shchukin DG, Gorin DA. Atomic force microscopy characterization of ultrasound-sensitive nanocomposite microcapsules. *Nanotechnologies in Russia*. 2008;3(9):560–569. doi:10.1134/S1995078008090048
- Sun Q, Chen JF, Routh AF. Coated colloidosomes as novel drug delivery carriers. *Exp Opin Drug Deliv*. 2019;16(9):903–906. doi:10.1080/17425247.2019.1652594
- Kataoka K, Matsumoto T, Yokoyama M, et al. Doxorubicin-loaded poly(ethylene glycol)–poly(β -benzyl-L-aspartate) copolymer micelles: Their pharmaceutical characteristics and biological significance. *J Controlled Release*. 2000;64(1–3):143–153. doi:10.1016/S0168-3659(99)00133-9
- Wei H, Cheng SX, Zhang XZ, Zhuo RX. Thermo-sensitive polymeric micelles based on poly(N-isopropylacrylamide) as drug carriers. *Prog Polym Sci*. 2009;34(9):893–910. doi:10.1016/j.progpolymsci.2009.05.002
- Rad A, Asiaee F, Jafari S, Shayanfar A, Lavasanifar A, Molavi O. Poly(ethylene glycol)–poly(ϵ -caprolactone)-based micelles for solubilization and tumor-targeted delivery of silibinin. *Bioimpacts*. 2019;10(2):87–95. doi:10.34172/bi.2020.11
- Dhaliwal A, Zheng G. Improving accessibility of EPR-insensitive tumor phenotypes using EPR-adaptive strategies: Designing a new perspective in nanomedicine delivery. *Theranostics*. 2019;9(26):8091–8108. doi:10.7150/thno.37204
- Conniot J, Silva J, Fernandes J, et al. Cancer immunotherapy: Nanodelivery approaches for immune cell targeting and tracking. *Front Chem*. 2014;2:1. doi:10.3389/fchem.2014.00105
- Kong SD, Zhang W, Lee JH, et al. Magnetically vectored nanocapsules for tumor penetration and remotely switchable on-demand drug release. *Nano Lett*. 2010;10(12):5088–5092. doi:10.1021/nl1033733
- Liu X, Zhang Y, Guo Y, et al. Electromagnetic field-programmed magnetic vortex nanodelivery system for efficacious cancer therapy. *Adv Sci (Weinh)*. 2021;8(18):2100950. doi:10.1002/advs.202100950
- Kubiak T. The use of shells made of poly(ethylene glycol) and chitosan to ensure the biocompatibility of nanoparticles in biomedical applications [in Polish]. *Polim Med*. 2014;44(2):119–127. PMID:24967783.

28. Rodrigues S, Dionisio M, Remuñán-López C, Grenha A. Biocompatibility of chitosan carriers with application in drug delivery. *J Funct Biomater*. 2012;3(3):615–641. doi:10.3390/jfb3030615
29. Krzymiński R, Kubiak T, Dobosz B, Schroeder G, Kurczewska J. EPR spectroscopy and imaging of TEMPO-labeled magnetite nanoparticles. *Curr Appl Phys*. 2014;14(5):798–804. doi:10.1016/j.cap.2014.03.021
30. Kubiak T, Krzymiński R, Dobosz B, Schroeder G, Kurczewska J, Hałupka-Bryl M. A study of magnetite nanoparticles in whole human blood by means of electron paramagnetic resonance [in Polish]. *Inżynieria Biomedyczna Acta Bio-Optica et Informatica Medica*. 2015;21:9–15. <http://yadda.icm.edu.pl/baztech/element/bwmeta1.element.baztech-46fd6649-cfe9-4ed2-aec5-7382ef9e429d>
31. Kubiak T. Nanoparticles as radiosensitizers in photon and hadron radiotherapy. *Acta Bio-Optica et Informatica Medica Inżynieria Biomedyczna*. 2017;23:29–36. <http://yadda.icm.edu.pl/baztech/element/bwmeta1.element.baztech-0799f4ea-89b2-4c4b-908a-726e9c0c5618>
32. Borvinskaya E, Gurkov A, Shchapova E, Baduev B, Meglinski I, Timofeyev M. Distribution of PEG-coated hollow polyelectrolyte microcapsules after introduction into the circulatory system and muscles of zebrafish. *Biol Open*. 2018;7(1):bio030015. doi:10.1242/bio.030015
33. Cosco D, Paolino D, De Angelis F, et al. Aqueous-core PEG-coated PLA nanocapsules for an efficient entrapment of water soluble anticancer drugs and a smart therapeutic response. *Eur J Pharm Biopharm*. 2014;89:30–39. doi:10.1016/j.ejpb.2014.11.012
34. Prego C, Torres D, Fernandez-Megia E, Novoa-Carballal R, Quiñoa E, Alonso MJ. Chitosan-PEG nanocapsules as new carriers for oral peptide delivery: Effect of chitosan pegylation degree. *J Control Release*. 2006;111(3):299–308. doi:10.1016/j.jconrel.2005.12.015
35. Hinz A, Szczepanowicz K, Cierniak A, et al. In vivo studies on pharmacokinetics, toxicity and immunogenicity of polyelectrolyte nanocapsules functionalized with two different polymers: Poly-L-glutamic acid or PEG. *Int J Nanomedicine*. 2019;14:9587–9602. doi:10.2147/IJN.S230865
36. Xu K, Liu X, Bu L, Zhang H, Zhu C, Li Y. Stimuli-responsive micelles with detachable poly(2-ethyl-2-oxazoline) shell based on amphiphilic polyurethane for improved intracellular delivery of doxorubicin. *Polymers (Basel)*. 2020;12(11):2642. doi:10.3390/polym12112642
37. Kakkar D, Mazzaferro S, Thevenot J, et al. Amphiphilic PEO-b-PBLG diblock and PBLG-b-PEO-b-PBLG triblock copolymer based nanoparticles: Doxorubicin loading and in vitro evaluation. *Macromol Biosci*. 2015;215(1):124–137. doi:10.1002/mabi.201400451
38. Katragadda U, Fan W, Wang Y, Teng Q, Tan C. Combined delivery of paclitaxel and tanespimycin via micellar nanocarriers: Pharmacokinetics, efficacy and metabolomic analysis. *PLoS One*. 2013;8(3):e58619. doi:10.1371/journal.pone.0058619
39. Xiong MP, Yáñez JA, Kwon GS, Davies NM, Laird Forrest M. A Cremophor-free formulation for tanespimycin (17-AAG) using PEO-b-PDLLA micelles: Characterization and pharmacokinetics in rats. *J Pharm Sci*. 2009;98(4):1577–1586. doi:10.1002/jps.21509
40. Liu Z, Liu D, Wang L, Zhang J, Zhang N. Docetaxel-loaded Pluronic p123 polymeric micelles: In vitro and in vivo evaluation. *Int J Mol Sci*. 2011;12(3):1684–1696. doi:10.3390/ijms12031684
41. Liu Z, Wang Y, Zhang J, Li M, Liu Y, Zhang N. Pluronic P123-docetaxel conjugate micelles: Synthesis, characterization, and antitumor activity. *J Biomed Nanotechnol*. 2013;9(12):2007–2016. doi:10.1166/jbn.2013.1706
42. Liang Y, Su Z, Yao Y, Zhang N. Preparation of pH sensitive Pluronic-docetaxel conjugate micelles to balance the stability and controlled release issues. *Materials (Basel)*. 2015;8(2):379–391. doi:10.3390/ma8020379
43. He Z, Alexandridis P. Micellization thermodynamics of Pluronic P123 (EO20PO70EO20) amphiphilic block copolymer in aqueous ethylammonium nitrate (EAN) solutions. *Polymers (Basel)*. 2017;10(1):32. doi:10.3390/polym10010032
44. Ullah RS, Wang L, Yu H, et al. Synthesis of polyphosphazenes with different side groups and various tactics for drug delivery. *RSC Advances*. 2017;7(38):23363–23391. doi:10.1039/C6RA27103K
45. Zhang JX, Qiu LY, Jin Y, Zhu KJ. Physicochemical characterization of polymeric micelles constructed from novel amphiphilic polyphosphazene with poly(N-isopropylacrylamide) and ethyl 4-aminobenzoate as side groups. *Colloids Surf B Biointerfaces*. 2005;43(3):123–130. doi:10.1016/j.colsurfb.2005.03.012
46. Qiu LY, Wu XL, Jin Y. Doxorubicin-loaded polymeric micelles based on amphiphilic polyphosphazenes with poly(N-isopropylacrylamide-co-N,N-dimethylacrylamide) and ethyl glycinate as side groups: Synthesis, preparation and in vitro evaluation. *Pharm Res*. 2009;26(4):946–957. doi:10.1007/s11095-008-9797-7
47. Ogueri KS, Ogueri KS, Ude CC, Allcock HR, Laurencin CT. Biomedical applications of polyphosphazenes. *Med Devices Sens*. 2020;3(6):e10113. doi:10.1002/mds3.10113
48. Soleymani Abyaneh H, Vakili MR, Lavasanifar A. The effect of polymerization method in stereo-active block copolymers on the stability of polymeric micelles and their drug release profile. *Pharm Res*. 2014;31(6):1485–1500. doi:10.1007/s11095-013-1255-5
49. Sun J, Wei Q, Shen N, Tang Z, Chen X. Predicting the loading capability of mPEG-PDLLA to hydrophobic drugs using solubility parameters. *Chin J Chem*. 2020;38(7):690–696. doi:10.1002/cjoc.202000078
50. Kim SC, Kim DW, Shim YH, et al. In vivo evaluation of polymeric micellar paclitaxel formulation: Toxicity and efficacy. *J Control Release*. 2001;72(1):191–202. doi:10.1016/S0168-3659(01)00275-9
51. Guthi JS, Yang SG, Huang G, et al. MRI-visible micellar nanomedicine for targeted drug delivery to lung cancer cells. *Mol Pharm*. 2010;7(1):32–40. doi:10.1021/mp9001393
52. Shuai X, Ai H, Nasongkla N, Kim S, Gao J. Micellar carriers based on block copolymers of poly(caprolactone) and poly(ethylene glycol) for doxorubicin delivery. *J Control Release*. 2004;98(3):415–426. doi:10.1016/j.jconrel.2004.06.003
53. Shuai X, Merdan T, Schaper AK, Xi F, Kissel T. Core-cross-linked polymeric micelles as paclitaxel carriers. *Bioconjugate Chem*. 2004;15(3):441–448. doi:10.1021/bc034113u
54. Yusuf O, Ali R, Alomrani AH, et al. Design and development of D- α -tocopheryl polyethylene glycol succinate-block-poly(ϵ -caprolactone) (TPGS-b-PCL) nanocarriers for solubilization and controlled release of paclitaxel. *Molecules*. 2021;26(9):2690. doi:10.3390/molecules26092690
55. Muthu MS, Kulkarni S, Liu Y, Feng SS. Development of docetaxel-loaded vitamin E TPGS micelles: Formulation optimization, effects on brain cancer cells and biodistribution in rats. *Nanomedicine (Lond)*. 2012;7(3):353–364. doi:10.2217/nmm.11.111
56. Nam JP, Lee KJ, Choi JW, Yun CO, Nah JW. Targeting delivery of tocopherol and doxorubicin grafted-chitosan polymeric micelles for cancer therapy: In vitro and in vivo evaluation. *Colloids Surf B Biointerfaces*. 2015;133:254–262. doi:10.1016/j.colsurfb.2015.06.018
57. Shin HC, Alani AWG, Rao DA, Rockich NC, Kwon GS. Multi-drug loaded polymeric micelles for simultaneous delivery of poorly soluble anticancer drugs. *J Control Release*. 2009;140(3):294–300. doi:10.1016/j.jconrel.2009.04.024
58. Li S, Dong S, Xu W, Jiang Y, Li Z. Polymer nanoformulation of sorafenib and all-trans retinoic acid for synergistic inhibition of thyroid cancer. *Front Pharmacol*. 2020;10:1676. doi:10.3389/fphar.2019.01676
59. Xie X, Chen Y, Chen Z, et al. Polymeric hybrid nanomicelles for cancer theranostics: An efficient and precise anticancer strategy for the co-delivery of doxorubicin/miR-34a and magnetic resonance imaging. *ACS Appl Mater Interfaces*. 2019;11(47):43865–43878. doi:10.1021/acsami.9b14908
60. Voci S, Gagliardi A, Molinaro R, Fresta M, Cosco D. Recent advances of taxol-loaded biocompatible nanocarriers embedded in natural polymer-based hydrogels. *Gels*. 2021;7(2):33. doi:10.3390/gels7020033
61. Do VQ, Park KH, Park JM, Lee MY. Comparative in vitro toxicity study of docetaxel and nanoxel, a docetaxel-loaded micellar formulation using cultured and blood cells. *Toxicol Res*. 2019;35(2):201–207. doi:10.5487/TR.2019.35.2.201
62. Zheng X, Xie J, Zhang X, et al. An overview of polymeric nanomicelles in clinical trials and on the market. *Chin Chem Lett*. 2021;32(1):243–257. doi:10.1016/j.ccllet.2020.11.029
63. Khanna C, Rosenberg M, Vail DY. A review of paclitaxel and novel formulations, including those suitable for use in dogs. *J Vet Intern Med*. 2015;29(4):1006–1012. doi:10.1111/jvim.12596
64. Matsumura Y, Hamaguchi T, Ura T, et al. Phase I clinical trial and pharmacokinetic evaluation of NK911, a micelle-encapsulated doxorubicin. *Br J Cancer*. 2004;91(10):1775–1781. doi:10.1038/sj.bjc.6602204

65. Kim TY, Kim DW, Chung JY, et al. Phase I and pharmacokinetic study of Genexol-PM, a Cremophor-free, polymeric micelle-formulated paclitaxel, in patients with advanced malignancies. *Clin Cancer Res.* 2004;10(11):3708–3716. doi:10.1158/1078-0432.CCR-03-0655
66. Lim WT, Tan EH, Toh CK, et al. Phase I pharmacokinetic study of a weekly liposomal paclitaxel formulation (Genexol-PM) in patients with solid tumors. *Ann Oncol.* 2010;21(2):382–388. doi:10.1093/annonc/mdp315
67. Lee SW, Kim YM, Kim YT, Kang SB. An open-label, multicenter, phase I trial of a Cremophor-free, polymeric micelle formulation of paclitaxel combined with carboplatin as a first-line treatment for advanced ovarian cancer: A Korean Gynecologic Oncology Group study (KGOG-3016). *J Gynecol Oncol.* 2017;28(3):e26. doi:10.3802/jgo.2017.28.e26
68. Lee SW, Kim YM, Cho CH, et al. An open-label, randomized, parallel, phase II trial to evaluate the efficacy and safety of a Cremophor-free polymeric micelle formulation of paclitaxel as first-line treatment for ovarian cancer: A Korean Gynecologic Oncology Group study (KGOG-3021). *Cancer Res Treat.* 2018;50(1):195–203. doi:10.4143/crt.2016.376
69. Kim DW, Kim SY, Kim HK, et al. Multicenter phase II trial of Genexol-PM, a novel Cremophor-free, polymeric micelle formulation of paclitaxel, with cisplatin in patients with advanced non-small-cell lung cancer. *Ann Oncol.* 2007;18(12):2009–2014. doi:10.1093/annonc/mdm374
70. Keam B, Lee KW, Lee SH, et al. A phase II study of Genexol-PM and cisplatin as induction chemotherapy in locally advanced head and neck squamous cell carcinoma. *Oncologist.* 2019;24(6):751–e231. doi:10.1634/theoncologist.2019-0070
71. Ahn HK, Jung M, Sym SJ, et al. A phase II trial of Cremophor EL-free paclitaxel (Genexol-PM) and gemcitabine in patients with advanced non-small cell lung cancer. *Cancer Chemother Pharmacol.* 2014;74(2):277–282. doi:10.1007/s00280-014-2498-5
72. Kim JY, Do YR, Song HS, et al. Multicenter phase II clinical trial of Genexol-PM® with gemcitabine in advanced biliary tract cancer. *Anticancer Res.* 2017;37(3):1467–1473. doi:10.21873/anticancer.11471
73. Kim HS, Lee JY, Lim SH, et al. A prospective phase II study of cisplatin and Cremophor EL-free paclitaxel (Genexol-PM) in patients with unresectable thymic epithelial tumors. *J Thoracic Oncol.* 2015;10(12):1800–1806. doi:10.1097/JTO.0000000000000692
74. Lee KS, Chung HC, Im SA, et al. Multicenter phase II trial of Genexol-PM, a Cremophor-free, polymeric micelle formulation of paclitaxel, in patients with metastatic breast cancer. *Breast Cancer Res Treatment.* 2008;108(2):241–250. doi:10.1007/s10549-007-9591-y
75. Lee JL, Ahn JH, Park SH, et al. Phase II study of a Cremophor-free, polymeric micelle formulation of paclitaxel for patients with advanced urothelial cancer previously treated with gemcitabine and platinum. *Invest New Drugs.* 2012;30(5):1984–1990. doi:10.1007/s10637-011-9757-7
76. Park IH, Sohn JH, Kim SB, et al. An open-label, randomized, parallel, phase III trial evaluating the efficacy and safety of polymeric micelle-formulated paclitaxel compared to conventional Cremophor EL-based paclitaxel for recurrent or metastatic HER2-negative breast cancer. *Cancer Res Treat.* 2017;49(3):569–577. doi:10.4143/crt.2016.289
77. Kim TH, Gwak G, Chung MS, et al. Multicenter trial for safety and toxicity of a nanoparticle docetaxel formulation in breast cancer. *Ann Oncol.* 2018;29(Suppl 9):ix3. doi:10.1093/annonc/mdy426.010
78. Mukai H, Kato K, Esaki T, et al. Phase I study of NK105, a nanomicellar paclitaxel formulation, administered on a weekly schedule in patients with solid tumors. *Invest New Drugs.* 2016;34(6):750–759. doi:10.1007/s10637-016-0381-4
79. Hamaguchi T, Kato K, Yasui H, et al. A phase I and pharmacokinetic study of NK105, a paclitaxel-incorporating micellar nanoparticle formulation. *Br J Cancer.* 2007;97(2):170–176. doi:10.1038/sj.bjc.6603855
80. Kato K, Chin K, Yoshikawa T, et al. Phase II study of NK105, a paclitaxel-incorporating micellar nanoparticle, for previously treated advanced or recurrent gastric cancer. *Invest New Drugs.* 2012;30(4):1621–1627. doi:10.1007/s10637-011-9709-2
81. Saeki T, Mukai H, Ro J, et al. A global phase III clinical study comparing NK105 and paclitaxel in metastatic or recurrent breast cancer patients. *Ann Oncol.* 2017;28(Suppl 5):v80–v81. doi:10.1093/annonc/mdx365.013
82. Fujiwara Y, Mukai H, Saeki T, et al. A multi-national, randomised, open-label, parallel, phase III non-inferiority study comparing NK105 and paclitaxel in metastatic or recurrent breast cancer patients. *Br J Cancer.* 2019;120(5):475–480. doi:10.1038/s41416-019-0391-z
83. Burris HA, Infante JR, Anthony Greco F, et al. A phase I dose escalation study of NK012, an SN-38 incorporating macromolecular polymeric micelle. *Cancer Chemother Pharmacol.* 2016;77(5):1079–1086. doi:10.1007/s00280-016-2986-x
84. Hamaguchi T, Doi T, Eguchi-Nakajima T, et al. Phase I study of NK012, a novel SN-38-incorporating micellar nanoparticle, in adult patients with solid tumors. *Clin Cancer Res.* 2010;16(20):5058. doi:10.1158/1078-0432.CCR-10-0387
85. Jones SF, Burris HA, Infante JR, et al. A phase I study of NK012 in combination with 5-fluorouracil with or without leucovorin in patients (pts) with advanced solid tumors. *J Clin Oncol.* 2012;30(15 Suppl):e13076–e13076. doi:10.1200/jco.2012.30.15_suppl.e13076
86. Ri M, Suzuki K, Iida S, et al. A phase I/II study for dose-finding, and to investigate the safety, pharmacokinetics and preliminary efficacy of NK012, an SN-38-incorporating macromolecular polymeric micelle, in patients with multiple myeloma. *Intern Med.* 2018;57(7):939–946. doi:10.2169/internalmedicine.9567-17
87. Hamaguchi T, Tsuji A, Yamaguchi K, et al. A phase II study of NK012, a polymeric micelle formulation of SN-38, in unresectable, metastatic or recurrent colorectal cancer patients. *Cancer Chemother Pharmacol.* 2018;82(6):1021–1029. doi:10.1007/s00280-018-3693-6
88. Plummer R, Wilson RH, Calvert H, et al. A phase I clinical study of cisplatin-incorporated polymeric micelles (NC-6004) in patients with solid tumours. *Br J Cancer.* 2011;104(4):593–598. doi:10.1038/bjc.2011.6
89. Doi T, Hamaguchi T, Shitara K, et al. NC-6004 phase I study in combination with gemcitabine for advanced solid tumors and population PK/PD analysis. *Cancer Chemother Pharmacol.* 2017;79(3):569–578. doi:10.1007/s00280-017-3254-4
90. Subbiah V, Grilley-Olson JE, Combest AJ, et al. Phase Ib/II trial of NC-6004 (nanoparticle cisplatin) plus gemcitabine in patients with advanced solid tumors. *Clin Cancer Res.* 2018;24(1):43–51. doi:10.1158/1078-0432.CCR-17-1114
91. Volovat SR, Ciuleanu TE, Koralewski P, et al. A multicenter, single-arm, basket design, phase II study of NC-6004 plus gemcitabine in patients with advanced unresectable lung, biliary tract, or bladder cancer. *Oncotarget.* 2020;11(33):3105–3117. doi:10.18632/oncotarget.27684
92. Mukai H, Kogawa T, Matsubara N, Naito Y, Sasaki M, Hosono A. A first-in-human phase 1 study of epirubicin-conjugated polymer micelles (K-912/NC-6300) in patients with advanced or recurrent solid tumors. *Invest New Drugs.* 2017;35(3):307–314. doi:10.1007/s10637-016-0422-z
93. Riedel RF, Chua VS, Kim T, et al. Results of NC-6300 (nanoparticle epirubicin) in an expansion cohort of patients with angiosarcoma. *J Clin Oncol.* 2021;39(15 Suppl):11543–11543. doi:10.1200/JCO.2021.39.15_suppl.11543
94. Chawla SP, Goel S, Chow W, et al. A phase 1b dose escalation trial of NC-6300 (nanoparticle epirubicin) in patients with advanced solid tumors or advanced, metastatic, or unresectable soft-tissue sarcoma. *Clin Cancer Res.* 2020;26(16):4225–4232. doi:10.1158/1078-0432.CCR-20-0591
95. Von Hoff DD, Mita MM, Ramanathan RK, et al. Phase I study of PSMA-targeted docetaxel-containing nanoparticle BIND-014 in patients with advanced solid tumors. *Clin Cancer Res.* 2016;22(13):3157–3163. doi:10.1158/1078-0432.CCR-15-2548
96. Autio KA, Garcia JA, Alva AS, et al. A phase 2 study of BIND-014 (PSMA-targeted docetaxel nanoparticle) administered to patients with chemotherapy-naïve metastatic castration-resistant prostate cancer (mCRPC). *J Clin Oncol.* 2016;34(2 Suppl):233–233. doi:10.1200/jco.2016.34.2_suppl.233
97. Autio KA, Dreicer R, Anderson J, et al. Safety and efficacy of BIND-014, a docetaxel nanoparticle targeting prostate-specific membrane antigen for patients with metastatic castration-resistant prostate cancer: A phase 2 clinical trial. *JAMA Oncol.* 2018;4(10):1344–1351. doi:10.1001/jamaoncol.2018.2168
98. Danson S, Ferry D, Alakhov V, et al. Phase I dose escalation and pharmacokinetic study of Pluronic polymer-bound doxorubicin (SP1049C) in patients with advanced cancer. *Br J Cancer.* 2004;90(11):2085–2091. doi:10.1038/sj.bjc.6601856
99. Armstrong A, Brewer J, Newman C, et al. SP1049C as first-line therapy in advanced (inoperable or metastatic) adenocarcinoma of the oesophagus: A phase II window study. *J Clin Oncol.* 2006;24(18 Suppl):4080. doi:10.1200/jco.2006.24.18_suppl.4080

100. Valle JW, Armstrong A, Newman C, et al. A phase 2 study of SP1049C, doxorubicin in P-glycoprotein-targeting Pluronic, in patients with advanced adenocarcinoma of the esophagus and gastroesophageal junction. *Invest New Drugs*. 2011;29(5):1029–1037. doi:10.1007/s10637-010-9399-1
101. Miller T, Hill A, Uezguen S, Weigandt M, Goepferich A. Analysis of immediate stress mechanisms upon injection of polymeric micelles and related colloidal drug carriers: Implications on drug targeting. *Biomacromolecules*. 2012;13(6):1707–1718. doi:10.1021/bm3002045
102. Miller T, Breyer S, van Colen G, et al. Premature drug release of polymeric micelles and its effects on tumor targeting. *Int J Pharm*. 2013;445(1):117–124. doi:10.1016/j.ijpharm.2013.01.059
103. Soleymani Abyaneh H, Vakili M, Zhan F, Choi P, Lavasanifar A. Rationale design of block copolymer micelles to control burst drug release at a nanoscale dimension. *Acta Biomater*. 2015;24:127–139. doi:10.1016/j.actbio.2015.06.017
104. Rozynek Z, Bielas R, Józefczak A. Efficient formation of oil-in-oil Pickering emulsions with narrow size distributions by using electric fields. *Soft Matter*. 2018;14(24):5140–5149. doi:10.1039/C8SM00671G
105. Dommersnes P, Rozynek Z, Mikkelsen A, et al. Active structuring of colloidal armour on liquid drops. *Nat Commun*. 2013;4:2066. doi:10.1038/ncomms3066
106. Kubiak T, Banaszak J, Józefczak A, Rozynek Z. Direction-specific release from capsules with homogeneous or Janus shells using an ultrasound approach. *ACS Appl Mater Interfaces*. 2020;12(13):15810–15822. doi:10.1021/acsami.9b21484
107. Rozynek Z, Mikkelsen A, Dommersnes P, Fossum JO. Electroformation of Janus and patchy capsules. *Nat Commun*. 2014;5:3945. doi:10.1038/ncomms4945
108. Rozynek Z, Józefczak A. Patchy colloidosomes: An emerging class of structures. *Eur Phys J Special Topics*. 2016;225(4):741–756. doi:10.1140/epjst/e2015-50267-7
109. Kubiak T, Zubko M, Józefczak A. Ultrasound-triggered directional release from turmeric capsules. *Particuology*. 2021;57:19–27. doi:10.1016/j.partic.2020.12.010
110. Dinsmore AD, Hsu MF, Nikolaidis MG, Marquez M, Bausch AR, Weitz DA. Colloidosomes: Selectively permeable capsules composed of colloidal particles. *Science*. 2002;298(5595):1006–1009. doi:10.1126/science.1074868
111. Bielas R, Surdeko D, Kaczmarek K, Józefczak A. The potential of magnetic heating for fabricating Pickering-emulsion-based capsules. *Colloids Surf B Biointerfaces*. 2020;192:111070. doi:10.1016/j.colsurfb.2020.111070
112. Sobczak G, Wojciechowski T, Sashuk V. Submicron colloidosomes of tunable size and wall thickness. *Langmuir*. 2017;33(7):1725–1731. doi:10.1021/acs.langmuir.6b04159
113. Chen Y, Wang C, Chen J, Liu X, Tong Z. Growth of lightly crosslinked PHEMA brushes and capsule formation using Pickering emulsion interface-initiated ATRP. *J Polym Sci A Polym Chem*. 2009;47(5):1354–1367. doi:10.1002/pola.23244
114. Sander JS, Studart AR. Monodisperse functional colloidosomes with tailored nanoparticle shells. *Langmuir*. 2011;27(7):3301–3307. doi:10.1021/la1035344
115. Li Z, Lee D, Rubner MF, Cohen RE. Layer-by-layer assembled Janus microcapsules. *Macromolecules*. 2005;38(19):7876–7879. doi:10.1021/ma0513012
116. Shchukin DG, Shchukina E. Capsules with external navigation and triggered release. *Curr Opin Pharmacol*. 2014;18:42–46. doi:10.1016/j.coph.2014.09.002
117. Guan BY, Yu L, Lou XW. Chemically assisted formation of monolayer colloidosomes on functional particles. *Adv Mater*. 2016;28(43):9596–9601. doi:10.1002/adma.201603622
118. Thompson KL, Williams M, Armes SP. Colloidosomes: Synthesis, properties and applications. *J Colloid Interface Sci*. 2014;447:217–228. doi:10.1016/j.jcis.2014.11.058
119. Zhang Z, Wang S, Yang Y, Li W, Liu P, Wang WJ. Hierarchical assembly of two-dimensional polymers into colloidosomes and microcapsules. *ACS Macro Letters*. 2021;10(7):933–939. doi:10.1021/acsmacrolett.1c00380
120. Subramaniam AB, Abkarian M, Stone HA. Controlled assembly of jammed colloidal shells on fluid droplets. *Nat Mater*. 2005;4(7):553–556. doi:10.1038/nmat1412
121. Noble PF, Cayre OJ, Alargova RG, Velev OD, Paunov VN. Fabrication of “hairy” colloidosomes with shells of polymeric microrods. *J Am Chem Soc*. 2004;126(26):8092–8093. doi:10.1021/ja047808u
122. Su Y, Zhao H, Wu J, Xu J. One-step fabrication of silica colloidosomes with in situ drug encapsulation. *RSC Advances*. 2016;6(113):112292–112299. doi:10.1039/C6RA19048K
123. Sun Q, Gao H, Sukhorukov GB, Routh AF. Silver-coated colloidosomes as carriers for an anticancer drug. *ACS Appl Mater Interfaces*. 2017;9(38):32599–32606. doi:10.1021/acsami.7b11128
124. Sun Q, Du Y, Hall EAH, Luo D, Sukhorukov GB, Routh AF. A fabrication method of gold coated colloidosomes and their application as targeted drug carriers. *Soft Matter*. 2018;14(14):2594–2603. doi:10.1039/c7sm02485a
125. Sun Q, Du Y, Zhao Z, et al. Functional silver-coated colloidosomes as targeted carriers for small molecules. *Langmuir*. 2017;33(15):3755–3764. doi:10.1021/acs.langmuir.6b04594
126. White AL, Langton C, Wille ML, et al. Ultrasound-triggered release from metal shell microcapsules. *J Colloid Interface Sci*. 2019;554:444–452. doi:10.1016/j.jcis.2019.07.020
127. Zhang K, Wang Q, Meng H, Wang M, Wu W, Chen J. Preparation of polyacrylamide/silica composite capsules by inverse Pickering emulsion polymerization. *Particuology*. 2014;14:12–18. doi:10.1016/j.partic.2013.02.010
128. Hitchcock JP, Tasker AL, Baxter EA, Biggs S, Cayre OJ. Long-term retention of small, volatile molecular species within metallic microcapsules. *ACS Appl Mater Interfaces*. 2015;7(27):14808–14815. doi:10.1021/acsami.5b03116
129. Stavarache CE, Paniwnyk L. Controlled rupture of magnetic LbL polyelectrolyte capsules and subsequent release of contents employing high intensity focused ultrasound. *J Drug Deliv Sci Technol*. 2018;45:60–69. doi:10.1016/j.jddst.2018.02.011
130. Li B, Cai M, Lin L, et al. MRI-visible and pH-sensitive micelles loaded with doxorubicin for hepatoma treatment. *Biomater Sci*. 2019;7(4):1529–1542. doi:10.1039/C8BM01501E
131. Yang X, Han X, Zhu Y. (PAH/PSS)5 microcapsules templated on silica core: Encapsulation of anticancer drug DOX and controlled release study. *Colloids Surf A Physicochem Engineering Aspects*. 2005;264(1–3):49–54. doi:10.1016/j.colsurfa.2005.05.017
132. Bu L, Zhang H, Xu K, Du B, Zhu C, Li Y. pH and reduction dual-responsive micelles based on novel polyurethanes with detachable poly(2-ethyl-2-oxazoline) shell for controlled release of doxorubicin. *Drug Deliv*. 2019;26(1):300–308. doi:10.1080/10717544.2019.1580323
133. Sun F, Wang Y, Wei Y, Cheng G, Ma G. Thermo-triggered drug delivery from polymeric micelles of poly(N-isopropylacrylamide-co-acrylamide)-b-poly(n-butyl methacrylate) for tumor targeting. *J Bioactive Compatible Polym*. 2014;29(4):301–317. doi:10.1177/0883911514535288
134. Schild HG. Poly(N-isopropylacrylamide): Experiment, theory and application. *Prog Polym Sci*. 1992;17(2):163–249. doi:10.1016/0079-6700(92)90023-R
135. Yang M, Ding Y, Zhang L, Qian X, Jiang X, Liu B. Novel thermosensitive polymeric micelles for docetaxel delivery. *J Biomed Mater Res A*. 2007;81A(4):847–857. doi:10.1002/jbm.a.31129
136. Liu SQ, Tong YW, Yang YY. Incorporation and in vitro release of doxorubicin in thermally sensitive micelles made from poly(N-isopropylacrylamide-co-N,N-dimethylacrylamide)-b-poly(d,l-lactide-co-glycolide) with varying compositions. *Biomaterials*. 2005;26(24):5064–5074. doi:10.1016/j.biomaterials.2005.01.030
137. Kaczmarek K, Mrówczyński R, Hornowski T, Bielas R, Józefczak A. The effect of tissue-mimicking phantom compressibility on magnetic hyperthermia. *Nanomaterials (Basel)*. 2019;9(5):803. doi:10.3390/nano9050803
138. Kim HC, Kim E, Jeong SW, et al. Magnetic nanoparticle-conjugated polymeric micelles for combined hyperthermia and chemotherapy. *Nanoscale*. 2015;7(39):16470–16480. doi:10.1039/C5NR04130A
139. Kijewska K, Głowala P, Wiktorska K, et al. Bromide-doped polypyrrole microcapsules modified with gold nanoparticles. *Polymer*. 2012;53(23):5320–5329. doi:10.1016/j.polymer.2012.09.029
140. Timin AS, Muslimov AR, Lepik KV, et al. Intracellular breakable and ultrasound-responsive hybrid micro-sized containers for selective drug release into cancerous cells. *Part Part Syst Char*. 2017;34(5):1600417. doi:10.1002/ppsc.201600417

141. Chen J, Ratnayaka S, Alford A, et al. Theranostic multilayer capsules for ultrasound imaging and guided drug delivery. *ACS Nano*. 2017;11(3):3135–3146. doi:10.1021/acsnano.7b00151
142. Cao Y, Chen Y, Yu T, et al. Drug release from phase-changeable nanodroplets triggered by low-intensity focused ultrasound. *Theranostics*. 2018;8(5):1327–1339. doi:10.7150/thno.21492
143. Liu TY, Huang TC. A novel drug vehicle capable of ultrasound-triggered release with MRI functions. *Acta Biomater*. 2011;7(11):3927–3934. doi:10.1016/j.actbio.2011.06.038
144. Cabane E, Malinova V, Meier W. Synthesis of photocleavable amphiphilic block copolymers: Toward the design of photosensitive nanocarriers. *Macromol Chem Phys*. 2010;211(17):1847–1856. doi:10.1002/macp.201000151
145. Lo YL, Tsai MF, Soorni Y, Hsu C, Liao ZX, Wang LF. Dual stimuli-responsive block copolymers with adjacent redox- and photo-cleavable linkages for smart drug delivery. *Biomacromolecules*. 2020;21(8):3342–3352. doi:10.1021/acs.biomac.0c00773
146. Dispinar T, Colard CAL, Du Prez FE. Polyurea microcapsules with a photocleavable shell: UV-triggered release. *Polym Chem*. 2013;4(3):763–772. doi:10.1039/C2PY20735D
147. Liu X, Tian Z, Chen C, Allcock HR. UV-cleavable unimolecular micelles: Synthesis and characterization toward photocontrolled drug release carriers. *Polym Chem*. 2013;4(4):1115–1125. doi:10.1039/C2PY20825C
148. Chen J, Qian C, Ren P, et al. Light-responsive micelles loaded with doxorubicin for osteosarcoma suppression. *Front Pharmacol*. 2021;12:679610. doi:10.3389/fphar.2021.679610
149. Rosenbauer EM, Wagner M, Musyanovych A, Landfester K. Controlled release from polyurethane nanocapsules via pH-, UV-light- or temperature-induced stimuli. *Macromolecules*. 2010;43(11):5083–5093. doi:10.1021/ma100481s